THE

STUDY OF PROTON-DONOR PROTON-ACCEPTOR INTERACTIONS BY INFRARED SPECTROSCOPY AND COMPUTER MODELLING

RAHIMA DILSHAD M.Sc.

A THESIS SUBMITTED IN PARTIAL FULFILMENT

OF THE REQUIREMENTS

FOR

THE DEGREE OF MASTER OF PHILOSOPHY

TO THE UNIVERSITY OF GLAMORGAN

NOVEMBER 1994

SCHOOL OF APPLIED SCIENCES

UNIVERSITY OF GLAMORGAN IN COLLABORATION WITH

CHEMICAL DESIGN LIMITED (OXFORD)

ABSTRACT

Infrared spectroscopy has been used to determine thermodynamic parameters for the reaction between ethanol and acetone in CCl_4 and in the vapour phase in which a hydrogen-bonded complex is formed. In carbon tetrachloride, $\Delta H_f^{\ominus} = -15.3$ kJ mol^{-1} and $\Delta S_f^{\ominus} = -50.8$ J mol^{-1} K^{-1}. These values are consistent with data reported in the literature for related alcohols. Equilibrium constants for the vapour phase reaction were not reproducible, possibly due to a combination of adsorption and pressure effects.

The IR spectra of propionic and acetic acids was studied in dilute CCl_4 and for acetic acid (at low acid pressure) in gaseous argon mixtures. Bands were assigned to the monomer and dimer. Spectra confirm that carboxylic acids are much more strongly hydrogen-bonded than the corresponding alcohols.

The IR spectra of acetic, propionic, butyric, benzoic, o-methoxyl and o-ethoxy benzoic, p-methoxyl and p-ethoxy benzoic and o-acetyl salicylic acids was studied in CCl_4. The effect of inter and intramolecular hydrogen-bonding is discussed.

Models of monomer and dimer carboxylic acids were constructed using the Chem-X computer modelling package (Chemical Design Ltd.). Molecular energies were generated for the most stable acid conformations. For o-methoxy benzoic acid, the variation of molecular energy with the degree of internal rotation for the four bonds for which internal rotation was feasible was plotted using Chem-X. The J-CAMP.DX file protocol was used to import IR spectra into the Chem-X package. The future potential of combining modelling and spectroscopic packages is discussed.

DECLARATION

This dissertation has not been nor is currently being submitted for the award of any other Degree or similar qualification.

Rahima Dilshad

RAHIMA DILSHAD

Candidate

Dated November 1994.

ACKNOWLEDGEMENT

I wish to express my thanks and indebtedness to my director of studies Dr.Rhobert Lewis, for his kindness, help, excellent guidance and thoughtful suggestions during the period of my research project. I would like to thank and express my gratitude to Professor W.O. George, my second supervisor, for his expert direction during the molecular modelling part of the project. Thanks is also due to Professor J.R. Dixon, for his many interesting suggestions and for allowing me the use of the departmental facilities. I also acknowledge the help provided by Chemical Design (Oxford) Ltd. who kindly collaborated with the department during this project.

My thanks are expressed to both the University of Glamorgan and the Association of Commonwealth Universities for providing me with an "Overseas Development Administration Shared Scholarship Scheme" Award (ODASSS).

My appreciation is expressed to all the staff and technicians in the department especially Mr.Brian Minty and Mr.R. Hancock who gave help during my studies.

Finally, special thanks are due to my husband A.S.M. Kamruzzahan and all other family members for their invaluable encouragement over the last two years.

DEDICATION

TO

MY PARENTS

INDEX

CONTENTS

CHAPTER ONE

INTRODUCTION

1.INTRODUCTION

1.1. General aspects of hydrogen bond

"Hydrogen bond" is the term given to the relatively weak secondary interaction between a hydrogen atom bound to an electronegative atom and another atom that is also generally electronegative or part of a π electron group, where lone pairs electrons or π electrons are available[1]. We can thus represent a hydrogen bond between a functional group A-H, the proton donor, and an atom, or group of atoms, B, which contains the proton acceptor, in the following generalised form:

$$A^{\delta-}- H^{\delta+}...B$$

where ... represents the hydrogen bond. A and B may be the same.

A hydrogen bond exists, when there is evidence of bond formation (association) and there is evidence that this new bond linking A-H and B specifically involves[2,3] the hydrogen atom already bonded to A. This differentiates the hydrogen bond from other types of associative interaction. Since the atom A of the proton donor A-H must be electronegative, the bond will be associated with a dipole moment[4,5] $A^{\delta-}- H^{\delta+}$, where δ represents only a fraction of full electronic charge. This leads to the view of the hydrogen bond as one kind of dipole - dipole interaction.

Hamilton and Ibers[6] provide an operational definition of a hydrogen bond. A hydrogen bond exists when a hydrogen atom is bonded to two or more atoms. Since in the electron pair theory of chemical bonding[7] a hydrogen atom possesses only one electron to engage in covalent bonding, the hydrogen bond is not a simple covalent orbital overlap bond.

The above considerations are summarised in the following operational criteria for the existence of hydrogen bonding:

1. The requirement for the formation of hydrogen bonds is a sufficiently polar bond between hydrogen and strongly electronegative atoms[8,9], such as nitrogen, oxygen and fluorine. Commonly encountered hydrogen bonds are O-H...O and N-H...O.

2. The bonding mechanism is primarily electrostatic attraction. The local interaction between the net charges on the proton donor group and the proton acceptor group holds the molecules together[10].

3. The presence of a hydrogen bond confers unusual properties to molecules. Classic examples are the apparently abnormally high melting points and boiling points of ammonia, water and hydrogen fluoride. Microscopically, the effects observed include changes in dipole moment, monomer bond lengths and in vibrational frequency.

4. In many hydrogen bonds, A-H...B, the atoms A and B are closer together than the sum of the van der Waal's radii. Owing to the smallness of the hydrogen atom and to the consequent uniquely intense field round the atomic core[4], it can occupy a position very close to the unshared electrons of an electronegative atom, and hence the dipolar A-H can get closer to atom B. A very strong electrostatic attraction results. Atoms larger than hydrogen atom cannot occupy positions so near to each other, consequently, dipole - dipole attraction between other atoms are weaker. Observations suggest that the total bond length contraction due to H-bond formation is equal to or greater than twice the van der Waal's radius of the hydrogen atom[11].

5. The bond dissociation energies of hydrogen bonds generally fall in the range 4 - 40 kJ mol^{-1}, weaker by a factor of ten than covalent bonds between atoms[11]. The strongest hydrogen bonds are found in the bifluoride ion $[F-H...F]^-$ and in hydrogen fluoride. Less strong and most common hydrogen bonds are found when proton is donated by a carboxyl, hydroxyl, amine or amide group. Weaker hydrogen bonds are found when C-H and S-H groups are bound to a strongly electronegative group, for example $CHCl_3$.

6. Hydrogen-bonding is an associative phenomenon. It causes a decrease in the total number of free molecules and an increase in the average molecular mass in solution except in the case of intramolecular hydrogen bonds. At ordinary temperatures, only a fraction of the molecules may be

associated while, at equilibrium, a certain number of new complexes are continually formed and an equal number of complexes are continually broken down[11].

In a molecule capable of self association, i.e. one that possesses both donor and acceptor sites, the hydrogen bond interaction causes an increase in the bond length A-H in both molecules.

All molecules can be conveniently classified into four types with respect to their ability to participate in hydrogen-bonding (table 1.1). Hydrogen-bonding molecules can be divided into types 1 to 3, while molecules incapable of hydrogen-bonding form type 4.

Type 1 and type 2 molecules are capable of forming hydrogen bonded complexes frequently in a simple ratio, 1:1. Type 4 molecules are largely incapable of forming hydrogen bonds which are used as inert solvents in studies of hydrogen bonding in solution. The strength of the hydrogen-bonding depends primarily on the relative acidity of 1 and the relative basicity of 2. This strength is at a maximum when the proton donor group and the axis of the lone pair orbital are co-linear[12]. The strength of the bond is often found to be inversely proportional to the distance between A and B.

Self associated hydrogen-bonded complexes are formed by type 3 molecules. The bonding may be either intermolecular or intramolecular.

TABLE 1.1[11]

Classification of molecules for H-bonding

Type	Description	Examples
1	Molecules with one or more donor groups (acids) and no acceptor groups.	Haloforms, highly halogenated compounds, alkynes.
2	Molecules with one or more acceptor groups (bases) and no donor groups.	Ketones, ethers, esters, alkenes, aromatics, tertiary amines, nitriles, isonitriles.
3	Molecules with both donor and acceptor groups.	Alcohols, water, phenols, inorganic and carboxylic acids, primary and secondary amines.
4	Molecules with neither donor or acceptor groups.	Saturated hydrocarbons, carbon tetrachloride, and carbon disulfide.

1.2. Types of hydrogen bond

Generally two types of hydrogen-bonded complexes are formed:

a. ***Intermolecular hydrogen bonds*** involving association of two or more separate molecules of the same or different compounds. This is the most commonly occurring H-bond and is not limited to dimeric linkages. They can occur in the form of chains as in hydrogen fluoride (fig.1.1), or rings as in the case of carboxylic acids in dimer molecules (fig.1.2). In neat samples or concentrated solutions, multiple bonding may occur[13].

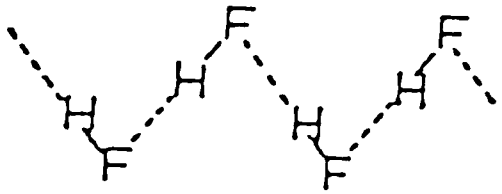

fig.1.1

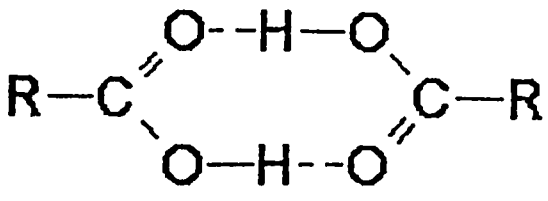

fig.1.2

b. ***Intramolecular hydrogen-bonding*** is hydrogen-bonding within a molecule. A favourable spatial configuration is required. This bond is formed by one part of a molecule donating a proton to an acceptor in another part. For a example, in o-hydroxy benzoic acid molecule[4], the bond between the phenolic group and carboxyl group is an intramolecular H-bond (fig.1.3).

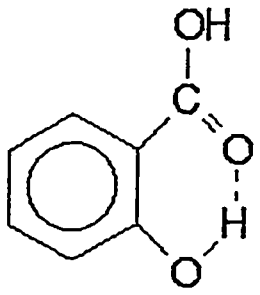

fig.1.3

Intramolecular hydrogen bonds are often weaker than intermolecular hydrogen bonds and are less sensitive to temperature and changes in concentration.

1.3. Methods for studying hydrogen-bonding

Many physical methods have been developed since 1920 [14] for studying molecular structure, and most of them have been applied to hydrogen bond. Evidence comes from X-ray and neutron diffraction crystallographic studies and from infrared and nuclear magnetic resonance spectra.

The accurate location of hydrogen atoms is not generally possible by X-ray diffraction[15] which only allows a determination of the overall A-B distance. When the sum of the van der Waal's radii for A and B are significantly

shorter than non bonded atoms, a hydrogen bond is assumed to be present. More recently, this method has been supplemented by neutron diffraction methods[16] which enables the proton in A-H...B to be located because the scattering of neutrons of thermal energies is roughly similar for all nuclei, regardless of atomic number.

Although X-ray and neutron diffraction are very powerful methods, they are applicable only to crystalline solids and spectroscopic methods are needed to study the effect of hydrogen-bonding in other phases. The types of spectra which have been used for the detection of hydrogen-bonding include microwave[17], infrared, Raman, UV-visible and nuclear magnetic resonance.

When a complex contains a chromophore which is perturbed by hydrogen bond formation, UV and visible spectroscopy may be used to study hydrogen-bonding[18]. Generally, hydrogen bonding causes a red (bathochromic) shift when chromophores are acting as proton donors and a blue shift (hypsochromic) when chromophores are acting as proton acceptors.

Proton nmr has been important to studies of hydrogen bonding since the early days of nmr[19,20]. This gives evidence of H-bond formation by showing a shift (usually to lower fields) of the proton involved[21]. The shifting of the A-H proton resonance signal to lower field indicates less shielding and hence lower electron density around the proton. Only one peak intermediate between those for pure A-H and A-H...B is observed.

Infrared spectroscopy has been more widely used in hydrogen bonding studies than any other spectroscopic method[16,22,23]. A number of favourable factors influence this dominance. The measurements are relatively easy to make in all phases[24], and there are no severe limitations on temperature variation. The studies reported in this thesis are mainly concerned with the stretching and deformation vibrations of the donor and acceptor groups and the decrease observed for hydrogen-bonded A-H...B.

1.4. The Vibrational spectra of hydrogen-bonded complexes

One of the most prominent effects of hydrogen-bonding is to cause substantial changes in the spectra of the interacting molecules[25]. The main types of vibrations which are affected by H-bond formation are shown diagrammatically[26] in fig.(1.4). Infrared absorption bands are associated with simple vibrational modes of proton - donor and proton - acceptor molecules and with the complexes formed by hydrogen-bonded association.

There are four types of modes which are involved in hydrogen bond: the low frequency stretching and bending modes ν_σ and ν_β, and higher frequency stretching and bending modes ν_S and ν_B. These normal modes are used as a basis for the discussion of the characteristic spectral changes that occur when hydrogen-bonding takes place in any state of matter[27].

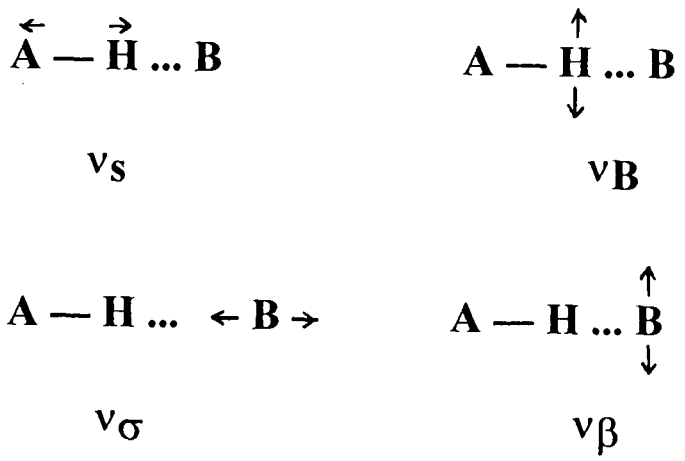

Fig.1.4: Diagrammatic representation of modes associated with the hydrogen bond for A-H...B complex.

The following are the most pronounced changes that occur in the formation of the A-H...B bond:

1. The A-H stretching frequency ν_S, decreases often by an amount corresponding to 30 cm^{-1} to several hundred cm^{-1} or more due to the hydrogen bond weakening the force constant for the A-H stretching mode.

2. The A-H bending frequency shifts to higher frequencies because hydrogen bond constrains the deformation vibrations and hence increases the force constants for these modes[11].

3. The breadth of the A-H stretching frequency increases markedly, as does its intensity. The possible causes of these broad absorption bands are discussed later (section 1.5). A large increase in intensity also occurs, probably because the bond moment $\mu_{(A-H)}$ is increased by H-bonding [25,28,29].

4. The absorptions due to the hydrogen bond H...B stretch in A-H...B complexes are found at low frequencies in the far-infrared region. Because of the weakness of the H-

bond, the force constants of these vibrations are small so causing absorptions to lie below 500 cm^{-1}. Assignments of hydrogen bond modes is complicated by the presence of a variety of other vibrations that occur in this region. Moreover, the stretching vibration couples with other vibrational modes making the assignments of bands difficult.

5. Hydrogen-bonding shifts the vibrational modes of acceptor groups B. These effects are much smaller than those observed for A-H vibrations.

Frequency shifts and changes in band intensities are valuable probes of hydrogen-bonding. The frequency shift, $\Delta\nu_S$, is generally represented as the difference between the stretching frequency for the monomeric A-H and the lowered stretching frequency for A-H...B complex, i.e.

$$\Delta\nu_S = \nu_S \text{ (A-H)} - \nu_S \text{ (A-H)complex}$$

The stronger is the hydrogen-bonding, the greater are the frequency shifts. For example, the centre of HCl(g)[30] fundamental occurs at 2886 cm^{-1}. When HCl enters into a hydrogen bond with CH_2=CHCN(g), a broad absorption band centred at about 2746 cm^{-1} is observed. The decrease in frequency, $\Delta\nu_S$ is, 140 cm^{-1}. For HCN...HCl complex, $\Delta\nu_S$ = 41 cm^{-1}, clearly indicating that CH_2=CHCN(g) participates more strongly in a H-bonding interaction than HCN(g). To measure the frequency shift in solution Allerhand and Schleyer[31] recommended the use of an inert solvent.

1.5. Origin of broad band structure in infrared spectra of hydrogen-bonded complexes

It has already been noted that the frequency lowering of the ν_S band by H-bond formation is accompanied with a marked increase in the integrated band area and in the breadth of $\nu_{(A - H)}$ absorption band. This is the most characteristic and interesting spectral change brought about by hydrogen bond formation and is observed in all three phases (gas, liquid, solid) in which the hydrogen-bonding occurs.

Several factors which may lead to broadening in the infrared spectra of hydrogen-bonded systems have been identified[32]. These include:

1. The presence of dimers, trimers or polymers, may contribute to broadening by increasing the chance of overlapping bands. It is difficult to know which species or whether more than one species, is contributing to a particular absorption band. The intermolecular interaction in solid or liquid phases is an added complication. Hydrogen-bonding studies in the gas phase at low pressure have the advantage of isolating the intermolecular contribution to the band broadening. Investigation of the effect of changing partial pressures in the infrared spectra of hydrogen-bonded system ether and hydrogen chloride[33], showed that the spectrum obtained is due to a single hydrogen-bonded species. Partial pressures of HCl and ether in the ratio of 1:2 and 2:1 mixture gave rise to

almost identical spectra. The intensity measurements showed that the observed absorption bands could be attributed to a 1:1 ether-hydrogen chloride complex and rejected band broadening due to multimers.

2. The observation of a band arising from unresolved rotational fine structure.

3. Occurrence of ν_S Fermi resonance with overtones or combinations of other internal vibrations in the region of hydrogen stretching vibrations. The observed overtone and summation frequencies are supposed to be intensified over a correspondingly wider range of frequencies and somewhat shifted in frequency as a result of resonance interaction. Evidence, proving that Fermi resonance is not the origin of the breadth or structure of the band has been provided by Bertie[33] for the dimers $(CH_3)_2O...HCl$ and $(CD_3)_2O...HCl$. The opportunities for Fermi resonance were found to be quite different but each mixture showed identical dimer spectra within experimental accuracy, which eliminates the possibility of broadening due to such interactions. This conclusion has also been supported by similar comparisons of $(CH_3)_2O...HF$ and $(CD_3)_2O...HF$[34] spectra.

4. Frequency modulation, i.e. anharmonic coupling between ν_S and low frequency vibrations (such as ν_σ and ν_S) giving a series of sum and difference bands $\nu_S \pm n\nu_\sigma$ where n is integral[35]. When a hydrogen bond is formed, the bond length (r_{A-H}) expands as the A...B distance (r_{A-B}) contracts causing a lowering of the A-H force constant. In effect,

the A-H vibration is frequency modulated by the (A-H ... B) vibration and strongly coupled in the region of the excited hydrogen stretching levels[36]. Thus the simple hydrogen band is replaced in the infrared spectra of a series of sub-bands which are not normally resolved. The band structure is interpreted as a strong central peak ν_s with side bands $\nu_s + \nu_\sigma$ and $\nu_s - \nu_\sigma$. This explanation is supported by the detailed experimental work of Millen et al[37,38].

CHAPTER TWO

INSTRUMENTATION AND EXPERIMENTAL TECHNIQUES

2. INSTRUMENTATION AND EXPERIMENTAL TECHNIQUES

2.1. Introduction

Two distinct families of infrared spectrometer are in general use[39]. One is the double beam dispersive spectrometer which involves passing the beam through a prism or reflecting it from a grating so that each frequency is distinguished spatially. The another is the Fourier transform spectrometer where interference techniques are involved. The use of an interferometer rather than a monochromator and the manner of its operation gives important advantages for the measurement of infrared spectra[40].

This chapter will summarize the essential theory of FT-IR spectrometers and then describe the experimental techniques used in the present study. Familiarity with dispersive instruments will be assumed. The two types of spectrometers are compared in fig.2.1.

2.2. Fourier transform infrared spectrometer

The criteria governing the measurement of spectra by Fourier transform infrared (FT-IR) spectroscopy are the same as for dispersive spectroscopy[39]. The technique of FT-IR spectroscopy is based on that of Michelson interferometer[42,43]. It basically consists of two parts: (1) an optical system which uses an interferometer (2) a dedicated computer and VDU. A computer controls optical

components, collects and stores data, performs computation on data and the VDU displays spectra.

The simplest form of an interferometer is shown[44] in fig. 2.1B. It consists of two plane mirrors which are mutually perpendicular, one of which is stationary while the other can move backwards and forwards along the axis but information is only collected during forward movement. Between these mirrors is a beamsplitter, at which the light from an infrared source is divided into two beams. One of two beams travels to the fixed mirror and is reflected right back to the beamsplitter. The other beam is transmitted to moving mirror. After each beam has been returned along the same path they recombine at the beamsplitter under going interference. An interference is obtained when two or more wave motions meet to reinforce or oppose each other[45]. The two beams recombine when the fixed and moving mirrors are equidistant from the beamsplitter. This position is called zero path difference (ZPD) and the addition is completely constructive. This reconstructed beam then passes through the sample and is focused on the detector. To eliminate unwanted high wavenumber flux, a spectral filter is used.

To obtain the spectrum from interferogram the Fourier transform mathematical operation is applied[44]. This operation can be done in analog fashion by means of a wave analyser. Interferograms for monochromatic radiation and

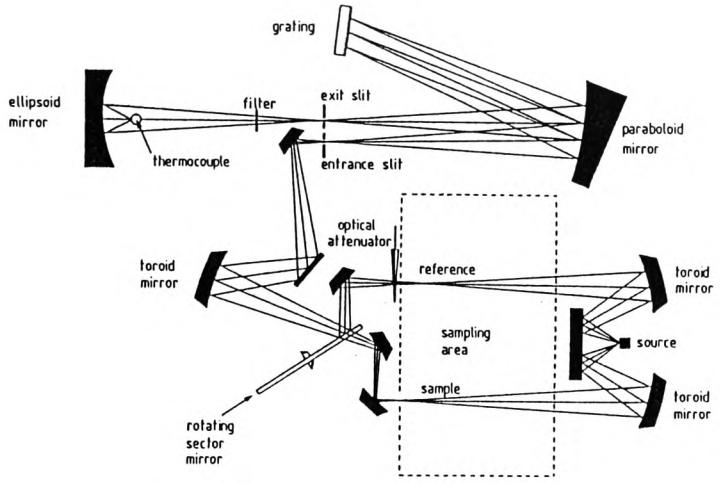

Fig.2.1A. A typical double beam infrared spectrometer[41].

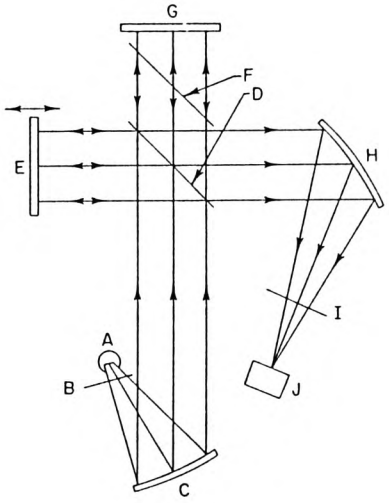

Fig.2.1B. Basic Michelson interferometer[44].

A: Source. **B:** Chopper. **C:** Collimator. **D:** Beamsplitter. **E:** Movable mirror. **F:** Compensator. **G:** Fixed mirror. **H:** Focusing mirror. **I:** Spectral filters. **J:** Detector.

white light are shown in fig.2.2. These represent the variation of intensity falling on the detector as a function of the optical path difference between the two beams. If $I(\delta)$ is the intensity of the detector signal at displacement δ and $I(\tilde{\nu})$ is the intensity of the source at wavenumber $\tilde{\nu}$ then the interferogram from a monochromatic source is given by the equation

$$I(\delta) = I(\tilde{\nu}) \cos (2\pi\delta\tilde{\nu}) \quad \ldots\ldots \quad (1)$$

For polychromatic source consisting of n frequencies of radiation the measured interferogram is the sum of n such

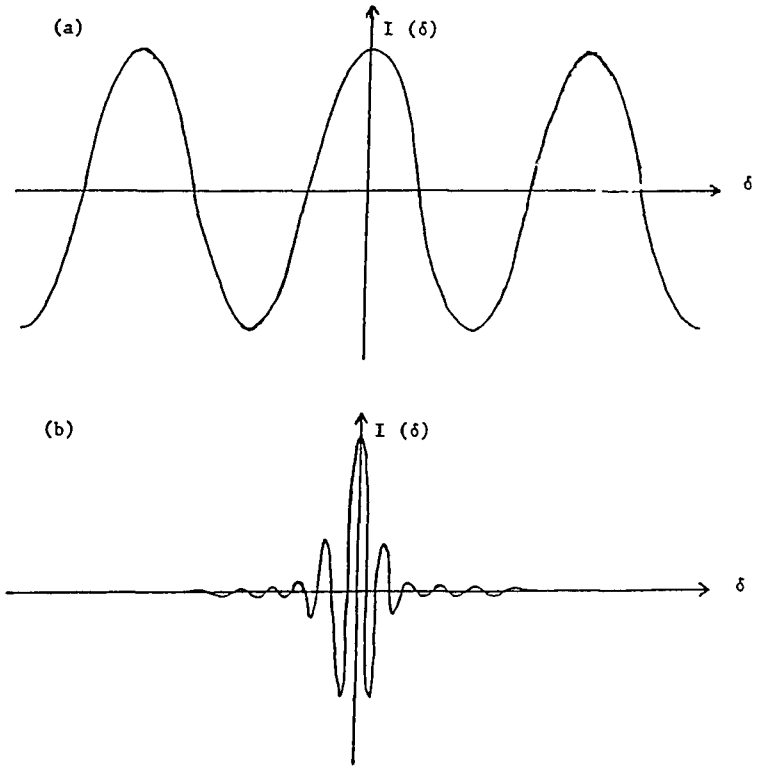

Fig.2.2. Interferograms for (a) monochromatic radiation (b) white light[49].

equations. When the source is a continuum, the interferogram is the integral of the contributions from all wave numbers in the spectrum, i.e.

$$I(\delta) = \int_{-\infty}^{+\infty} I(\tilde{\nu}) \, \mathrm{Cos} \, (2\pi\delta\tilde{\nu}) \, d\tilde{\nu} \quad \ldots\ldots \quad (2)$$

For either of the above cases, the spectrum can be calculated by computing the cosine Fourier transform as in the following equation,

$$I(\tilde{\nu}) = \int_{-\infty}^{+\infty} I(\delta) \, \mathrm{Cos} \, (2\pi\tilde{\nu}\delta) \, d\delta \quad \ldots\ldots \quad (3)$$

In order to achieve this, the moving mirror of the interferometer would have to scan an infinitely long distance. In practice, the mirror movement is truncated[49].

2.3. Comparison of interferometer vs dispersive spectrometer.

2.3.1. Advantages

An interferometer or Fourier transform spectrometer offers certain inherent advantages compared with conventional dispersive spectroscopy. The three main theoretical advantages are :

(1). Multiplex advantage[46] (Felgett's advantage)

Dispersive spectrometers only provide information about the narrow wavenumber region which falls within the exit slit of the monochromator at any given time. Accordingly, the

whole spectrum is built up gradually. This will often take a few minutes. In a FT-IR instrument an interferometer gives information from all frequencies in the spectrum and so it scans all wavelengths simultaneously. Scans (4000 - 600 cm^{-1}) can be complete in < 1 ms and are routinely complete in 1 s.

(2). Throughput advantage[47] (Jacquinot's advantage)

This advantage represents the fact that on an FT-IR spectrometer the optical throughput of an interferometer is greater relative to that of a grating spectrometer at the same resolution. To achieve higher resolution using a dispersive instrument the slits must be reduced whereby a large proportion of the source intensity is lost. This reduces signal to noise. In a FT-IR spectrometer, high resolving power can be achieved by using large mirror displacement which can utilize their source output more efficiently and produce a satisfactory signal to noise ratio. This can be improved by the addition of a series of spectra collected from a number of scans.

(3). Conne's advantage[48]

A dispersive instrument has limited precision for frequency measurements and proper calibration must be carried out by recording the spectra of sample whose frequencies have been measured accurately. But an FT-IR instrument determines frequencies by direct comparison with a visible laser output (an internal laser whose frequency is known) which

measures the position of moving mirror. Thus, the system potentially offers an improvement in frequency accuracy.

(4). Additional advantages

There are several other advantages shared by FT-IR instruments over dispersive. These are

(a). The dispersive instruments have a fair number of moving parts. With time, these can lose their tolerance which requires recalibration. The only moving part in an FT-IR instrument is the moving mirror.

(b). Reduced stray light problems[49].

(c). FT-IR spectrometers enabled the examination of sample sizes down to a few micrometers[50] by coupling an optical microscope to a suitably adapted FT-IR spectrometer.

2.3.2. Disadvantages

Although it is simple in its design, the principal disadvantage of interferometry concerns the fact that digitization requires to transform the raw data of an interferogram into a spectrum[51]. To measure high resolution spectra the system must be made bigger[40]. Another disadvantage (particularly for a single beam technique) is that comparison of sample and reference spectra has always to be performed by computer subtraction[49]. For measuring infrared spectra at higher sensitivity double beam FT-IR spectrometers have recently become available[52].

2.4. Preparation of samples

A wide range of techniques are available for mounting the sample in the beam of the infrared spectrometer. These experimental techniques depend on whether the sample is a gas, a liquid, or a solid[53]. Samples that are liquid at room temperature are usually scanned in their neat form or in solution. In the case of solution spectra solute-solvent interactions must not be overlooked. As far as possible a inert solvent should be selected. Commonly, carbon tetrachloride is used as a solvent in infrared spectroscopy, but even this solvent may contribute to some hydrogen-bonding[54].

2.4.1. Preparation of solution samples

Pure, dry HPLC grade CCl_4 was used as solvent to make different concentrated solutions of alcohol-acetone and in the propionic acid experiments. Since CCl_4 is a volatile substance, for quantitative work ethanol-acetone and cyclohexanol-acetone solutions were prepared by weight and special care was taken to transfer solutions into the cell so that the evaporation of the solvent does not vitate the accuracy of the measurements. Non-quantitative studies using the propionic acid allowed solutions to be prepared by volume.

2.4.2. Preparation of gas samples

In the study of gas phase spectra by infrared spectroscopy, a vacuum gas handling system is required for the preparation of samples. In the present study a movable vacuum line was used. A schematic diagram is shown in fig.2.3. This was equipped with a rotary pump, mercury diffusion pump, pirani gauge, penning gauge and pressure indicator. The main evacuation line consisted of large bore tubing for effective pumping. The rotary pump was mainly used to evacuate the air or gases by closing tap A and opening tap B (attached pyrex tube) and by this means a nominal pressure of 0.1 torr could be maintained. The pressure indicator was used to measure the pressure of gases introduced into the vacuum line. Before analysis, the whole system was evacuated. The sample was then introduced into the gas line through the gas inlet pipe and then allowed to flow into the gas cell which has previously evacuated. The minor constituent to the mixture was first added to the gas cell and isolated from the gas line. The previously evacuated manifold was then pressurised with the second gas and allowed into the gas cell.

Ethanol, acetone and acetic acid have sufficient vapour pressure for measurement of spectra in the vapour phase.

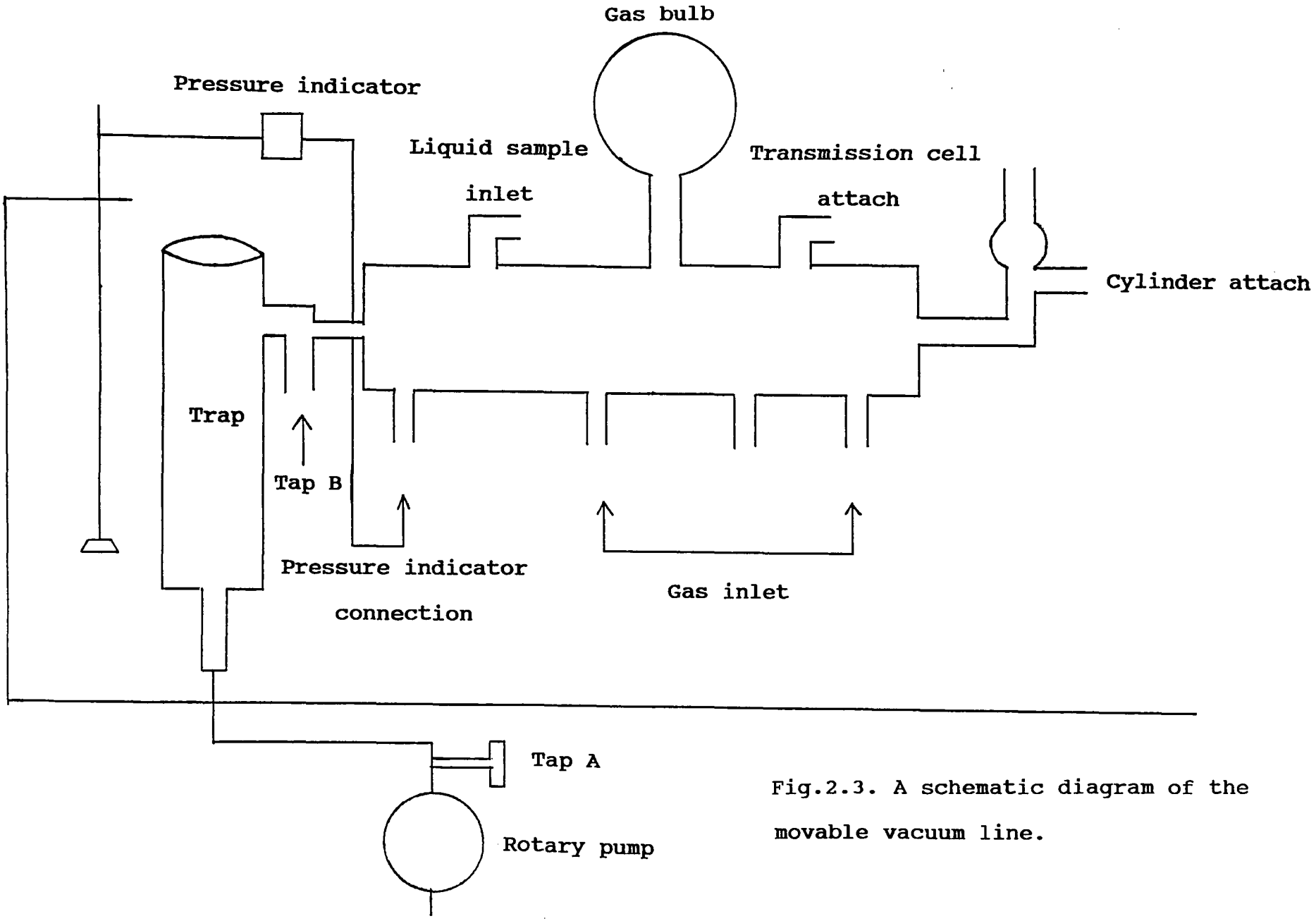

Fig.2.3. A schematic diagram of the movable vacuum line.

2.5. Infrared transmission cells

2.5.1. Liquid cells

A liquid sample must normally be contained in a cell for presentation to the spectrometer. A variety of such cells are now commercially available.

There are three types of cell in general use[53,55,57] : sealed (or permanent), demountable (or semipermable) and variable thickness cell. Since CCl_4 is a volatile solvent and the boiling point of ethanol and acetone is low, a enclosed cell of path length (1.0 mm) was used for recording the spectra at room temperature in the present study. An example of such a sealed precision path length cell is shown in fig.(2.4). The cell design incorporates inlet and outlet to make filling and cleaning fast and easy. For work with solutions of propionic acid a cell of 20 mm path length (fig.2.5) was used. These cells consist of a single piece of quartz into which a rectangular cavity has been bored. A conical hole above the cavity will accept a plastic stopper.

For quantitative measurements of alcohol-acetone complexes at various temperature, samples were examined in a variable temperature cell (fig.2.6) whose temperature can be increased gradually (up to +250^{o}C). A good thermal contact between the sample and the thermocouple conveniently heated the sample. The temperature regulation is maintained with a temperature controller (fig.2.7).

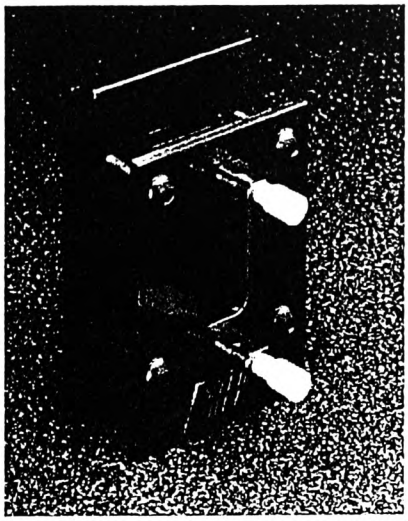

Fig. 2.4. A fixed path length sealed cell.

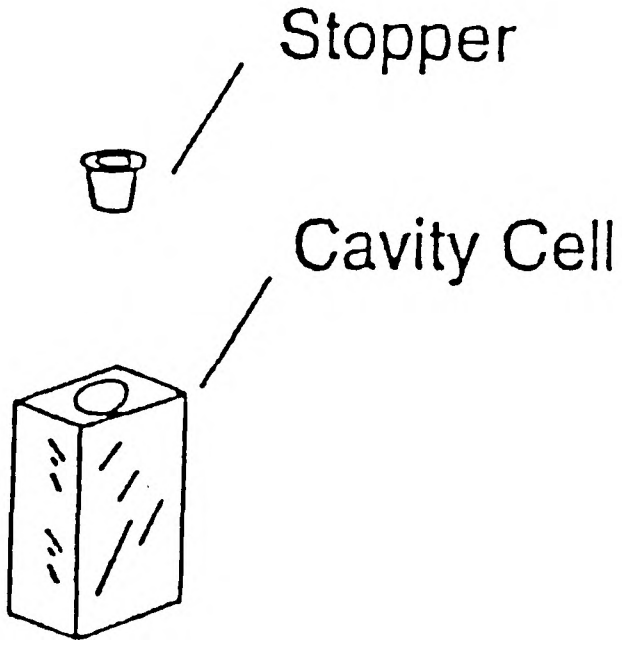

Fig.2.5. A 20 mm liquid cell.

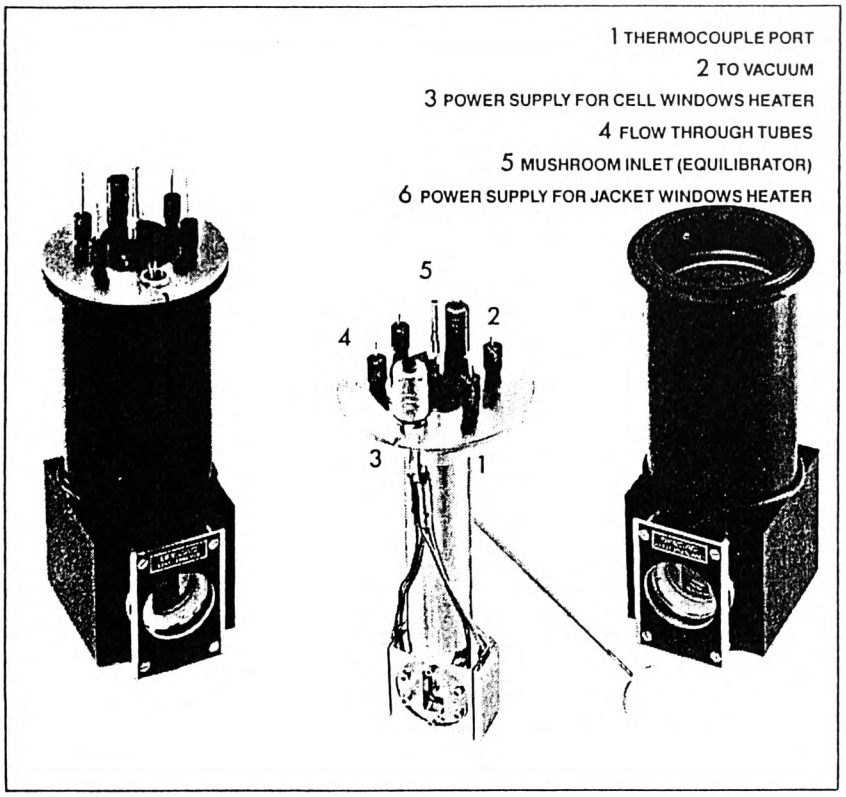

Fig.2.6. A temperature variable liquid cell.

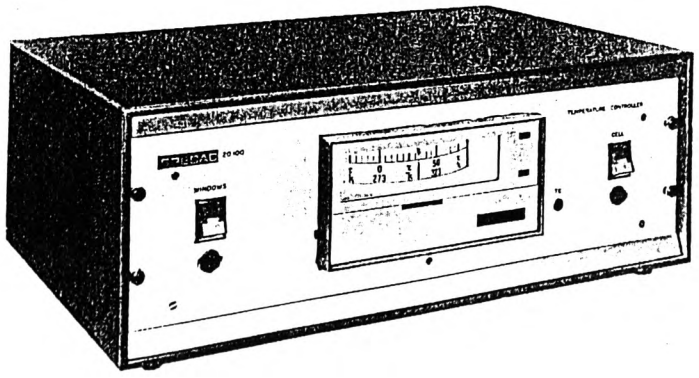

Fig.2.7. A temperature controller.

2.5.2. Gas cells

The spectrum of a substance in the gaseous state corresponds to the free molecules[56]. There are less absorbing molecules in a given volume of gas than in a condensed phase, hence path lengths must be correspondingly greater[57]. Design parameters for gas cell for infrared spectrophotometry vary depending on whether very low concentrations or very high concentrations of samples have to be measured. A Wilkes 20 metre variable path length gas cell was used to accomplish analyses of low concentration of gas in the present study. The cell consists with a folded (fig.2.8) path design[55] in which the entering beam is reflected back and forth several times through the same volume of sample before leaving the cell. This allowed an optical path length many times longer than the physical length of the cell. In many of these cells the optical path length can be varied by changing the angle of an internal pair of mirrors in discrete steps. This is adjusted by an externally located dial on the end of the cell in the range 0.75 metres to 20.25 metres in increments of 1.5 metres. The total volume of the cell is about 5.4 litres. The outer body is constructed from of aluminium metal (fig. 2.9) and the interior of the cell body is Teflon plastic coated which reduce the surface adsorption effects. To provide protection against chemically reactive samples (and to improve infrared reflectivity) the internal optics are front surface gold coated. Transfer optics mirrors (outside the cell) are front surface aluminium coated.

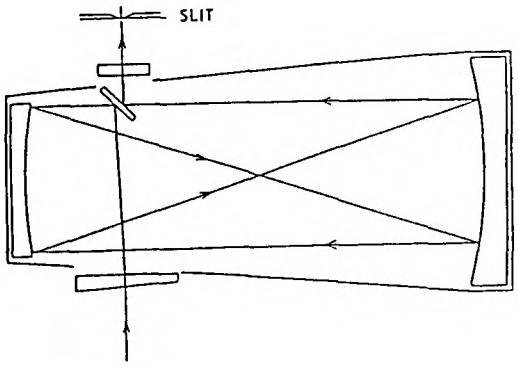

Fig.2.8. Optical path of a long path length gas cell[55].

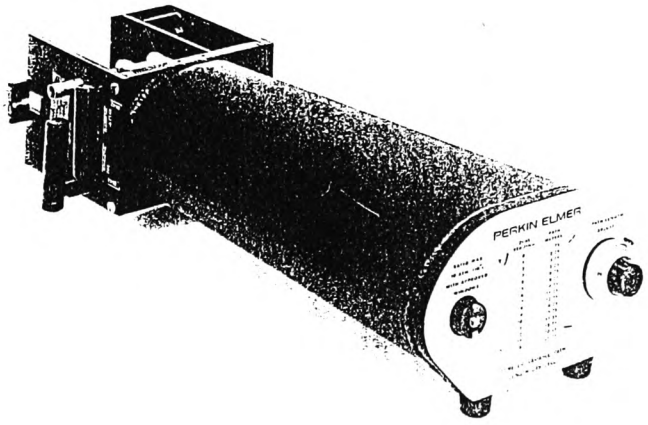

Fig.2.9. The twenty metre folded path gas cell for infrared spectroscopy.

This cell was used with the movable vacuum line and evacuated before introduction of the gas sample into the cell. The evacuated cell was used to record the background spectra in the Perkin Elmer FT-IR spectrometer. Each change in path length required that a new background spectrum (= evacuated cell) be taken.

2.6. Factor affecting the quality of a spectrum : Resolution

In modern infrared spectrometers there are many interrelated parameters which determine the quality of a spectrum. Some of these parameters are[58] resolution, signal to noise ratio, accuracy of absorbance measurements and speed of scan.

In dispersive instruments resolution is limited by the maximum slit width of the monochromator. High resolution is associated with small spectral slit widths[55,58]. In FT-IR instruments, a moving mirror controls the resolution. The further the moving mirror travels in the interferometer the higher the resolution.

Resolution may be regarded as the ability of an instrument to separate neighbouring bands in a spectrum. Unless the resolution of the instrument is less than the 'natural width' of a particular band it is found that the recorded absorbance will be less than the true absorbance[55]. Thus the observed appearance of a band which has a narrow 'natural width' is particularly dependent upon the

resolution. To demonstrate this, an experiment was carried out using 1% acetone solution in CCl_4. The spectrum of the $\nu_{C=O}$ band (1760 cm^{-1}) at various resolution is shown in fig.2.10. The apparent widths of the $\nu_{C=O}$ band at low resolutions (16, 8, 4, cm^{-1}) are large and the peak height is correspondingly small. As the resolution increases, the absorbance increases. The spectra suggest that a resolution of 2 cm^{-1} fully resolves the true band shape of the carbonyl absorption. Alpert et al.[55] carried out a similar experiment using two bands of cyclohexanol.

By way of comparison, the Doppler widths of the rotational vibrational lines of molecules in the gas phase may be as narrow as 0.001 cm^{-1} and may only be resolved using the most expensive FT-IR spectrometers currently available.

2.7. A simple theoretical treatment of infrared absorption

In the case of vibrational spectroscopy the dipolar changes within molecules are the basis of molecular vibrations leading to absorption in the infrared region[58].

A heteropolar diatomic molecule (A-B) gives rise to a single fundamental absorption band in the infrared region at a particular wavenumber which is characteristic of that molecule. By contrast, homopolar diatomic molecules (A-A, and for which there is no change of dipole moment during the vibration) do not absorb infrared radiation. This model may be developed further as follows:

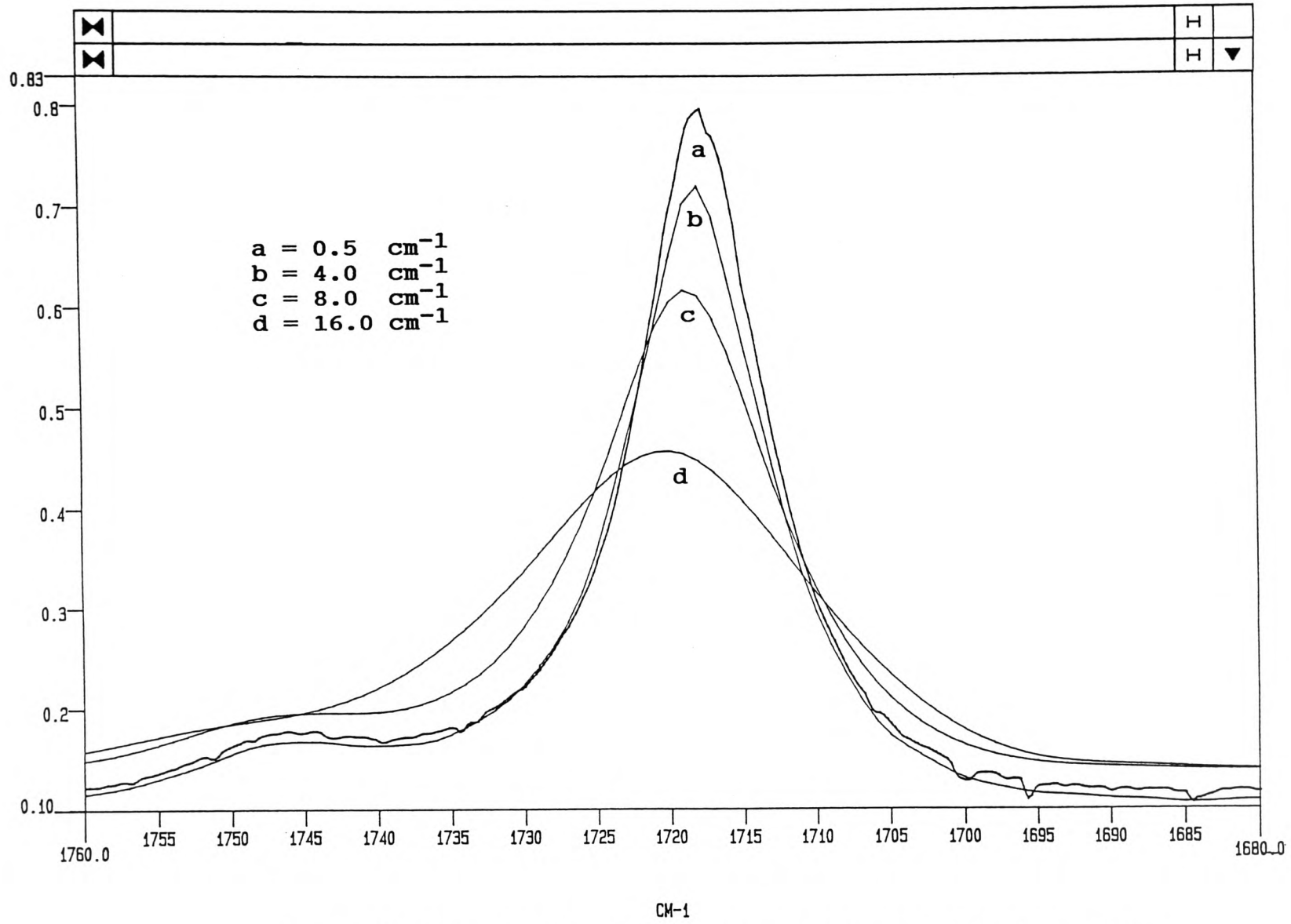

Fig.2.10. The carbonyl band of 1% acetone solution (in CCl_4) at various spectrometer resolutions.

Diatomic molecules may be considered as a model of two masses m_1 and m_2 joined by a bond which has spring like properties and maintains the two atoms at some equilibrium separation. The stiffness of the bond can be characterised by a force constant f, which is applied for the displacement in accordance with Hookes law. This law states that if the particle is removed a distance x, from its equilibrium position, it experiences an opposing restoring force F which is proportional to its displacement from the equilibrium position r_e. For such behaviour we can write

$$F = - fx$$

For a diatomic molecule the displacement, x represents the displacement from their equilibrium position r_e, to some value r:

$$x = r - r_e$$

If the masses m_1 and m_2 are different they must attract the bonding electrons to different extents. Due to electro-negativity differences among atoms in the molecule A-B, the electric dipole moment is permanent. Fig.2.11 represents a classical model for the interaction of electromagnetic radiation with a changing electric dipole of a diatomic molecule. In this figure the dipole moment is shown by an electric vector p.

By combining Hookes law with Newton's second law of motion it can be shown that a small displacement for each masses relative to the other will undergo simple harmonic motion.

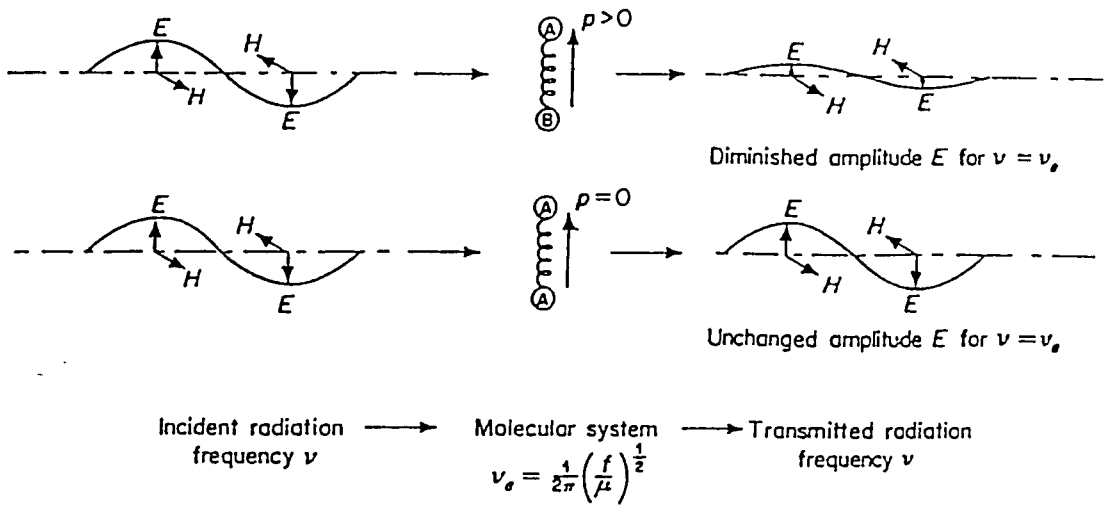

Fig.2.11. Classical model of the interaction of electromagnetic radiation with a diatomic molecule[58].

The system vibrates at equilibrium frequency, ν_e and is given by

$$\nu_e = \frac{1}{2\pi}\sqrt{\frac{f}{\mu}}$$

where μ is defined as " reduced mass " , such that

$$\frac{1}{\mu} = \frac{1}{m_1} + \frac{1}{m_2}$$

The coupling between the electrical vector of the incident radiation and the electrical dipole moment vectors causes the displacement of each of the masses relative to the other. When the frequency ν of radiation incident on the molecule (fig.2.11) is equal to ν_e, an interaction can take place between the incident radiation vector, E, and

the dipole moment p. This induces the molecule A-B to vibrate. As a result an absorption band at the corresponding frequency ν_e will appear in the spectrum. In case of a homonuclear diatomic molecule with no permanent dipole moment (A-A in fig.2.11) no electrical coupling can take place by this mechanism in the infrared region.

Molecules in the gaseous state show vibration bands with fine structure which arises from rotational-vibrational interactions. Molecules in the condensed state do not normally show rotational structure.

In the case of a non linear polyatomic molecule with N atoms there will be 3N - 6 vibrations. If we consider the spectra of a carboxylic acid in the monomer form many of these 3N - 6 vibration are skeletal vibrations which affect the whole molecule.

The mass effect of the hydrogen attached to heavier oxygen atom gives rise to a characteristic O-H stretching vibration. Also the existence of a double bond on the C=O group leads to a force constant for the group which is larger than that of the adjacent groups. This leads to a characteristic C=O stretching vibration. It is readily shown that the wavenumber value of these characteristic vibration is approximately given by the expressions:

$$\nu_{O-H} = \frac{1}{2\pi c}\sqrt{\frac{f_{O-H}}{\mu_{X-H}}}$$

$$\nu_{C=O} = \frac{1}{2\pi c}\sqrt{\frac{f_{C=O}}{\mu_{X=O}}}$$

Here μ_{X-H} and $\mu_{X=O}$ approximate to a reduced mass associated with the O-H and C=O groups and c is velocity of light.

In the case of the dimeric form of a carboxylic acid the structure has a center of symmetry[59] and the rule of mutual exclusion applies to the $3N_D - 6$ modes of vibration (where $N_D = 2N_M$). The rule of mutual exclusion states that the vibrations which preserve the centre of symmetry are Raman active but infrared inactive whereas the vibration which distort the centre of symmetry are infrared active but Raman inactive. Certain "silent vibrations" are inactive in both Raman and infrared. The infrared active vibrations of the O-H and C=O group in the dimer may be depicted as follows:

ν_{O-H}

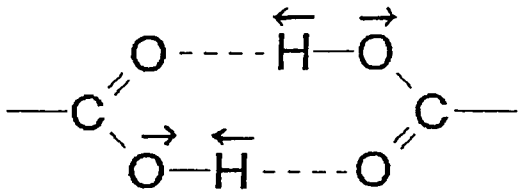

$\nu_{C=O}$

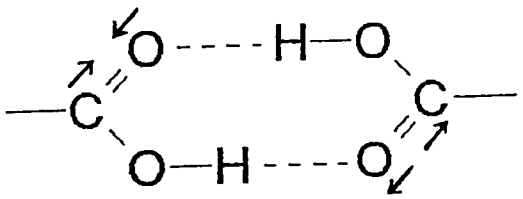

The difference in wavenumber values between symmetric modes which are Raman active and antisymmetric modes which are infrared active are fairly small.

CHAPTER THREE

SPECTROSCOPIC INVESTIGATION OF LIQUID AND GASEOUS HYDROGEN-BONDED COMPLEXES BY INFRARED SPECTROSCOPY

3. SPECTROSCOPIC INVESTIGATION OF LIQUID AND GASEOUS HYDROGEN-BONDED COMPLEXES BY INFRARED SPECTROSCOPY

3.1. Introduction

Infrared absorption spectroscopy is one of the most widely used methods in the investigation of hydrogen-bonded equilibria in solution[60-63]. Liddel and Becker[64] first described a method which used the intensities of IR bands to evaluate equilibrium constants of dimerization. Several other methods of evaluating equilibrium constants have also been reported. A graphical method has been reported by Geisler and Stockel[65]. Stepwise self association constants from infrared data have been calculated using a rigorous procedure developed by Vinogradov[66]. Concentration and temperature dependence of band intensity in the fundamental stretching region in the infrared absorption spectra have been used to obtain thermodynamic parameters of the specific hydrogen bond formation.

In this chapter infrared spectroscopy was used to obtain equilibrium constants for the complexation of alcohols with acetone. For the ethanol-acetone hydrogen-bonded complex, $\Delta H^{\ominus}$ and $\Delta S^{\ominus}$ were also calculated.

3.2. Equilibrium constants and bond energy

For the formation of a hydrogen bond between an acid HA and a base B ;

$$B + HA = B...HA$$

We can write,

$$\Delta H_f = - D_H (B...HA)$$

where D_H (B...HA) is the hydrogen bond dissociation energy of the complex at 298 K. The energy required to decompose the complex in its zero point vibrational energy into monomers in their zero point energy vibrational states, is defined as D_o (B...HA), deduced from spectroscopic data.

In case of gaseous complexes following the ideal gas law:

$$D_H (B...HA) = D_o (B...HA) + RT$$

hence, $\Delta H_f = - D_o (B...HA) - RT$

Recently, high resolution measurements of the intensity of the absorption bands of rotational transitions in microwave and infrared spectra have been directly used to obtain the bond dissociation energies of certain complexes. Such experiments have been limited to a few complexes including the prototype dimer[67] HCN...HF.

K_C may also be calculated by the knowledge of D_o, using the expression:

$$K_C = \frac{Q\ (A\text{-}H\ldots B)\ _{exp}\ (-\ D_o/\ RT)}{Q\ (A\text{-}H)\ Q\ (B)}$$

where Q represents the partition functions of each species, evaluated by substituting vibrational frequencies and rotational constants (B_o values) into standard expressions[30,68].

3.3 Previous determinations of equilibrium constant and ΔH for alcohol systems.

The infrared spectra of several sterically hindered alcohols were studied by Smith and Creitz[69] and equilibrium constants for H-bond formation in some of the lower alcohols were reported by Coggeshall and Saier[70]. Becker[71] obtained the equilibrium constants and enthalpies for the formation of 1:1 hydrogen-bonding complexes of alcohols with several donors in carbon tetrachloride solution by employing infrared spectroscopy. The $\Delta H^{\ominus}$ values for fifteen O-H...O complexes lie in the range 9.2-16.7 kJ mol^{-1}. Krueger and Mettee[72] used infrared spectroscopy to determine the equilibrium constants and $\Delta\nu_{OH}$ for the interaction of methanol with organic halides (RX) and aromatic hydrocarbons and questioned the usefulness of $\Delta\nu_{OH}$ as a measure of basicity of the donor. The increase in ν_{OH} shift determines the ionic character of the RX bond which would be expected to increase in the order R = C_6H_5 < $C_6H_5CH_2$ < n-Bu < t-Bu (for a given X atom). Dunken and Fritzsche[73-75] have determined the thermodynamic constants

of 1:1 complex formation for phenol with several donors. Quantitative hydrogen-bonding data between a number of aliphatic alcohols and benzophenone have been given by Singh et al[76] who found that K, $\Delta H^{\ominus}$ and $\Delta\nu_{OH}$ increase with the acidities of alcohols. Singh and Rao[77] have quantitatively studied the interaction of sterically hindered alcohols and phenols with various donors and found that enthalpies of formation of sterically hindered hydroxylic compounds are large and comparable with those of simple alcohols and phenols. $\Delta\nu_{OH}$ and $\Delta H^{\ominus}$ are not related in these sterically hindered systems. Hydrogen bond energies have been determined for the complexes formed between HBr, HCl and HI with acetone, dioxane and ether[78]. Pineau and Josien[79] have determined the enthalpy of 1:1 complex formation between butanol and a series of ketones. Hydrogen bonding between methanol and several donors has been studied by means of the first overtone of the O-H stretching vibration[80].

Many studies of hydrogen-bonded complexes in gaseous states have involved the binary halides complexes. Legon et al[81] have reported the spectra of gaseous complexes of HF with various alcohols and interpreted them in terms of the formation of hydrogen-bonded complexes ROH...HF. On the basis of the observed frequency shift ($\Delta\nu_{HF}$) of the H-F stretching vibration, the proton acceptor abilities of alcohols have been compared. Investigations of chlorosubstituted alcohols with hydrogen chloride in CCl_4 solutions have also been reported[82]. The infrared spectra of hydrogen

bonded complexes of HCl with CH_3OH, C_2H_5OH and $(CH_3)_2CHOH$ in the gas phase has also been reported[83] with the proton acceptor ability increasing along the series CH_3OH < C_2H_5OH < $(CH_3)_2CHOH$.

3.4 Determination of equilibrium constant for alcohol acetone hydrogen-bonded complexes in liquid and gas phase.

The infrared spectral characteristics of H-bonded alcohols in the fundamental OH stretching region were established over 58 years ago by Errera et al[84,85]. The OH stretching vibration of methanol, ethanol and t-butanol have been investigated[86]. The sharp band in the region of 3630 cm^{-1} is assigned to the OH stretching mode of the monomer. In the presence of a proton acceptor, a new broad band appears around 3300 - 3500 cm^{-1} region and this is considered as evidence for the formation of a complex. The intensity of free OH is related to the concentration of monomeric alcohol. The band at approximately 3500 cm^{-1} has been assigned[69,87] to dimers. Measurements of the relative intensities of such bands before and after the complex formation allow a determination of the complex formation constant.

When a hydrogen-bonded complex formed between an acid HA and a base B, the equilibrium is represented as follows :

$$A\text{-}H + B \underset{\text{dissociation}}{\overset{\text{association}}{\rightleftharpoons}} A\text{-}H\ldots B$$

In case of an alcohol-acetone association complex of the type R-OH...O=C$(CH_3)_2$, the equilibrium constant of the hydrogen-bonded complex

$$K_H = \frac{[\text{H-bonded complex}]}{[\text{R-OH}]\ [CH_3\text{-}\underset{\displaystyle CH_3}{\overset{\displaystyle |}{C}}\text{=O}]}$$

$$= \frac{C}{a_e \cdot a_{ce}} \qquad (1)$$

where C, a_e, a_{ce} are the equilibrium concentration of the hydrogen-bonded complex, alcohol and acetone respectively.

Alcohol dimerizes as

$$\text{R-OH} + \text{R-OH} = [\text{R-OH...OH-R}]$$

Then the dimerization equilibrium constant,

$$K_D = \frac{[\text{R-OH...OH-R}]}{[\text{R-OH}]^2}$$

$$= \frac{D}{a_e^2} \qquad (2)$$

If the initial concentration of alcohol and acetone are a_o and a_{co} respectively, then equilibrium complex concentration, C

$$C = a_o - a_e - 2D$$

$$= a_o - a_e - 2K_D\, a_e^2$$

and equilibrium acetone concentration,

$$\begin{aligned} a_{ce} &= a_{co} - C \\ &= a_{co} - (a_o - a_e - 2K_D\, a_e^2) \\ &= a_{co} - a_o + a_e + 2K_D\, a_e^2 \end{aligned}$$

From equation (1)

$$K_H = \frac{a_o - a_e - 2K_D\, a_e^2}{a_e\,(a_{co} - a_o + a_e + 2K_D\, a_e^2)} \qquad (3)$$

If alcohol dimerization is negligible, then equation (3) becomes

$$K_H = \frac{a_o - a_e}{a_e\,(a_{co} - a_o + a_e)}$$

$$= \frac{a_o - a_e}{a_e\,(a_{co} - (a_o - a_e))}$$

$\frac{o}{o}$ top and bottom by a_o gives,

$$K_H = \frac{1 - \frac{a_e}{a_o}}{\frac{a_e}{a_o}\,(a_{co} - (a_o - a_e))}$$

The term $(a_o - a_e)$ may also be expressed as

$$a_o\,(1 - \frac{a_e}{a_o})$$

Resubstituting,

$$K_H = \frac{(1 - \frac{a_e}{a_o})}{\frac{a_e}{a_o}\ (a_{co} - a_o\ (1 - \frac{a_e}{a_o}))} \qquad (4)$$

The value of this equation is that it contains only relative values of concentration, so that the calibration of absorbance values is unnecessary.

It is usually assumed that the standard enthalpy of formation $\Delta H^{\ominus}$ of the H-bond in a complex A-H...B and its standard entropy of formation $\Delta S^{\ominus}$ are independent of temperature. Then according to van't Hoff equation

$$\log K = - \frac{\Delta H^{\ominus}}{2.303\ RT} + \frac{\Delta S^{\ominus}}{2.303\ R} \qquad (5)$$

A plot of log K_C vs 1/T should therefore, give a straight line from which $\Delta H^{\ominus}$ can be calculated.

The entropy can be calculated from the intercept of the van't Hoff graph.

In the present calculation, K_p has been calculated for the $\Delta G^{\ominus}$ by using the equation

$$K_p = K_C / RT \qquad (6)$$

here T is the sample temperature.

3.5. Experiment

All of the samples of ethanol, acetone and carbon tetrachloride were commercially available. Absolute ethanol and spectroscopic grade acetone were used and kept over molecular sieves before use to eliminate traces of water. HPLC grade carbon tetrachloride was used as solvent and was checked for dryness before use. The concentration of ethanol was varied from 0.035 M to 0.056 M and acetone from 0.301 M to 0.498 M in order to prevent self association. The solutions were contained in a liquid sample cell of fixed path length 0.1 mm. K_C values at five different temperatures ranges from 26^{o}C to 42^{o}C were determined using a variable temperature liquid cell. The spectra were scanned 20 times at a resolution of 2.0 cm^{-1}.

3.6. Results and discussions

Fig.3.1 shows spectra of ethanol in CCl_4 at two different concentrations at room temperature. The bands near 3000 cm^{-1} are due essentially to the C-H stretching vibrations. The sharp band in the region of 3635 cm^{-1} is assigned to the OH stretching mode of the alcohol monomer. The intensity of this band is assumed to be proportional to the concentration of monomer. The broad band at lower frequencies around 3550 - 3050 cm^{-1} increases with increasing alcohol concentration and are assigned to OH stretching vibrations in H-bonded alcohol molecules. Fig.3.1b shows that the extent of self association decreases as the concentration of solution decreases from

0.2% to 0.05%. This is evidently the disappearance of the broad lower frequency band. The dilute solution reduces the formation of an appreciable number of alcohol-alcohol H-bonded species.

To study the H-bonding between ethanol and acetone, solutions were used with the alcohol concentration so low that self association was not significant. The acetone concentration used was at least five times higher than that of alcohol in order to favour the complex formation. Fig.3.2 shows a typical infrared spectrum of ethanol and acetone mixture in CCl_4. The sharp band at 3420 cm^{-1} is due to the first overtone of the carbonyl stretching vibration. The peak height of this band decreases when the concentration of acetone is lowered. The band at 3635 cm^{-1} is attributed to the free OH stretching of ethanol-acetone complex and the broad H-bonded complex band appear around 3523 cm^{-1} is essentially due to complexed ethanol-acetone molecules. All these assignments are supported by the variation of intensity with the concentration of acetone. These spectra show similar behaviour to that reported by Ying Sing Li et al[88] for 2-propanol-acetone complex and is consistent with their assignments. They used the infrared spectra of 2-propanol and acetone-propanol in CCl_4 solution to determine the equilibrium constant for the H-bonded complex.

Quantitative measurements of the intensity of the sharp OH band near 3635 cm^{-1} yielded values for the equilibrium

constants. This technique is possible because (as shown in fig.3.1b) the non-bonded OH stretch absorbs in this region and its band possesses sufficient intensity to be accurately measurable and yet is not submerged in the very broad band at 3550 - 3050 cm^{-1}. Equation (4) was used to computed K_C values. The calculated complex formation constants K_C at different concentrations of ethanol and acetone are listed in table 3.1 which shows that complex formation constant at 4 different concentrations of ethanol and acetone agree very well. The value 1.73 M^{-1} is excluded as an "outlier". The mean value of 1.23 $\pm$ 0.2 M^{-1} is comparable to the result (1.64 $\pm$ 0.18 M^{-1}) for the complex of n-butanol with methyl ethyl ketone[89], for the complex of 2-propanol-acetone[88] (3.34 $\pm$ 0.26 M^{-1}) and also for the complex of methanol-acetone[72] (1.60 M^{-1}).

$\Delta H^{\ominus}$ was obtained by measuring K_C at different temperature and is assumed to be primarily a measure of the hydrogen bond energy. The values of K_C for five different temperatures are listed in table 3.2. The increase in temperature decreases the number of H-bonds and essentially decreases the association equilibrium constant K_C. A van't Hoff plot of log K_C vs 1/T (using data in table 3.2) is presented in fig.3.3. The trend is linear and the hydrogen bond energy, $\Delta H^{\ominus}$, for the formation of ethanol-acetone complex was calculated from the slope of the straight line as -15.3 kJ mol^{-1} (correlation co-efficient 0.9909).

The significance of minus sign for $\Delta H^{\ominus}$ indicates that heat is liberated in the forward reaction, that is, the formation of the hydrogen bond is exothermic.

The extent of the forward reaction at equilibrium is measured by $\Delta G^{\ominus}$ as 7.88 kJ mol^{-1} by using equation

$$\Delta G = - RT \ln K_p$$

where R is molar gas constant, T is sample temperature ($26^{o}C$) and K_p is equilibrium constant in terms of partial pressure.

In the present study, $\Delta S^{\ominus}$ is -50.8 J mol^{-1} K^{-1}. The sign of $\Delta S^{\ominus}$ confirms a decrease in entropy or disorder upon complexation. Values of $\Delta S^{\ominus}$ and $\Delta H^{\ominus}$ for related system are given in table 3.3.

The frequency difference, $\Delta\nu_{OH}$, between the maxima of the monomer band and the complex was estimated to be about 146 cm^{-1}. The error involved in locating the complex maxima is at least $\pm$ 20 cm^{-1}. Table 3.3 lists values of $\Delta\nu_{OH}$ at $26^{o}C$. The bonded OH frequency shows a slight random shift when the temperature is increased 20^{o} C to 42^{o} C.

In conclusion, the information obtained in the literature[71] on the enthalpies, entropy and free energy values of H-bonded ethanol-acetone association is quite consistent with the present results. The main errors in the determination of K_C, $\Delta H^{\ominus}$ and $\Delta S^{\ominus}$ lie in the accurate determination of peak heights and in the maintenance and accurate measurement of solution temperature. In particular, the

determination of peak heights relies upon the absence of overlapping bands and upon the correct choice of baselines.

Table 3.1

Equilibrium constant for ethanol-acetone H-bonded complex at 293 K

Experiment	C_2H_5OH/M	$[(CH_3)_2C=O]$/M	K_c/M^{-1}
1	0.056	0.405	1.24
2	0.036	0.301	1.26
3	0.035	0.498	(1.73)
4	0.043	0.351	1.18
			av.1.23

Table 3.2

Data for van't Hoff plot

Temperature (^{o} K)	K_C/M^{-1}	log K_C	1/T
293.15	1.180	0.072	3.411×10^{-3}
299.15	1.036	0.015	3.342×10^{-3}
305.15	0.887	-0.051	3.277×10^{-3}
310.15	0.811	-0.090	3.224×10^{-3}
315.15	0.776	-0.110	3.173×10^{-3}

Table 3.3

Comparison of thermodynamic properties of various alcohols with acetone base

Alcohol	$-\Delta H$ kJ mol^{-1}	$-\Delta S$ J mol^{-1} K^{-1}	$\Delta \nu_{OH}$ cm^{-1}	Ref
Ethanol	15.3	50.8	146	This work
Ethanol	14.5	46.86	109	71
Methanol	10.55	30.55	112	71
t-Butanol	12.30	41.00	101	71

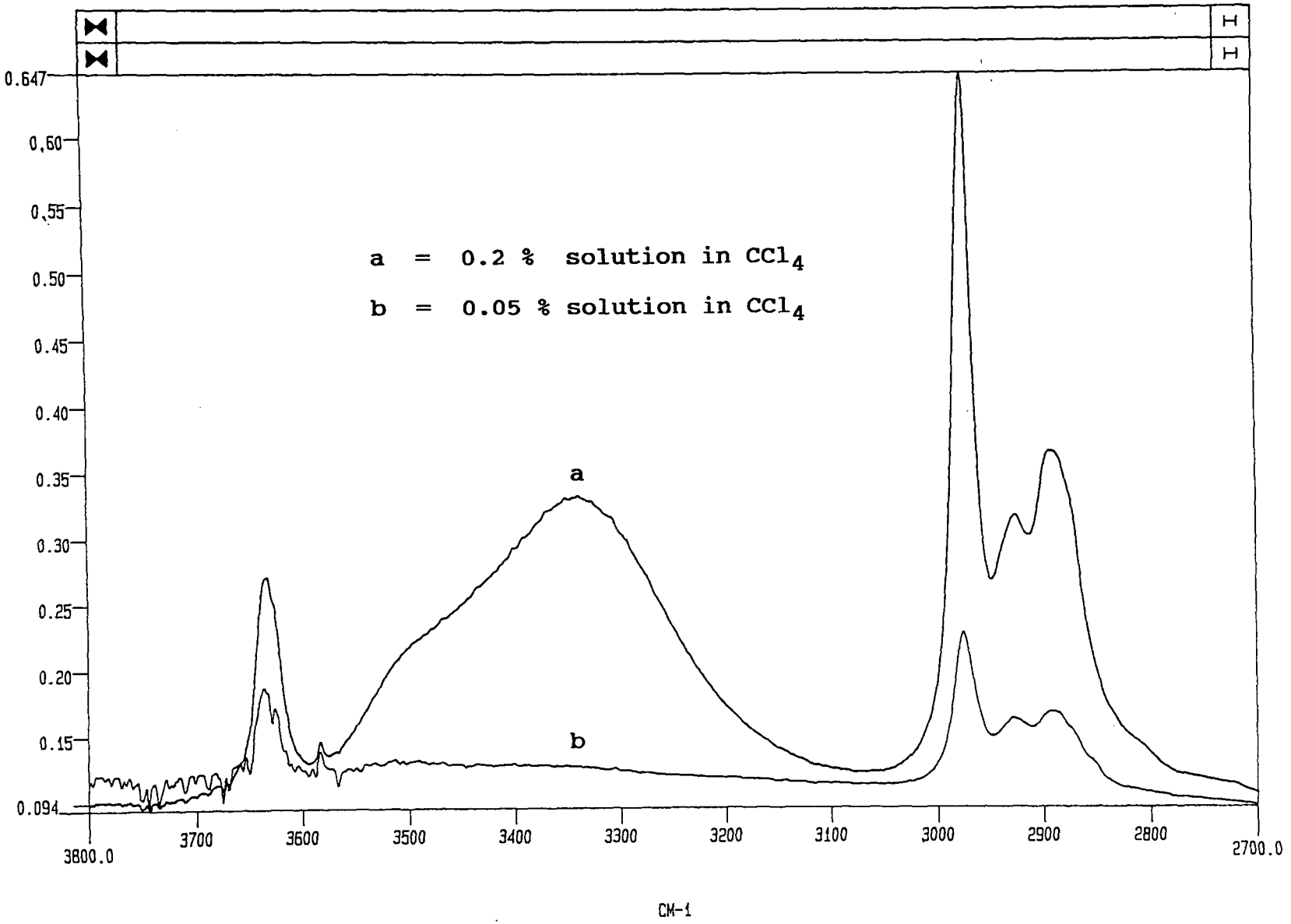

Fig.3.1. Infrared spectra of ethanol at resolution 2.0 cm^{-1}.

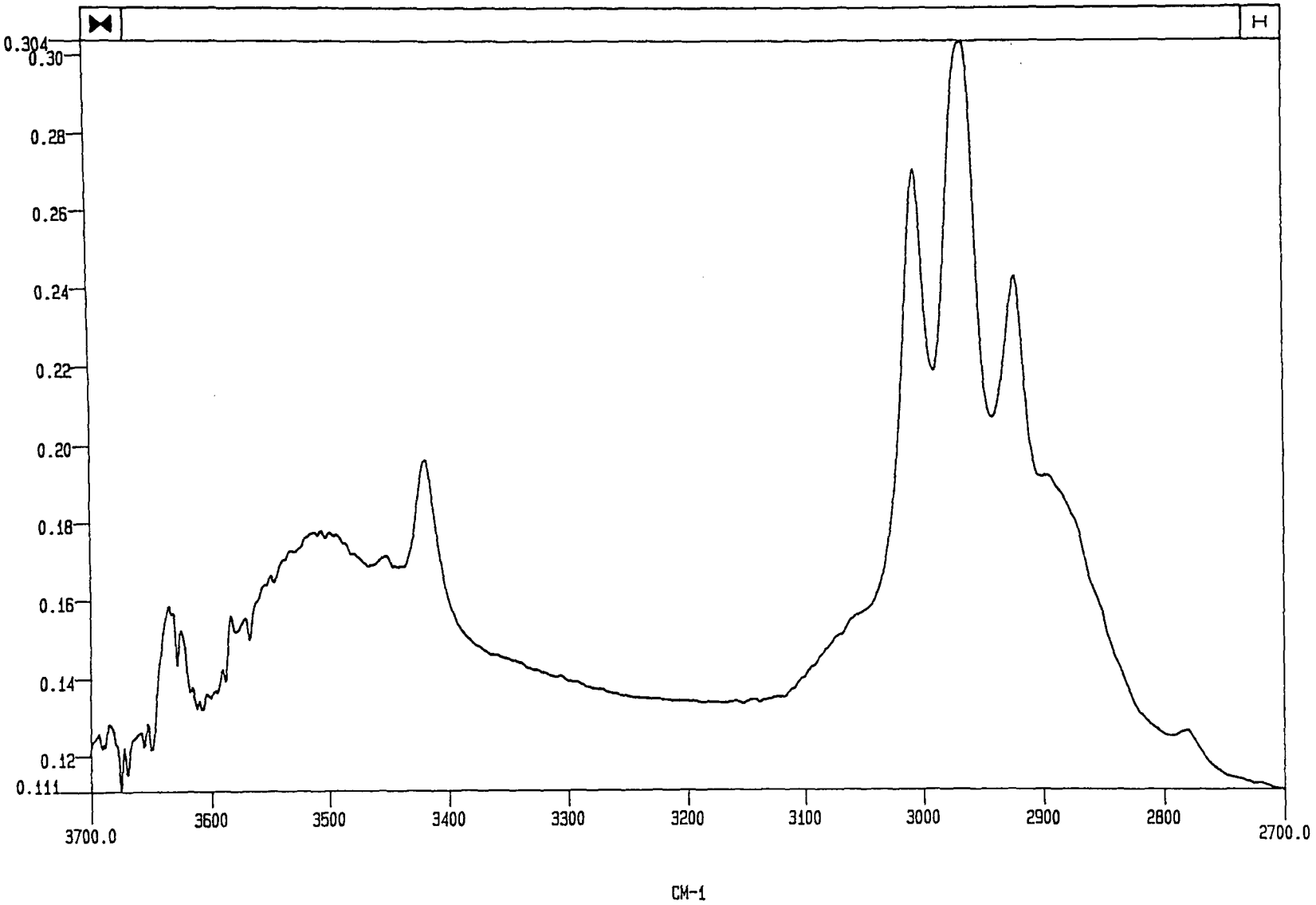

Fig.3.2. Infrared spectrum of ethanol-acetone H-bonded complex (0.3 % solution in CCl_4, resolution 2.0 cm^{-1}).

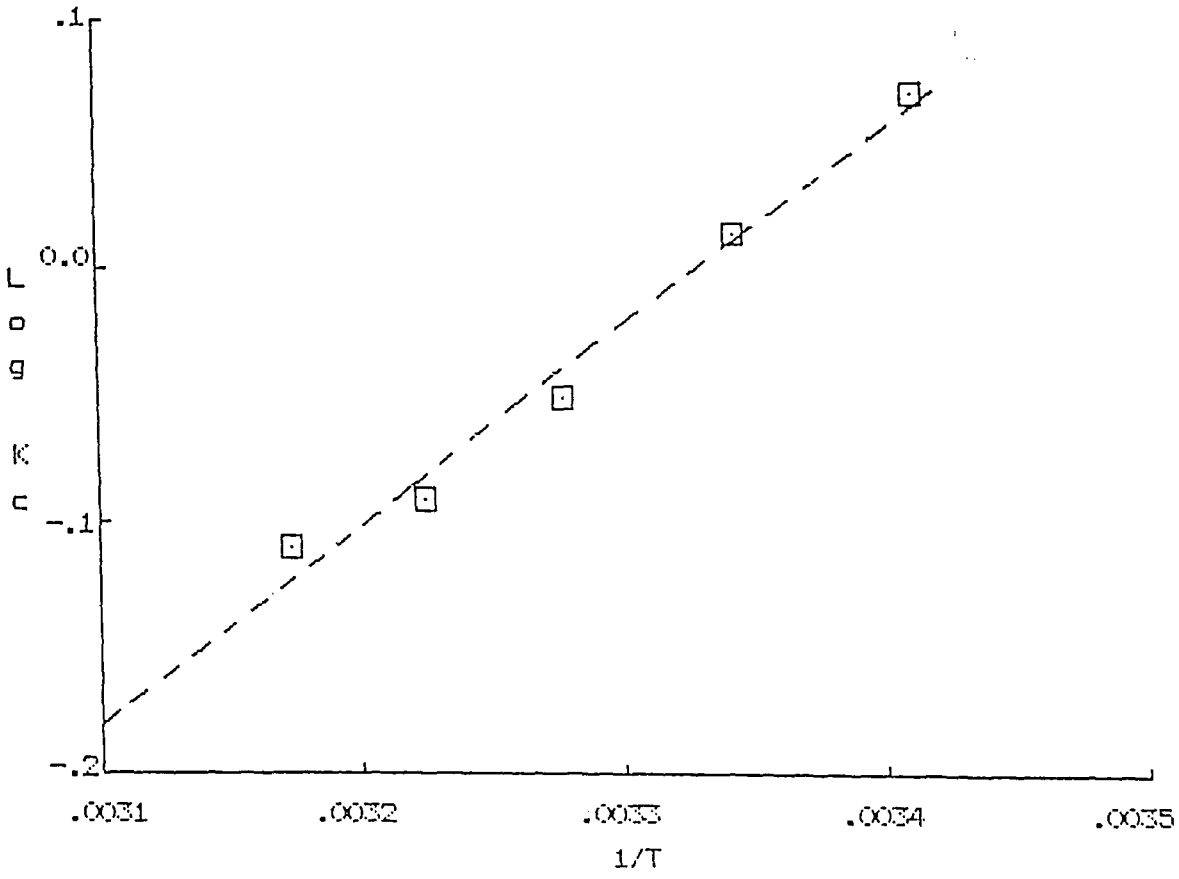

Fig.3.3. Van't Hoff plot for ethanol-acetone hydrogen-bonded complex.

3.7. Determination of equilibrium constant of cyclohexanol-acetone H-bonded complex in liquid phase.

The equilibrium constant K_C for cyclohexanol-acetone hydrogen bonded system was obtained using the method described in section 3.6. The result calculated at laboratory temperature is very similar (1.52 M^{-1}) to that obtained for the ethanol-acetone system (1.23 $\pm$ 0.2 M^{-1}). Studies were limited to determining K_C value due to the sensitivity of the spectra changes with temperature. When the spectra were recorded at higher temperature, the intensity of sharp ν_{OH} monomer band appeared as a doublet and therefore is not a true measure of free hydroxyl molecule. Quantitative thermodynamic data would, therefore, not be reliable.

3.8. Determination of equilibrium constant in gas phase for ethanol-acetone complex.

The thermodynamics of association of ethanol and acetone have been quantitatively investigated in liquid phase in section 3.6. Following these observations it was considered worth while to study quantitative aspects in gas phase. The studies in gas phase have advantages in the sense that we do not have to consider the solvent interactions[83]. The gaseous molecules are free from the interactions that characterise condensed phases and only energetic effects related to hydrogen-bonding are included[90]. Thus, the self association of ethanol is expected to be less important in the gas phase.

3.9. Experiment

The gas phase measurements were performed with a gas cell of path length 10 cm and fitted with gas inlet and outlet tubes for admission and evacuation of samples. A pressure gauge was attached to the vacuum line set up in order to measure the pressure of components. Measurements of pressures were judged to be accurate to ± 0.1 torr at room temperature. The partial pressures of the single component (ethanol) was kept low enough (typically 10 torr) to avoid self association of the alcohol. The partial pressures of acetone used was five times higher than the ethanol pressure in order to increase the probability for the formation of the $C_2H_5OH...O=C(CH_3)_2$ complex. The spectra were obtained by filling the gas cell with ethanol vapour, recording the spectrum and then added acetone vapour by opening a connecting tap, with subsequent recording of the spectra of the mixture which now contained the hydrogen bonded complex.

3.10. Results and discussions

It has already been mentioned in section 3.6 that in attempting quantitative measurements of hydrogen-bonded complex formation it is necessary to use a sufficiently dilute solution in order to preclude self association. Fig.3.4 shows the infrared spectra of ethanol in both solution and gas phase. It is evident that there is very little complexation of the ethanol in the vapour phase. The addition of acetone vapour to ethanol caused complexation

producing a broad association band in the range 3300-2700 cm^{-1} (fig.3.5) similar to the association band found in solution. Using the peak height of the free component ν_{OH} (3675 cm^{-1}) before and after the complex formation, an estimate of the equilibrium constant value was made. The calculation is similar to that used in solution. The two K_C values with concentration of ethanol and acetone vapour are listed in table 3.4 . The values which were determined for gas phase dimers in this experiment are much higher than those determined in solution (section 3.6) and were not reproducible.

In an effort to establish the factors which are likely to affect the reproducibility of these results an additional experiment was conducted to see if adsorption effects were important. Glass beads were added to a gas cell containing acetone only, and the pressure of vapour monitored against time with and without glass beads (fig.3.6 and 3.7). The plots suggests that adsorption effects are taking place and that these may compromise the reproducibility of results in the gas phase.

Another factor affecting the measurements of gaseous species using low resolution infrared spectroscopy has been reported by George, Lewis et al[91]. This effect termed spectral enhancement, involves the apparent increase in the absorbance of a band of a gas by a second (buffer) gas even if the buffer gas is optically transparent at the monitored wavelength. Applying this effect in present context, the peak height of the free ν_{OH} might be influenced by the

acetone molecules. Only if the free ν_{OH} is equally enhanced before and after the addition of acetone would spectral enhancement negligibly affect the determination of K_C.

Table 3.4

Equilibrium constants for ethanol-acetone H-bonded complex in vapour phase

Experiment	Ethanol (torr)	Acetone (torr)	K_C/M^{-1}
1	10	50	31.2
2	15	55	46.0

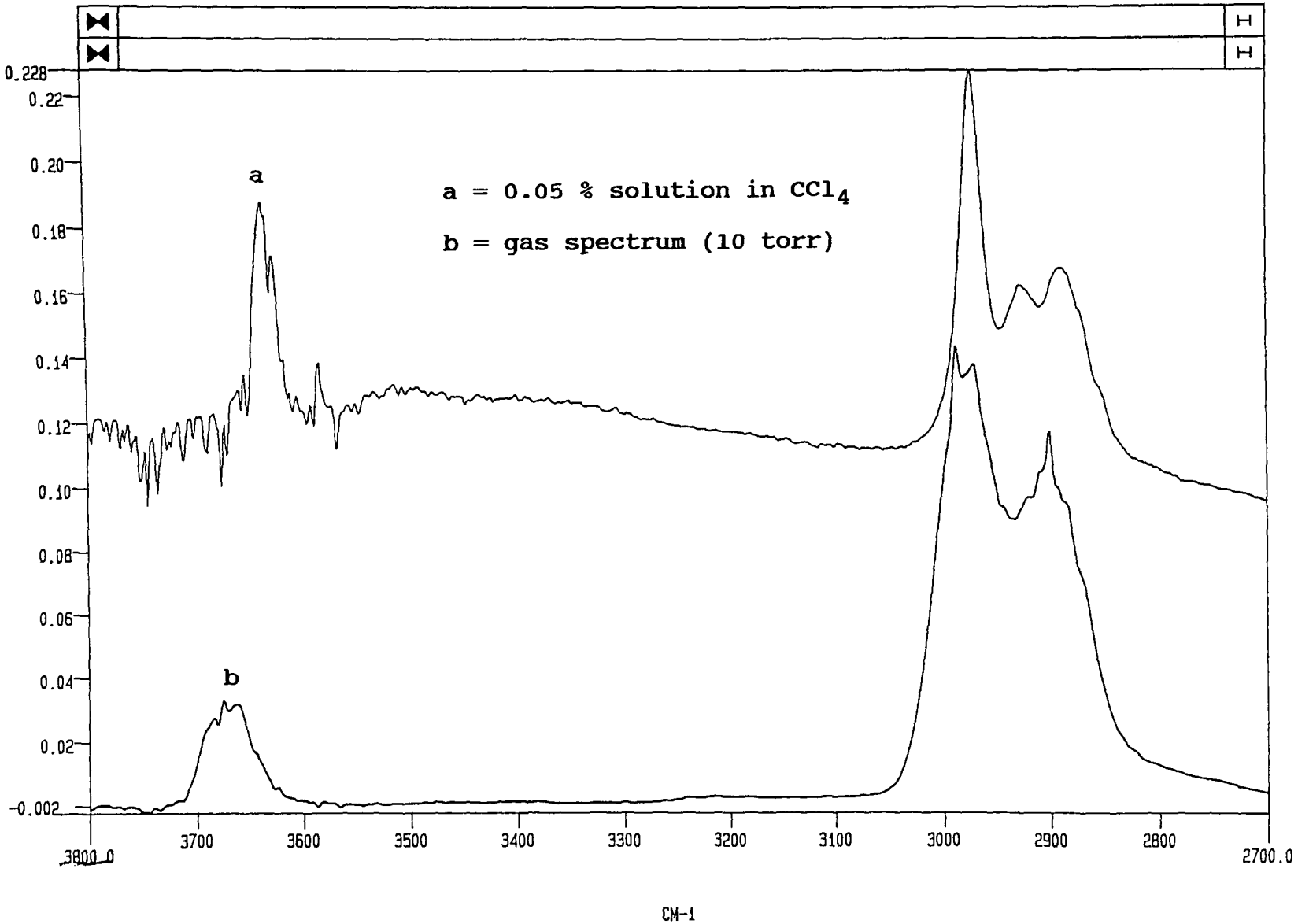

Fig. 3.4. Comparison of ethanol association in gas and liquid phases at 2.0 cm^{-1} resolution.

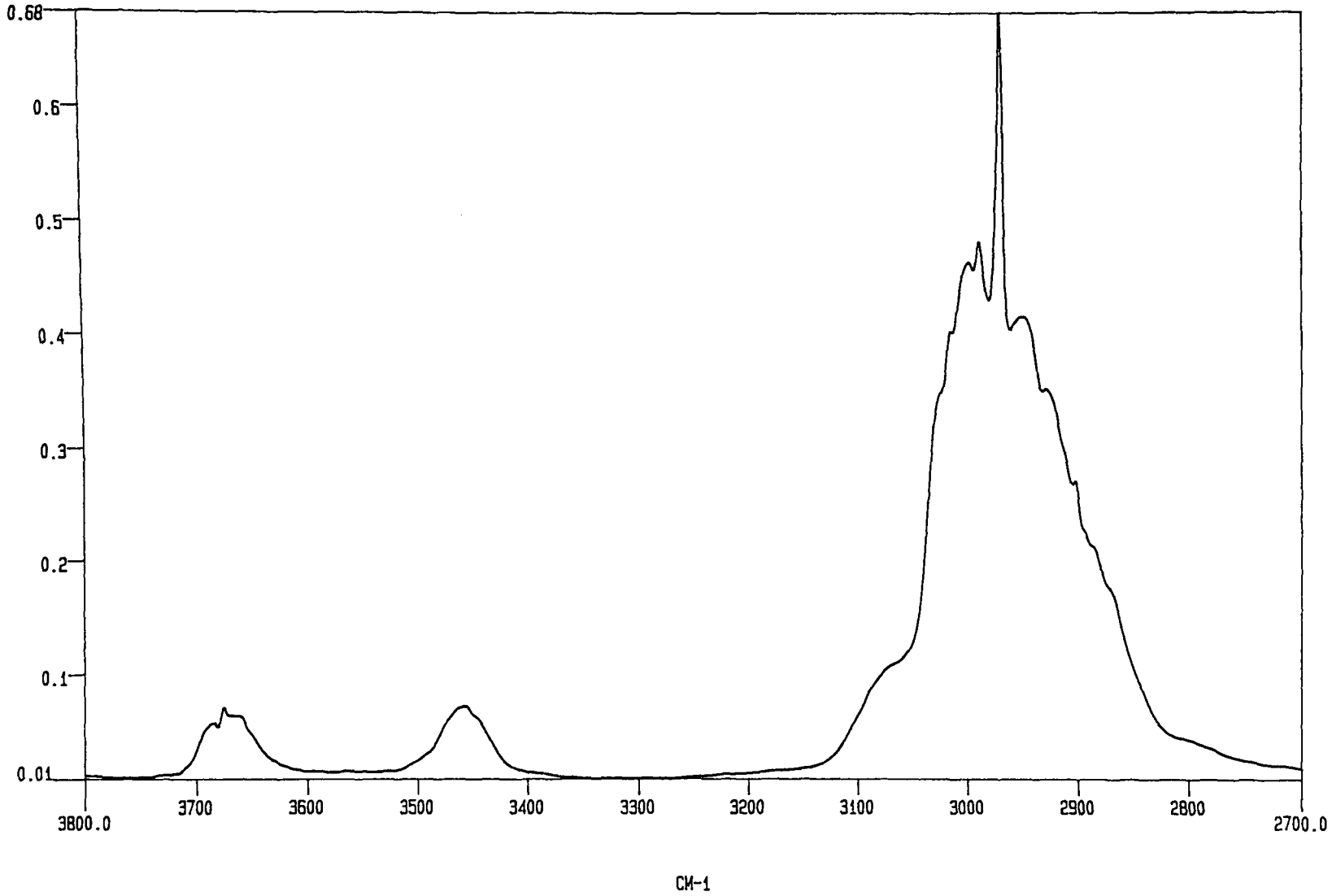

Fig.3.5. Infrared spectrum of ethanol-acetone H-bonded complex in vapour phase at resolution 2.0 cm^{-1} ($p_{ethanol}$ = 10 torr, $p_{acetone}$ = 50 torr, path length = 10 cm).

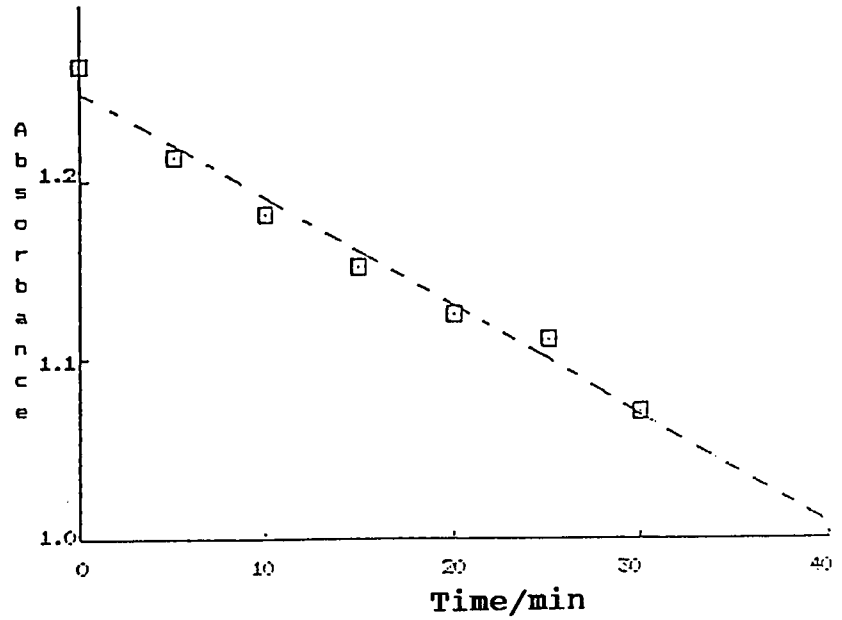

Fig.3.6. Apparent adsorption of acetone vapour with glass beads ($p_{acetone}$ = 20 torr, cell path length = 10 cm).

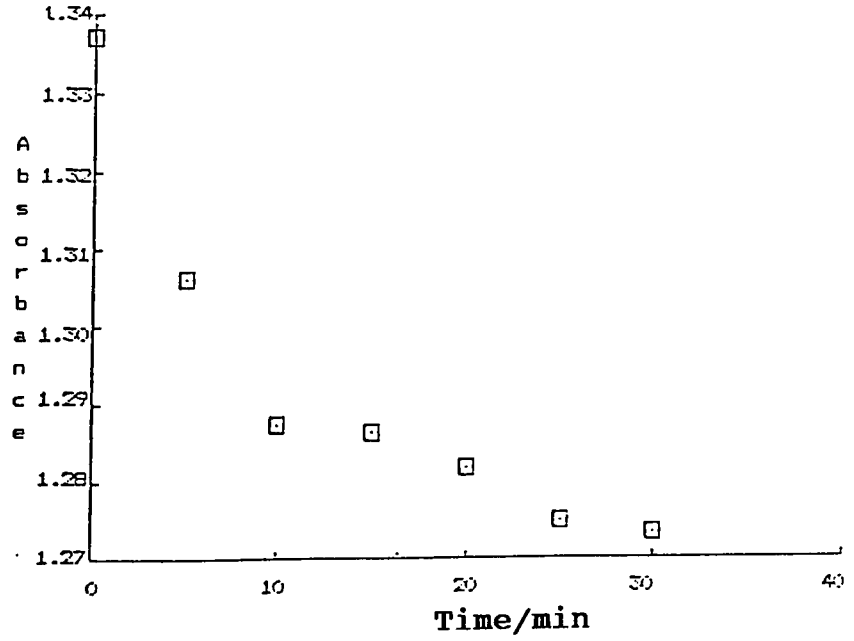

Fig.3.7. Apparent adsorption of acetone vapour without glass beads ($p_{acetone}$ = 20 torr, cell path length = 10 cm).

3.11. Studies of infrared spectra of propionic acid hydrogen-bonded system at different concentration in liquid phase.

In this experiment the concentration of propionic acid in CCl_4 was varied in order to determine the sensitivity of the spectrum to this variable. It is well known that carboxylic acids exist as dimers[92-94] due to strong intermolecular hydrogen-bonding in concentrated solution. The extent of the dimer form and the unbonded monomer form depends on the concentration of solution. In view of this importance observations were made over a range of concentration which extended down to infinite dilution. Particular attention was paid to the OH absorption band to study any intensity changes on lowering the concentration. Owing to the occurrence of a certain fraction of monomeric acid molecules in solution in CCl_4, the spectrum shows extra sharp and weak absorption bands corresponding to the ν_{OH} and $\nu_{C=O}$ vibrations of the single molecules[95,96].

3.12. Experiment

Spectra were measured with a Perkin Elmer Fourier transform infrared spectrometer. The solutions of propionic acid were made using HPLC grade carbon tetrachloride as solvent. Diluted solutions were prepared from 1%, v/v, acid solution using clean graduated pipettes by a factor of the ten each time. The concentration range was used from 1.0 - 0.00001%, v/v. All solutions were run in a longer "infrasil" quartz cell of (opaque below 2500 cm^{-1}) path length 20 mm with

scan limits 4000 - 3000 cm^{-1}. The spectra were improved by increasing the no. of scans to 64 at a resolution of 2.0 cm^{-1}. Bands due to carbon tetrachloride were subtracted from our samples spectrum in the region of interest. Spectra of pure propionic acid were also run to ensure that water bands were absent in the region of strongest water absorptions.

3.13. Results and discussions

The infrared spectra of pure propionic acid was recorded using a sodium chloride cell of path length 0.5 mm. The spectrum is shown in fig.3.8.

The most prominent feature in this spectra is the strong and broad band attributed to the COOH group in the region 3600 - 2500 cm^{-1} centred near 3000 cm^{-1}. This is caused by the stretching vibration of the ν_{OH} dimeric units[96,97]. The carbonyl stretching vibration of the dimeric units centred in the range 1720 - 1700 cm^{-1}. This peak is much more intense than that due to the ν_{OH} vibrations.

The concentration range used together with spectral changes are listed in table 3.5. The use of a longer path length cell permits observation of weak ν_{OH} monomer absorptions. Drastic spectral changes occurs in the region of ν_s near 3600 - 3500 cm^{-1} in going from lower to higher concentration. The narrow band at 3535 cm^{-1} due to the monomer O-H stretch dominates the lower frequency absorption in the dilute solutions. The characteristic

"association bands" were absent from the most dilute solution spectra. The monomeric ν_{OH} stretch was detected at solution concentrations greater than 0.0001%, v/v.

The intensity ν_{OH} is increased greatly in most concentrated solution (0.1%, v/v, fig.3.9). At high concentrated solution the broad band due to H-bonded dimer appears. Background spectra of carbon tetrachloride solution are subtracted from each of the solution spectra and thereby it is possible to obtain only acid spectra (fig.3.9).

Table - 3.5

Comparison of bands observed for propionic acid at dilute solutions (ν_{OH} monomer region only)

Concentration (% , v/v)	Path length mm	ν_{OH} ; 3800 - 3300 cm^{-1} region wavenumber
0.00001	20	monomeric species not present
0.0001	"	monomeric species not present
0.001	"	3537 ; monomeric free ν_{OH} stretch only , weak intensity
0.01	"	3535 ; monomeric free ν_{OH} stretch, sharp medium intensity
0.1	"	3535; monomeric free ν_{OH} stretch, sharp, increased intensity
1.0	"	3534; monomeric free ν_{OH} stretch, very sharp, intensity has greatly increased

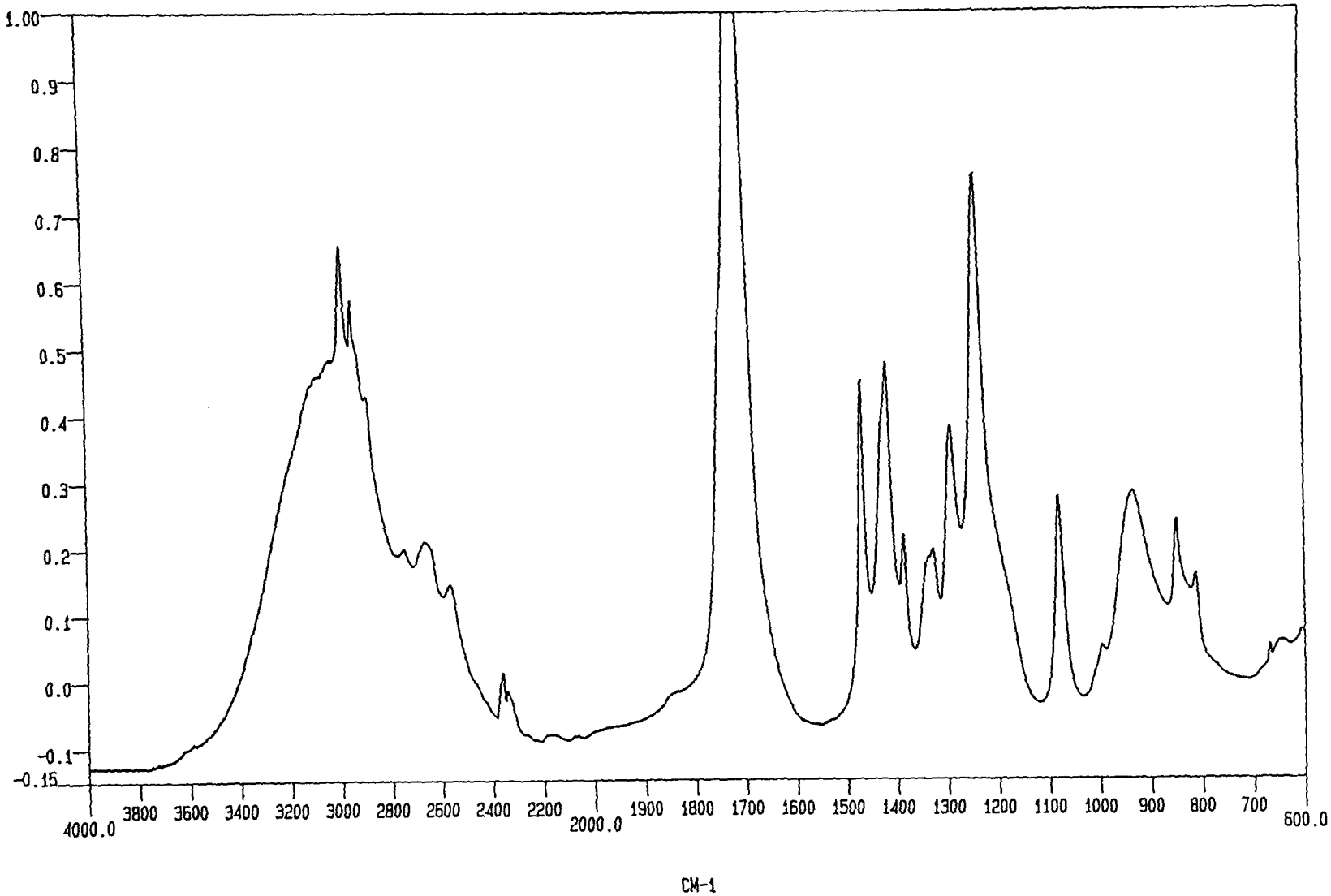

Fig.3.8. Infrared spectrum of pure propionic acid using sodium chloride cell of path length 0.5 mm.

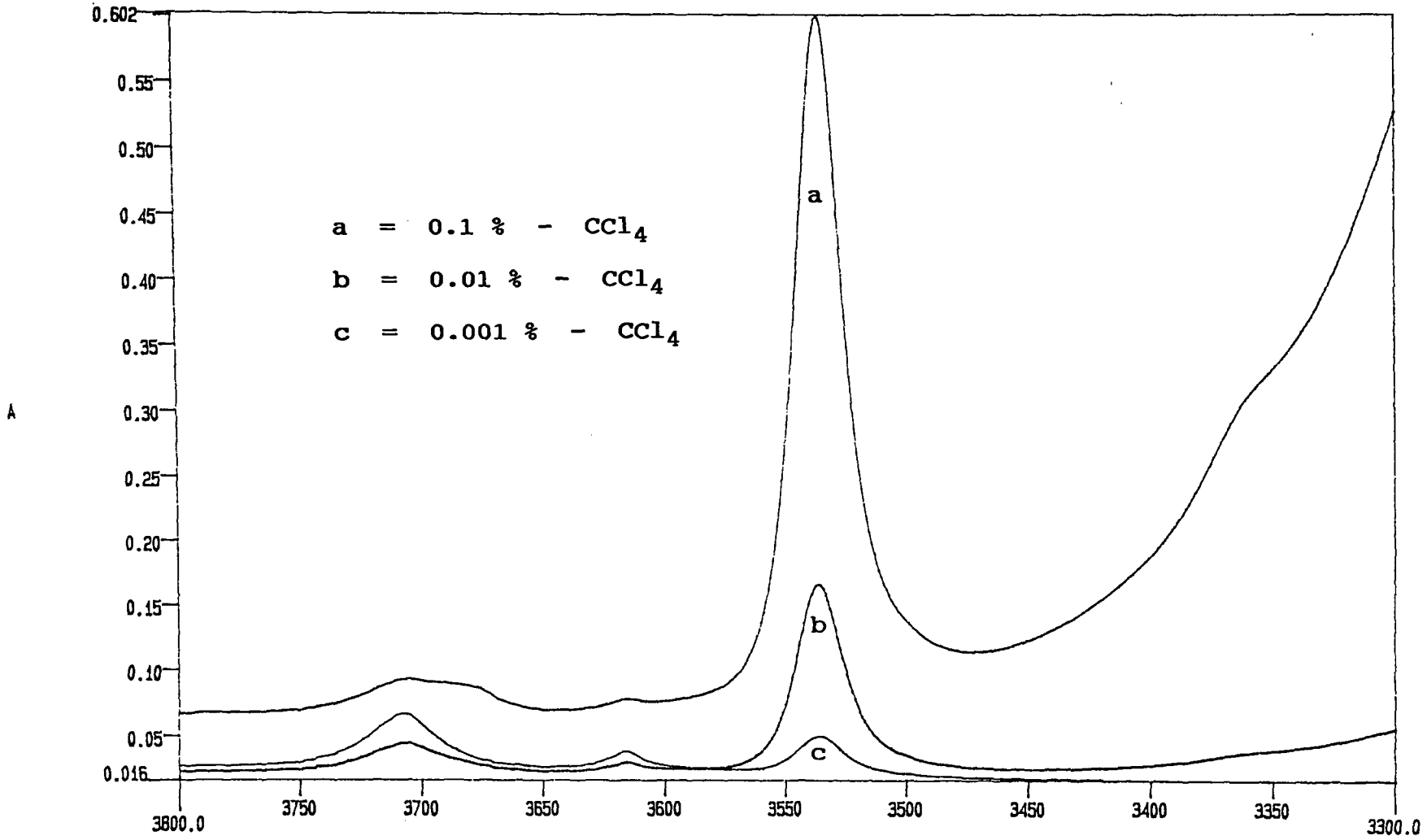

Fig.3.9. Infrared spectrum of propionic acid at different concentrated solutions (monomeric ν_{OH} stretch only, cell path length = 20 mm).

3.14. Investigation of the vapour phase association of acetic acid.

The present section reports infrared spectra of acetic acid vapour. At room temperature the vapour of acetic acid consists chiefly of 'double molecules' whose structure has been determined by electron diffraction study to be as follows[98-100]

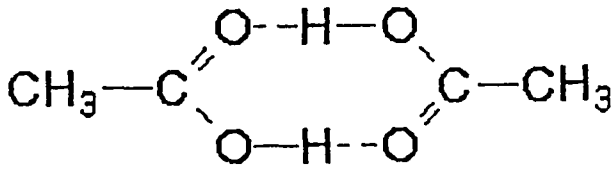

Both the monomer and dimer acetic acid infrared spectra has been reported[101-105].

3.15. Experiment

Spectra were recorded on Perkin Elmer Fourier Transform infrared spectrometer. The purity of acetic acid were confirmed by infrared spectra. Gas spectra were obtained at 10 cm path length cell averaged over 20 scans at resolution 0.5 cm^{-1}. A variable longer path length cell was required to record the spectra at low vapour pressures of acetic acid. The longer path length enabled measurements at low partial pressure of acetic acid, thus reducing self complexation. The chosen path lengths were 0.10 m to 2.25 m.

Spectra were obtained by mixing acetic acid with argon in the desired proportions.

3.16. Results and discussions

Values of the frequency measurement of the more prominent bands found in CH_3COOH vapour are tabulated in table 3.6. The complexity of all these spectra make impossible a complete assignment of bands at the present time. However, certain bands may be assigned with confidence using the work of Y.Marechal[106]. Such identification have been noted in the table 3.6.

Fig.3.10A shows the $\nu_{C=O}$ bands at three different path length cell and at different partial pressures of acetic acid. The second group of modes is shown in fig.3.10B. Fig.3.10C shows the high resolution spectra of ν_{OH} of acetic acid. Fig.3.10E shows ν_{OH} bands in acetic acid vapour at a longer path length (2.25 m). Fig.3.10D shows the ν_{OH} bands using a path length of 10 cm. On comparing the spectra obtained from different path lengths it is seen that the degree of hydrogen-bonding in acetic acid is concentration dependent. For the equilibrium between monomer and dimer, some of the acetic acid bands which can be attributed solely to the monomer or the dimer. The monomer and dimer spectra are quite different.

The monomer bands of $\nu_{C=O}$ appears at 1781 cm^{-1} and the dimer appears at 1734 cm^{-1} (fig.3.10A). The relative intensity of monomer and dimer falls as the pressure of acid

decreases. This confirms the identity of the bands. The band at 1296 cm^{-1} is for ν_{C-O} dimer and at 1183 cm^{-1} is for ν_{C-O} monomer (fig.3.10B). The bending O-H is observed at 948 cm^{-1} which vanishes at low pressure. The frequency at 3580 cm^{-1} is for monomer ν_{OH} band and the very broad band centres at 2980 cm^{-1} is for the dimeric ν_{OH} (fig. 3.10E and 3.10D). The ratio of dimer/monomer falls as pressure falls. The stretching vibration of ν_{OH} of acetic acid monomer is found at 3583 cm^{-1} in fig.3.10C and has a simple P, Q, and R branch[107,108] structure. The high frequency sharp peak diminishes in intensity at lower pressure.

Is it possible to obtain acetic acid vapour which is not appreciably dimerized ? Successively dilute acetic acid / Ar mixtures were prepared, correspondingly longer path length being used. Fig.3.10E shows the spectrum of 5 torr of acetic acid mixed with Argon (total p = 505 torr) at l = 2.25 m. It is seen that dimerization remains extensive. Extension of the experiment to further dilutions was limited by the low signal to noise ratio of the spectra under these conditions.

To provide additional information for interpreting the acetic acid spectra an experiment was devised in an attempt to demonstrate the formation of hydrogen bonds between unlike molecules. In this case ethanol vapour was added to acetic acid vapour at room temperature in a 10 cm path length gas cell. The spectra of vapour of ethanol (fig. 3.11a), of acetic acid (fig.3.11b) and of the two together

(fig.3.11c) were compared. On the addition of ethanol vapour there are no significant changes in the spectra (fig.3.11c). Only a slight broadness appears around 3500 - 3000 cm^{-1} and there is no evidence of a C=O absorption due to the complex in the 1700 cm^{-1} region (fig.3.12). It may be concluded that very little acid-alcohol complexation takes place.

In summary there is no evidence for the formation of an intermolecular bond between acetic acid and ethanol. Presumably, the acid dimer (with two hydrogen bonds) is preferred to the acid-alcohol dimer (one hydrogen bond).

Table - 3.6

Assignments of bands observed in acetic acid vapour

pCH_3CO_2H torr	Path length cm	Bands cm^{-1}	Assignment	Y.Marechal[104]
10	10	3583	ν_{OH} monomer	3583
		3050	ν_{OH} dimer	2965
		1781	$\nu_{C=O}$ monomer	1781
		1734	$\nu_{C=O}$ dimer	1734
		1296	ν_{C-O} dimer	1290
		1183	ν_{C-O} monomer	1178
		948	OH bend (dimer)	942
0.5	75	1781	$\nu_{C=O}$ monomer	
		1734	$\nu_{C=O}$ dimer	
		1294	ν_{C-O} dimer	
		1183	ν_{C-O} monomer	
		948	OH bend (dimer)	
0.05	225	3580	ν_{OH} monomer	
		2980	ν_{OH} dimer	
		1781	$\nu_{C=O}$ monomer	
		1732	$\nu_{C=O}$ dimer	
		1293	ν_{C-O} dimer	
		1184	ν_{C-O} monomer	
		991	OH bend (dimer)	

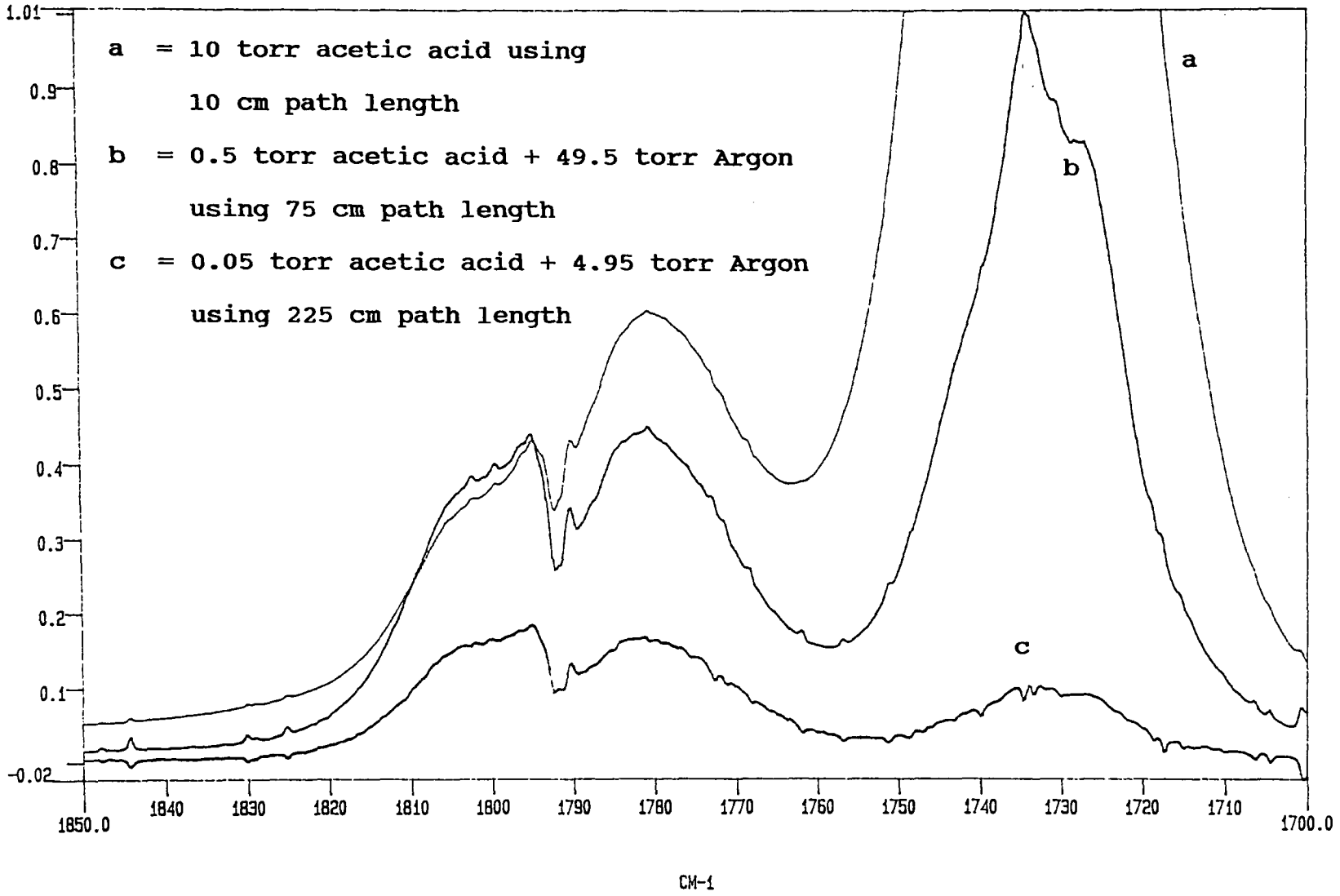

Fig.3.10A. Infrared spectra (carbonyl band region) of acetic acid at laboratory temperature [resolution 0.5 cm^{-1}].

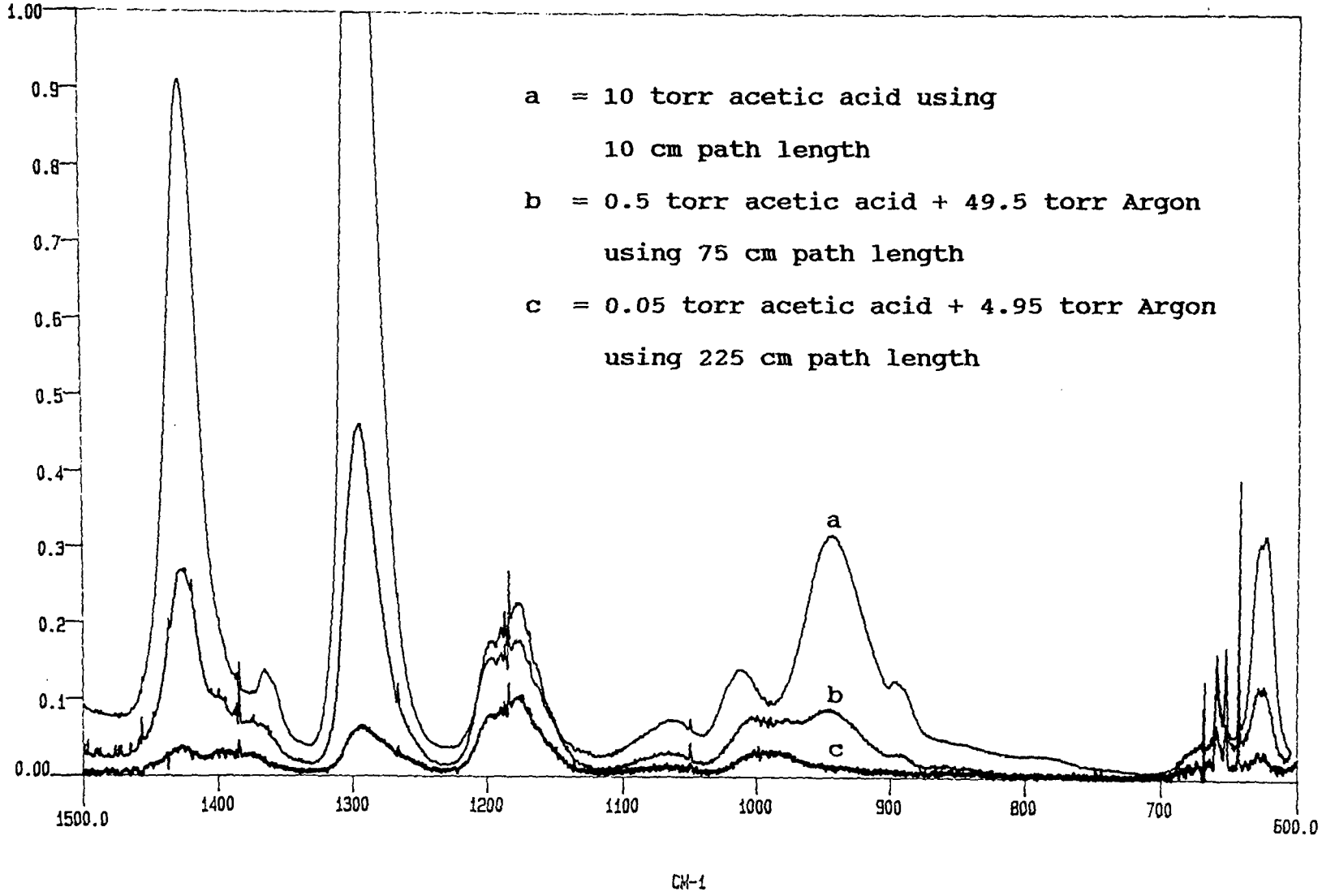

Fig.3.10B. Infrared spectra of acetic acid vapour (lower frequency region) at laboratory temperature [resolution 0.5 cm^{-1}].

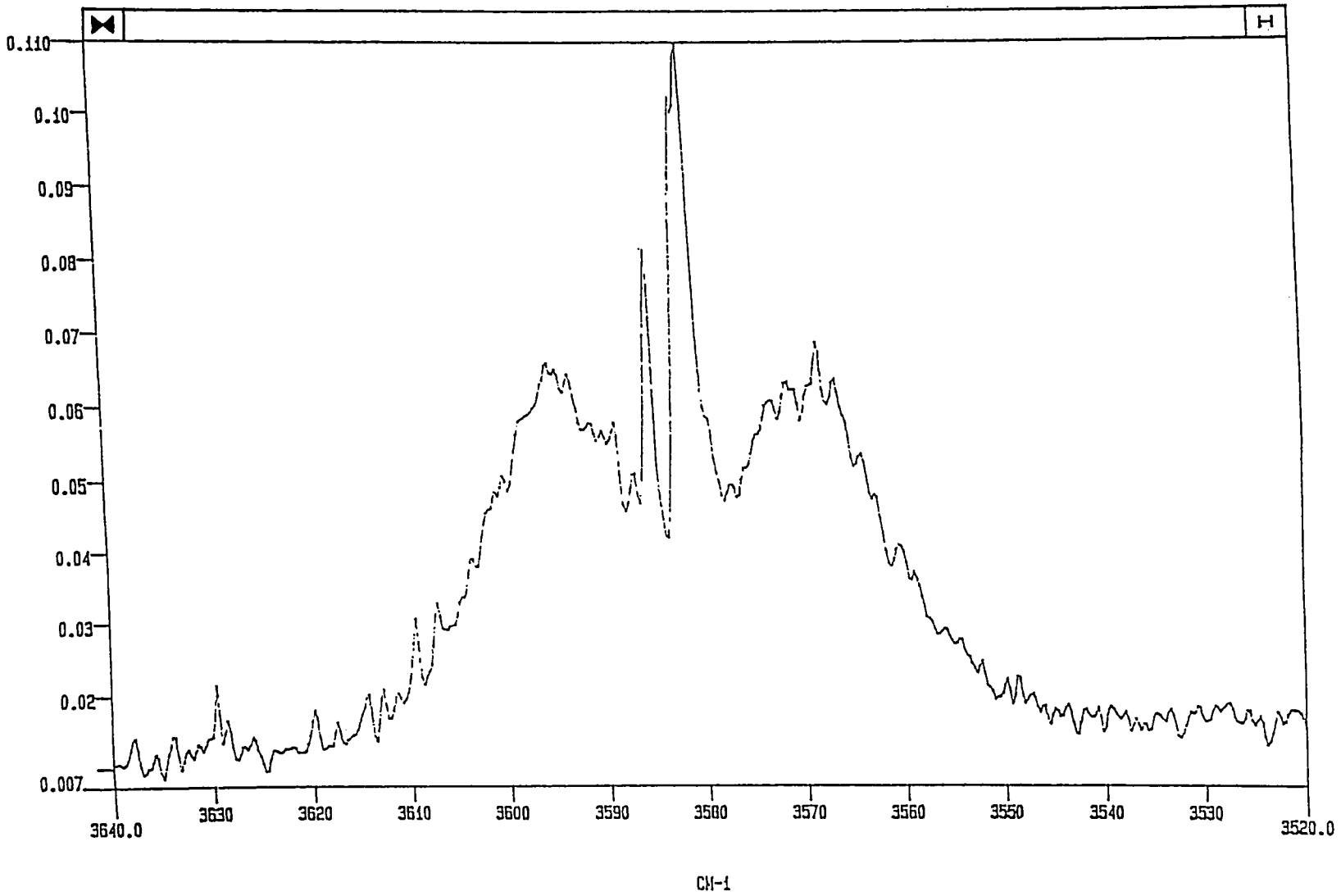

Fig.3.10C. Monomeric hydroxyl band of acetic acid vapour (resolution 0.5 cm^{-1}, partial pressure of acetic acid = 10 torr, path length 10 cm).

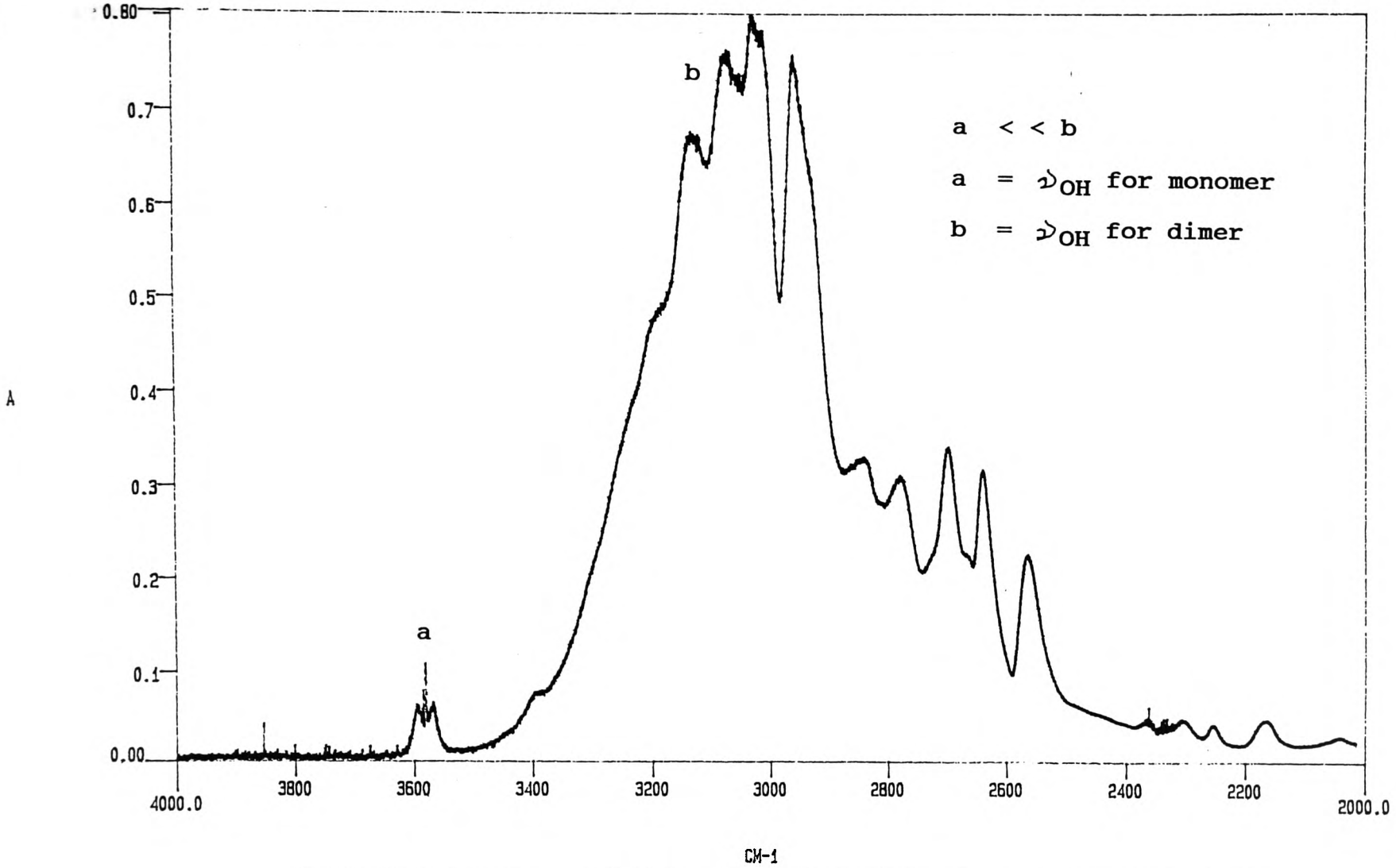

Fig.3.10D. Monomer and Polymer hydroxyl bands of pure acetic acid vapour (resolution 0.5 cm^{-1}, partial pressure of acetic acid = 10 torr, path length 10 cm).

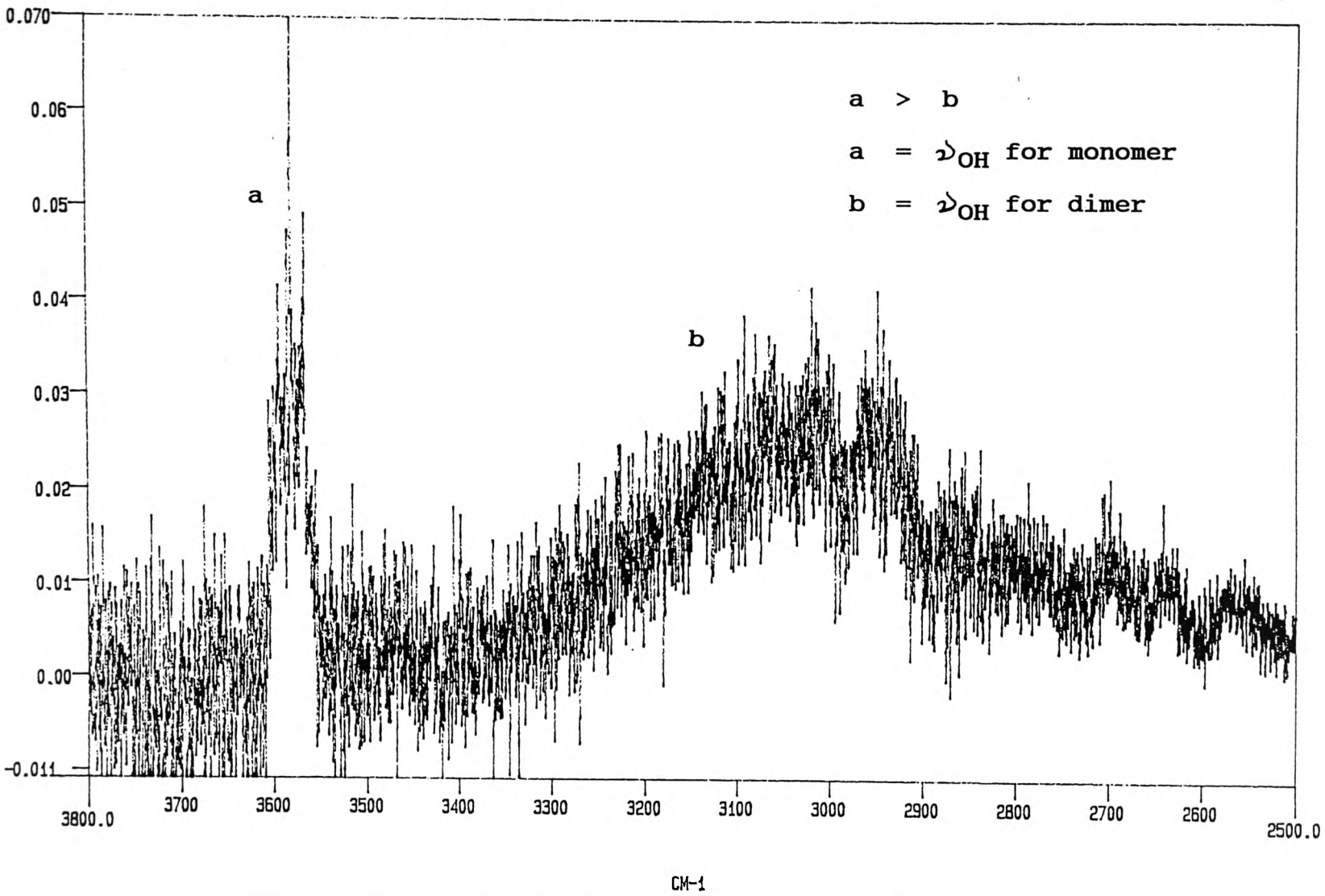

Fig.3.10E. Spectrum of acetic acid vapour/Argon mixture ($p_{acetic\ acid}$ = 0.05 torr, p_{Argon} = 4.95 torr) at laboratory temperature [resolution 0.5 cm^{-1}, path length 225 cm].

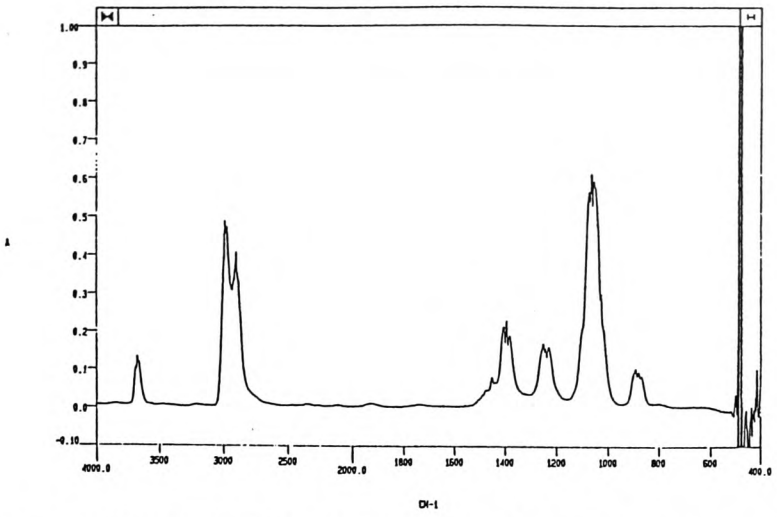

Fig.3.11a. Infrared spectrum of ethanol vapour at 4.0 cm^{-1} resolution (20 torr using 10 cm path length cell).

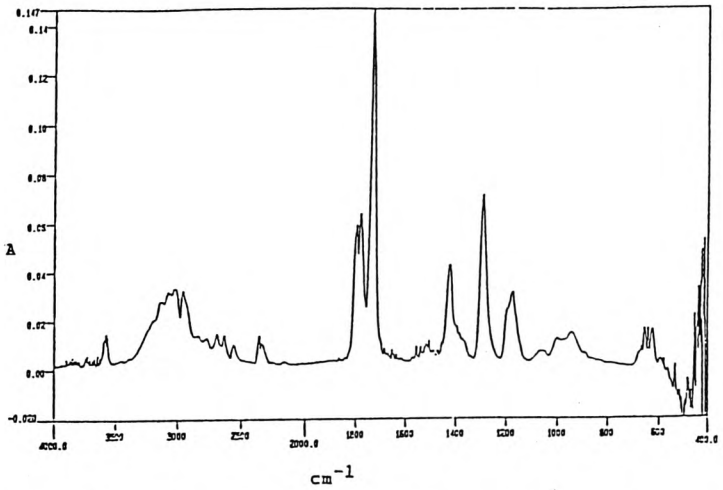

Fig.3.11b. Infrared spectrum of acetic acid vapour at 4.0 cm^{-1} resolution (0.8 torr using 10 cm path length cell).

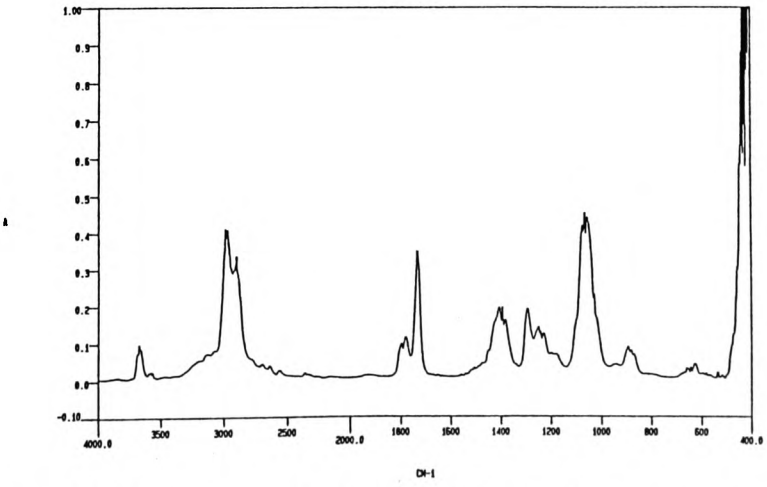

Fig.3.11c. Infrared spectrum of acetic acid and ethanol vapour at 4.0 cm^{-1} resolution (0.8 torr acetic acid + 20 torr ethanol using 10 cm path length cell).

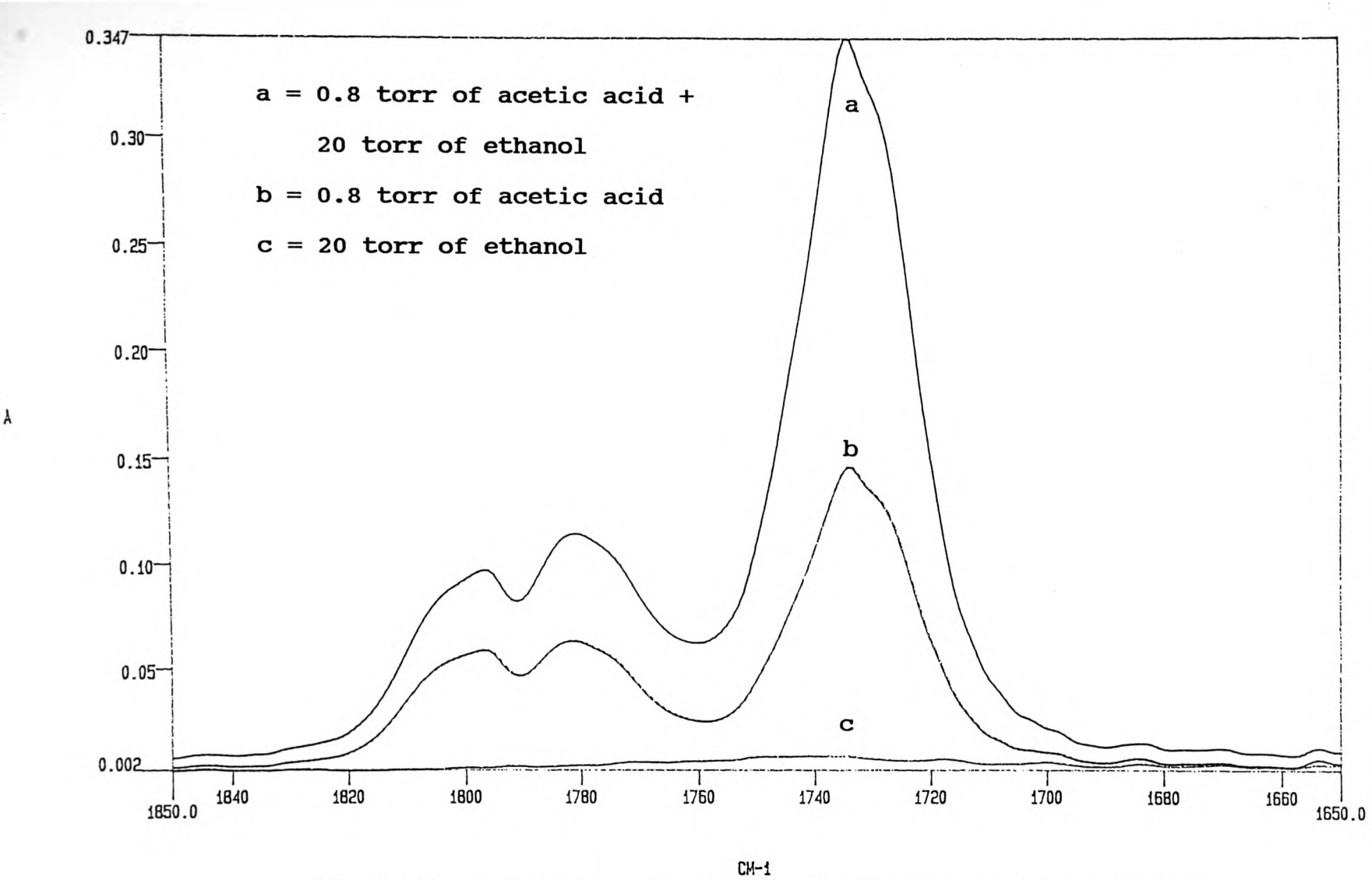

Fig.3.12. Comparison of spectra of ethanol, acetic acid and the two together in the C=O absorbing region (resolution 4.0 cm^{-1}, path length 10 cm).

CHAPTER FOUR

STUDIES OF HYDROGEN-BONDING IN CARBOXYLIC ACIDS BY INFRARED SPECTRA

4. STUDIES OF HYDROGEN-BONDING IN CARBOXYLIC ACIDS BY INFRARED SPECTRA

4.1. Introduction

The effect of hydrogen-bonding on the infrared spectra was reviewed in chapter one. As discussed previously hydrogen bonding in carboxylic acids leads to the formation of strongly hydrogen-bonded dimers[109-111]. This in turn leads to a shift of the band assigned to the OH stretching vibration to lower wavenumber together with much broadening. Also the band assigned to the C=O stretching vibration moves to lower wavenumber on hydrogen-bonding but with little change in band shape.

Some detailed studies of hydrogen-bonding on propionic acid and acetic acid were presented in chapter 3. This present chapter extends these studies to a larger family of aliphatic and aromatic carboxylic acids of greater complexity including the ortho- and para-alkoxy benzoic acids and ortho-acetyl salicylic acid (aspirin).

In general intermolecular hydrogen-bonding in carboxylic acid leads to equilibria of the type[112]

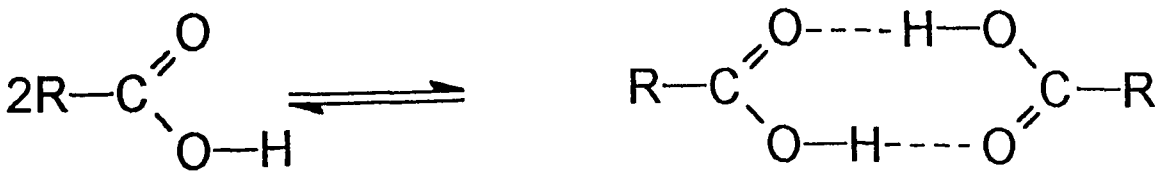

1 2

Evidence from electron diffraction data and dipole moment measurements indicates that the carboxyl group in monomeric carboxylic acid exists in a cis structure (form 1)[113-115].

In addition to intermolecular hydrogen bonds, intramolecular hydrogen-bonding is feasible when the geometrical arrangement of adjacent hydrogen donors and hydrogen acceptors are favourable. An example[116] is o-hydroxy acetophenone (form 3) in which the OH stretch and CO stretch are reduced with reference to p-hydroxy acetophenone (form 4). Thus in 4 there is a sharp OH absorption band near 3600 cm^{-1}. No such band is observed in 3 because intramolecular hydrogen-bonding shifts the sharp band at 3600 cm^{-1} to a broad weak band at lower wavenumber. Similarly, the CO stretching frequency in 4 falls to about 1646 cm^{-1}, corresponding to 3.

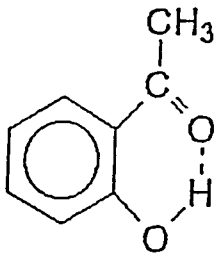

3

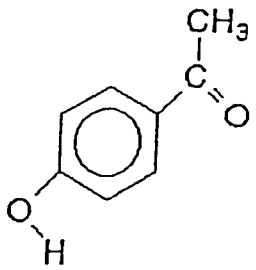

4

In the present work a series of carboxylic acid were examined including examples where both inter and intramolecular hydrogen bond were feasible.

4.2. Experiment

All carboxylic acids used in the investigation reported in this chapter were commercially available. HPLC grade CCl_4 was used as solvent and all acids were soluble in CCl_4 as dilute solutions which were examined at three different concentrations. The dilute solutions 6 X 10^{-3} M and 1.2 X 10^{-3} M were prepared from 3 X 10^{-2} M solution by graduated pipette. Perkin Elmer model 880 and FT-IR model 1760 spectrometers were used to record the spectra over the OH frequency range (3500 - 2700 cm^{-1}) and carbonyl frequency range (1800 - 1650 cm^{-1}). The accuracy of the OH frequency measurements is considered only to be about $\pm$ 4 cm^{-1} and C=O frequencies measurements are considered as $\pm$ 2 cm^{-1}. The optical path length of the cell used was 1.0 mm. All the measurements were carried out at room temperature. An absorption band near 3580 cm^{-1} is due to water present in carbon tetrachloride.

4.3. Results and discussions

The infrared absorption spectra of solutions of a series of carboxylic acids in carbon tetrachloride solution were studied at various concentrations in the hydroxyl and carboxyl stretching region. Table 4.1 lists the bands which were assigned to individual species. The results were considered in terms of equilibria involving inter and intramolecular hydrogen bonds. The IR spectra run at different concentrations showed no noticeable frequency

shifts for the carboxyl or hydroxyl bands. A marked increase in absorbance was seen in the bands assigned to C=O and O-H monomer in the spectra of the more dilute solutions.

4.3.1. Acetic acid

The infrared spectra of acetic acid is presented in fig.4.1. The sharp peak at 3535 cm^{-1} attributable to monomeric ν_{OH} and a very broad irregular dimer band extending from 3500 - 2700 cm^{-1} is assigned to dimeric ν_{O-H}. In the carbonyl region the spectra of acetic acid in solutions shows two fairly sharp peaks at 1764 and 1715 cm^{-1} attributable to monomer and dimer molecules respectively. Comparison of solutions at concentration 3 X 10^{-2} M, 6 X 10^{-3} M and 1.2 X 10^{-3} M show systematic changes associated with equilibria between monomer and dimer.

4.3.2. Propionic acid

The IR spectra of propionic acid is shown in fig.4.2. The monomeric O-H stretching vibration is observed at 3533 cm^{-1} and the dimeric band is a broad feature between 3500 to 2700 cm^{-1}. The monomeric and dimeric carbonyls are observed at 1757 and 1716 cm^{-1} respectively. On dilution the bands assigned to the monomeric form increase systematically. See also section 3.13.

4.3.3. Butyric acid

Infrared spectral changes of solutions of butyric acid showed the same characteristic bands as that observed in the case of solutions of similar concentrations of acetic acid and propionic acid. Fig.4.3 shows vibrational assignments for both the monomer and hydrogen-bonded dimer molecules. The band observed at 3533 cm^{-1} and 1758 cm^{-1} has been assigned to the monomeric ν_{OH} and ν_{CO} species. A typical broad band observed at 3500 - 2700 cm^{-1} and 1713 cm^{-1} which are assigned to the ν_{OH} and ν_{CO} vibrations involving hydrogen bond formation. Comparison of the spectra of different concentrated solutions showing the increase in intensity of the narrow monomer bands.

4.3.4. Benzoic acid

Fig.4.4 shows the most prominent peaks are observed in the infrared spectra of benzoic acid solutions in CCl_4. The O-H frequency occurs at 3533 cm^{-1} (monomer) and 3500 - 2700 cm^{-1}(dimer) respectively. The frequencies assigned to the C=O stretching bands are at 1742 cm^{-1} (monomer) and 1697 cm^{-1} (dimer)[120] respectively. Increasing dilution enhanced intensity in the monomer relative to the bonded dimer.

4.3.5. o-Methoxy benzoic acid

o-Methoxy benzoic acid has a structure which permits both inter and intramolecular hydrogen-bonding[117]. The measured frequencies for the OH and CO vibrations are shown in

fig.4.5. The spectra contains a new band of strong intensity centred at 3365 cm^{-1} and totally distinct from the absorptions in carboxylic acids considered earlier. The weak monomeric O-H absorption is found at 3523 cm^{-1} (3580 cm^{-1} band is probably due to water present in CCl_4). The band at 3365 cm^{-1} gives valuable information regarding the structure in relation to intramolecular H-bonding since its relative intensity remains reasonably constant with increase in concentration. A normal association band is also observed at 3500 - 2700 cm^{-1}. The frequency assigned to the C=O vibration in the spectrum at 1750 cm^{-1} is for the monomer and that of 1700 cm^{-1} is for the dimeric carbonyl band[117]. From these frequency measurements it can readily be deduced that an equilibrium between single and double molecules of o-methoxy benzoic acid of the following form really does exist in solution.

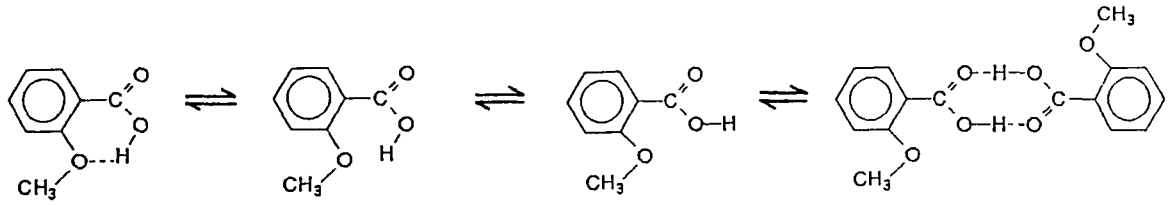

5 6 7 8

In form 5, interaction between the oxygen of the methoxy group and the O-H of the COOH group will reduce normal association of two COOH groups (form 8) and so a strong monomeric O-H band should be observed[118]. Examination at different concentrations confirms this interpretation. This

explain the absence of a band assigned to the C=O dimer form at concentration 1.2 X 10^{-3} M (fig.4.5c).

4.3.6. o-Ethoxy benzoic acid

o-Ethoxy benzoic acid is also capable of forming intramolecular hydrogen-bonding and possesses very similar spectra to that found in o-methoxy benzoic acid[117] (fig. 4.6). An intense O-H band at 3343 cm^{-1} arises from intramolecular H-bonding, whereas the broad absorption band extending from 3500 to 2700 cm^{-1} arises from associated dimeric molecules. A frequency of the free O-H is observed as a very weak band at 3525 cm^{-1}. The $\nu_{C=O}$ absorptions assigned to the monomer is at 1750 cm^{-1} and the dimer is at 1700 cm^{-1}. The dimeric $\nu_{C=O}$ band diminishes on dilution. This band is less prominent than in carboxylic acids which do not permit intramolecular hydrogen-bonding.

4.3.7. p-Methoxy benzoic acid

In assessing the contribution of the intramolecular interactions in the spectra, the ortho- and para- isomers form are useful comparison. It is observed that the para-methoxy benzoic acid gives the usual carboxylic acid dimer band (fig.4.7). The band arising from the contribution of intramolecular H-bonding is absent in the para compound. It is therefore to be expected that the hydrogen-bonding is intermolecular[119]. The ν_{O-H} and $\nu_{C=O}$ band possesses two bands one of which is presumably due to the monomer

molecule (3540 and 1735 cm^{-1} respectively) and the other to the dimer (3500 - 2700 and 1690 cm^{-1} respectively). The bands are affected by changing concentration as the normal monomer.

4.3.8. p-Ethoxy benzoic acid

The spectra of fig.4.8 are interpreted in terms of the characteristic vibrations of O-H and C=O stretching modes. The band at 3500 - 2700 cm^{-1} and 1690 cm^{-1} are assigned to the dimeric ν_{O-H} and $\nu_{C=O}$ of p-ethoxy benzoic acid in CCl_4 solution. The bands at 3541 and 1735 cm^{-1} for ν_{O-H} and $\nu_{C=O}$ increases in relative intensity as concentration is lowered. This is appropriate behaviour for the monomeric O-H and C=O functional groups.

4.3.9. o-Acetyl salicylic acid

Fig.4.9 shows the wavenumber of OH and CO bands of o-acetyl salicylic acid (aspirin) obtained from various concentrations. Upon comparing the infrared spectra for 3 dilute solutions it is possible to conclude that frequency at 3532 cm^{-1} and 3500 - 2500 cm^{-1} to frequency ν_{O-H} of monomeric and dimeric acid molecules. Three sharp frequencies are found in the carbonyl stretching region. The bands at 1745 and 1700 cm^{-1} are due to free and hydrogen-bonded carbonyl stretching frequency respectively. The acetoxyl C=O vibration is associated with the band at 1776 cm^{-1}. These assignments are consistent with the result found in the

literature[120,121]. Under the condition of present measurements no bands were observed which corresponded to structure involving intramolecular hydrogen-bonding[120-122].

Table 4.1 summarizes the frequencies found for the given series of carboxylic acids. Comparison of the spectra revealed that a carboxylic acid exhibits strong absorption band in the 3500 - 2700 cm^{-1} region for the hydrogen-bonded dimeric species even in the very dilute 1.2 X 10^{-3} M solution. Evidence for only a small portion of the monomer present which is detected by increased intensity of sharp peaks (around 3530 cm^{-1} for ν_{OH} and near 1750 cm^{-1} for ν_{CO}) with decreased concentration. Strong intermolecular hydrogen-bonding is also evidenced by the strong broad dimeric carbonyl band which is reflected in the decrease frequency about 1700 cm^{-1} region.

The solution spectra of o-methoxy and o-ethoxy benzoic acid suggest that intramolecular hydrogen-bonding exists within the acid molecule, between the carboxylic hydroxyl (a proton donor), and the oxygen of the methoxy group (a proton acceptor). However, when a carboxylic acid has a proton acceptor group at an α - position to the carboxyl group, the trans structure will be stabilised owing to the formation of an intramolecular hydrogen bond[115] (form A in table 4.1). This is observed in these two spectra. There is evidence for the formation of dimeric species which is broad (3500 - 2700 cm^{-1}) but is reduced in intensity compared with those carboxylic acids which do not possess

o-proton acceptors. In the aspirin spectra no intramolecular hydrogen-bonding is detected although it contains a proton accepting group in ortho- to the carboxyl group. Nakai et at[120], Nagibina et al[121] and Wojcik et al[122] also report that aspirin is associated with intermolecular hydrogen-bonding only.

The experimental information and assignments in carboxylic acids in this chapter serve as a basis for modelling structure in chapter 5.

Table 4.1

Comparison of infrared spectra of carboxylic acids.

R	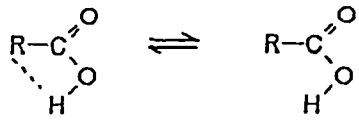 A		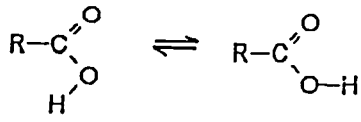 B		C		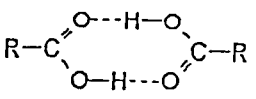 D	
	CO	OH	CO	OH	CO	OH	CO	OH
	cm^{-1}		cm^{-1}		cm^{-1}		cm^{-1}	
CH_3—					1764	3535	1715	3500-2700
C_2H_5—					1757	3533	1716	3500-2700
C_3H_7—					1758	3533	1713	3500-2700
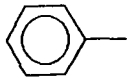					1742	3533	1697	3500-2700
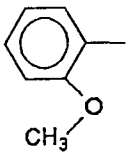	1750	3365			1750	3523	1700	3500-2700
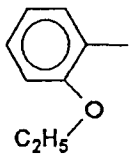	1750	3343			1750	3525	1700	3500-2700
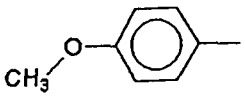					1735	3540	1690	3500-2700
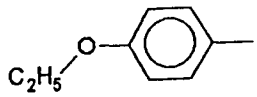					1735	3541	1690	3500-2700
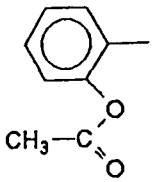					1745	3532	1700	3500-2700
					1776 (acetoxyl CO)			

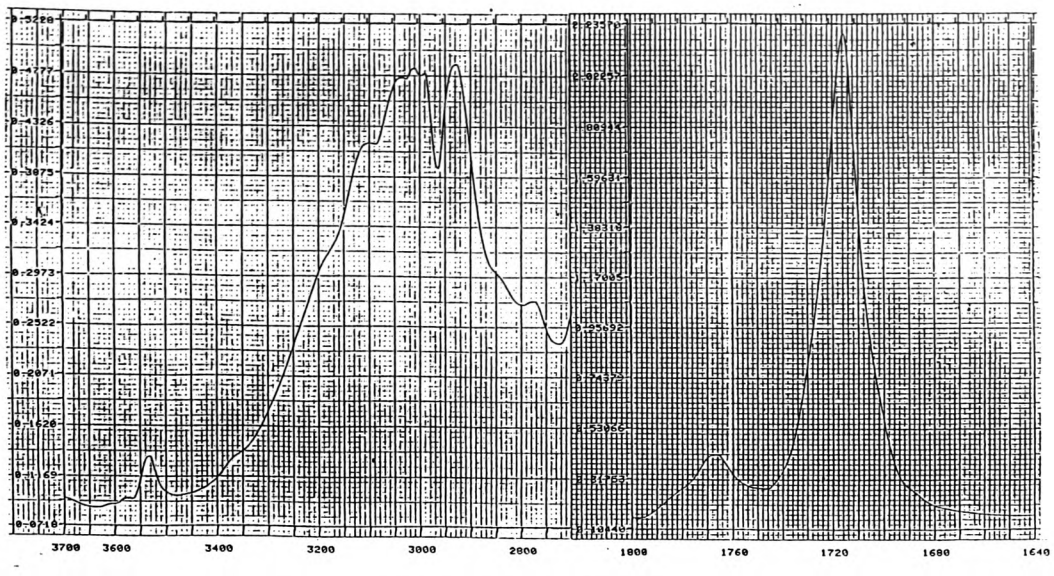

(a) 3 X 10 $^{-2}$ M

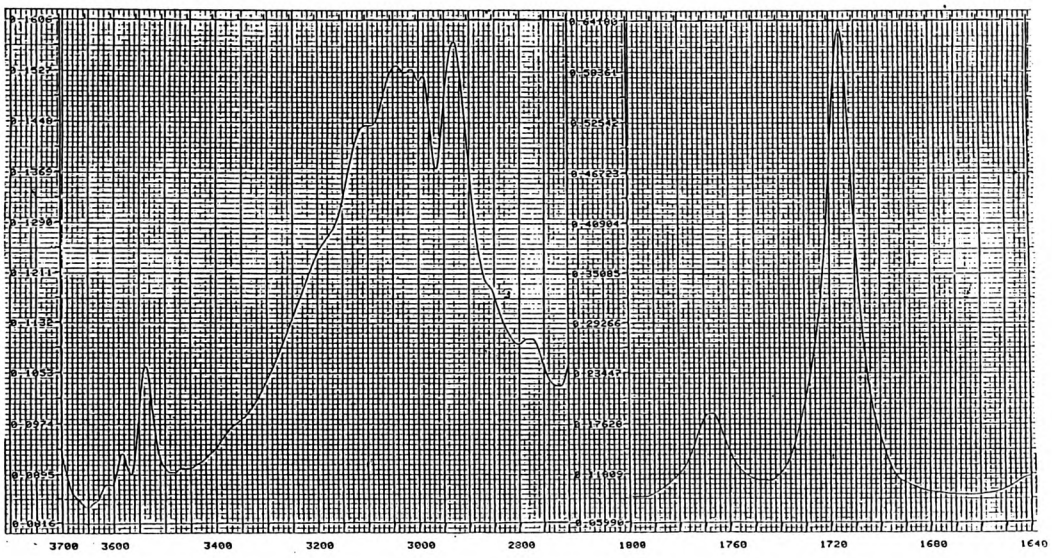

(b) 6 X 10 $^{-3}$ M

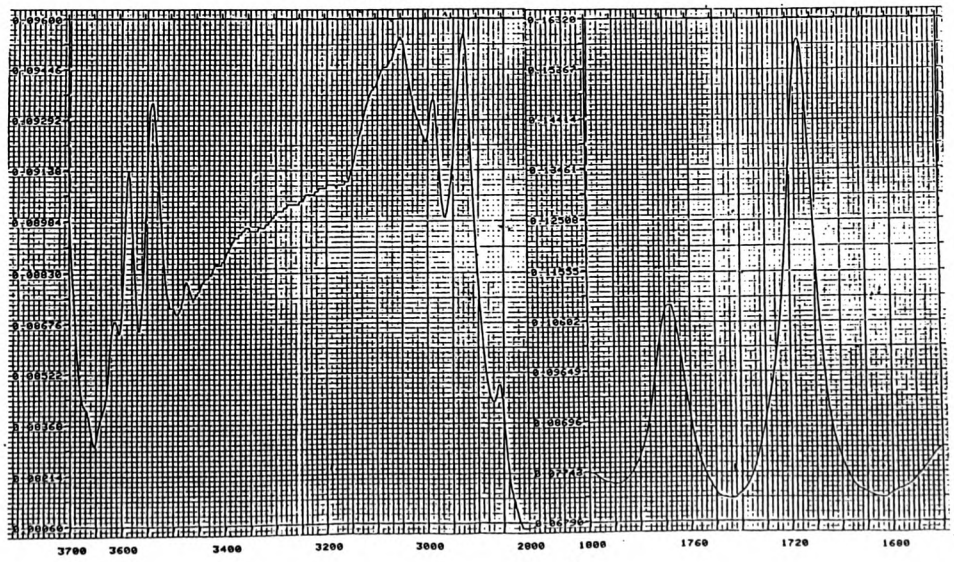

cm^{-1}

(c) 1.2 X 10 $^{-3}$ M

Fig.4.1. Infrared spectra of Glacial acetic acid in CCl_4 at 1.0 mm path length. PE 880, Slit prog.1, Filter 16, Smooth level 2.

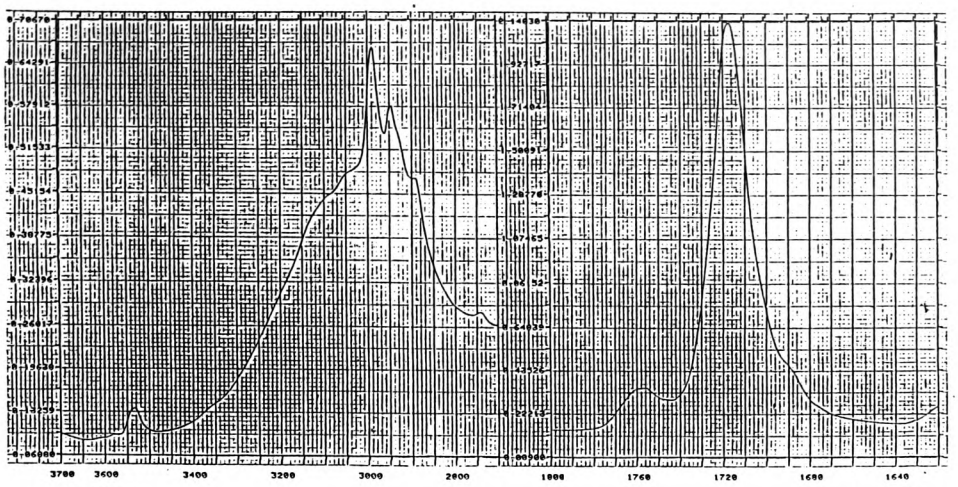

(a) 3 X 10 $^{-2}$ M

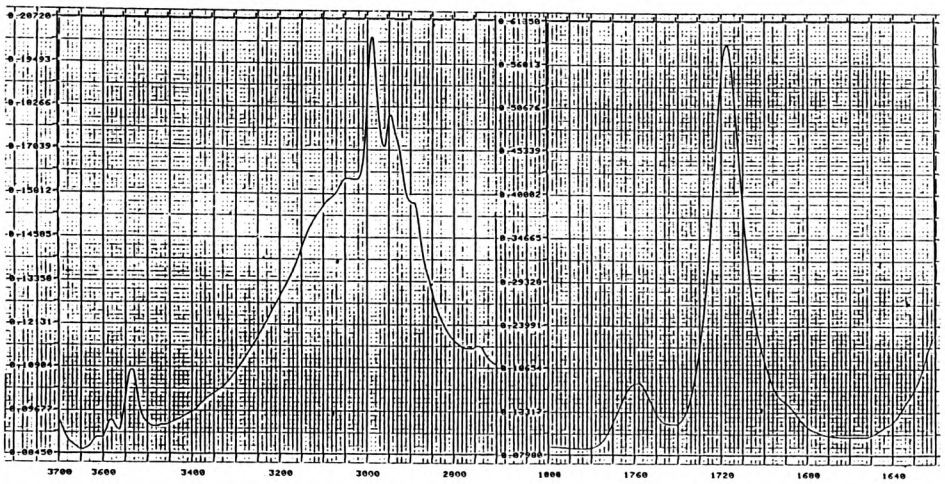

(b) 6 X 10 $^{-3}$ M

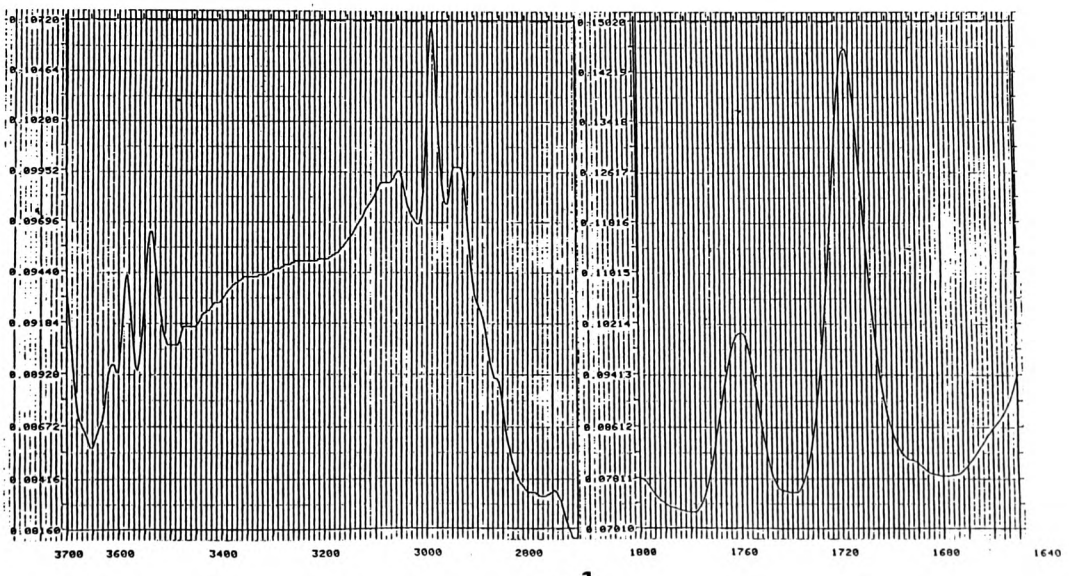

(c) 1.2 X 10 $^{-3}$ M

Fig.4.2. Infrared spectra of n-Propionic acid in CCl_4 at 1.0 mm path length. PE 880, Slit Prog.1, Filter 16, Smooth level 2.

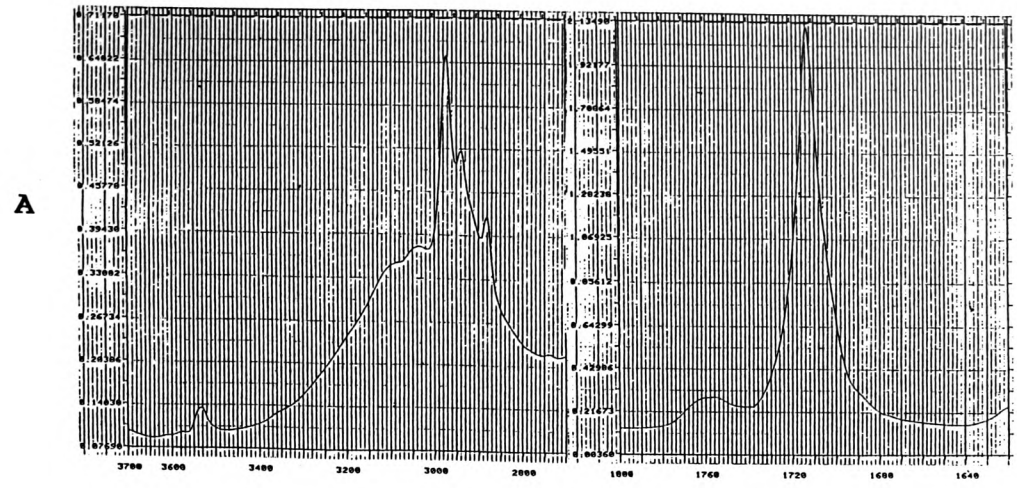

(a) 3 X 10 $^{-2}$ M

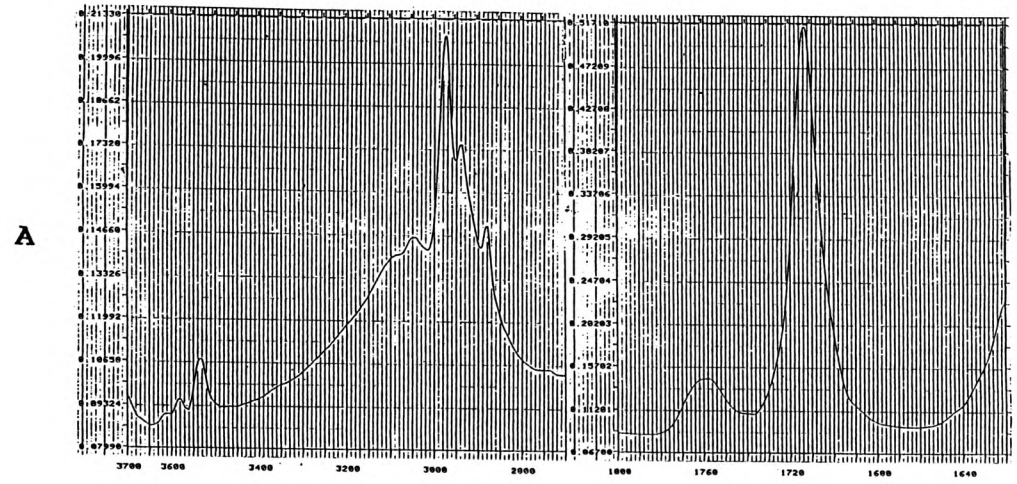

(b) 6 X 10 $^{-3}$ M

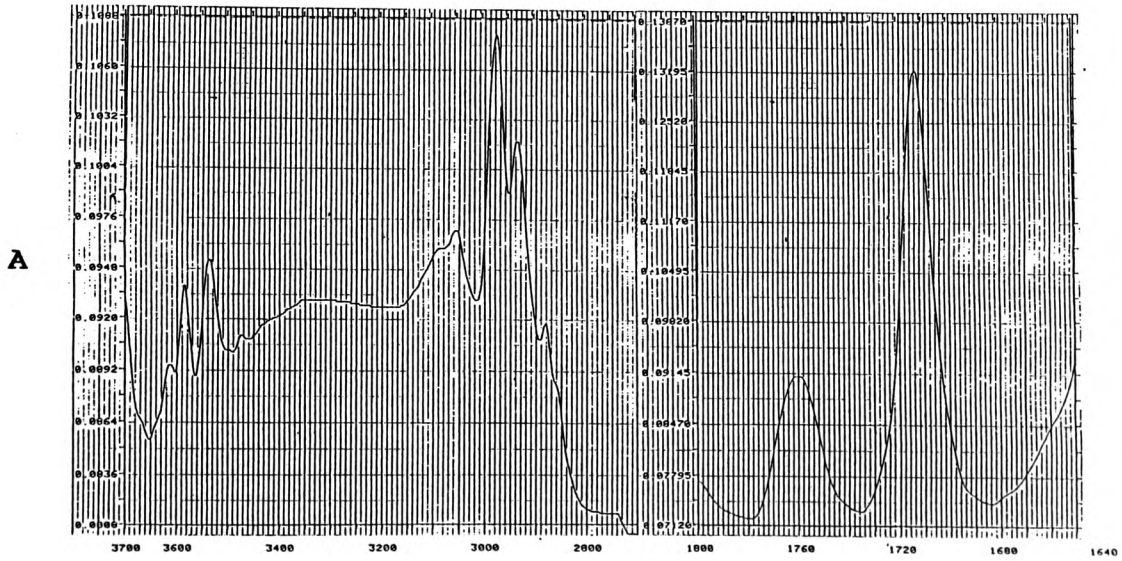

cm^{-1}

(c) 1.2 X 10 $^{-3}$ M

Fig.4.3. Infrared spectra of n-Butyric acid in CCl_4 at 1.0 mm path length. PE 880, Slit prog.1, Filter 16, Smooth level 2.

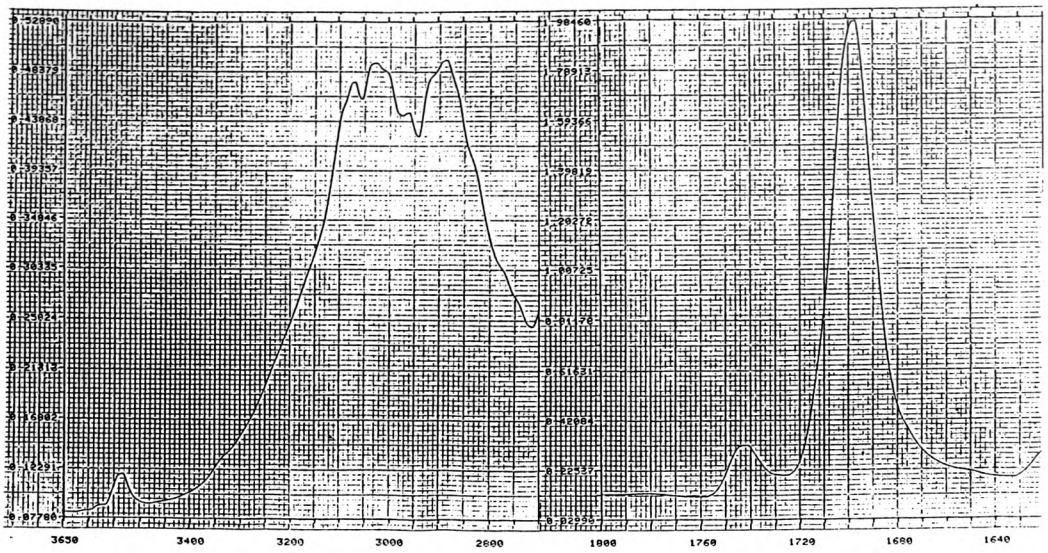

(a) 3 X 10 $^{-2}$ M

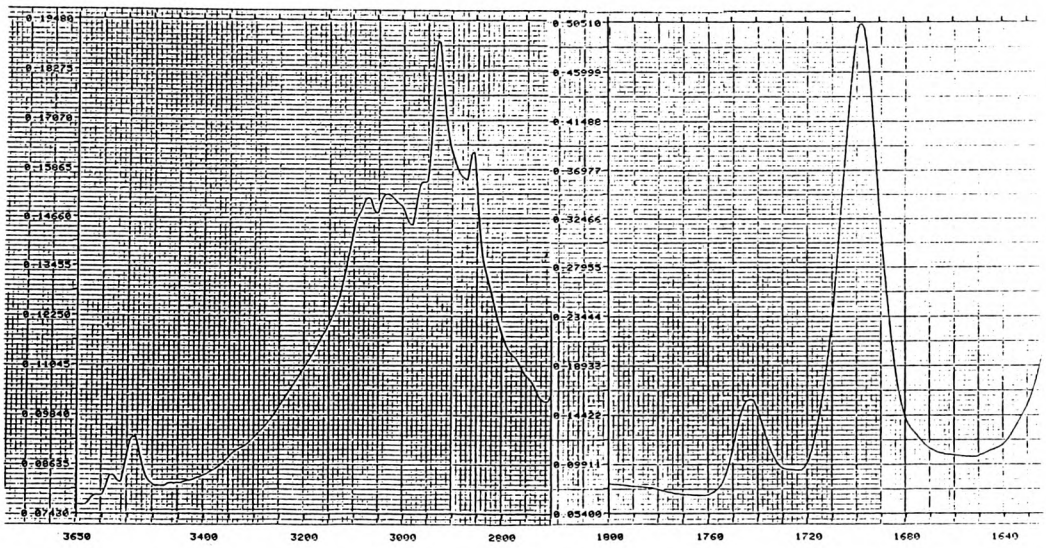

(b) 6 X 10 $^{-3}$ M

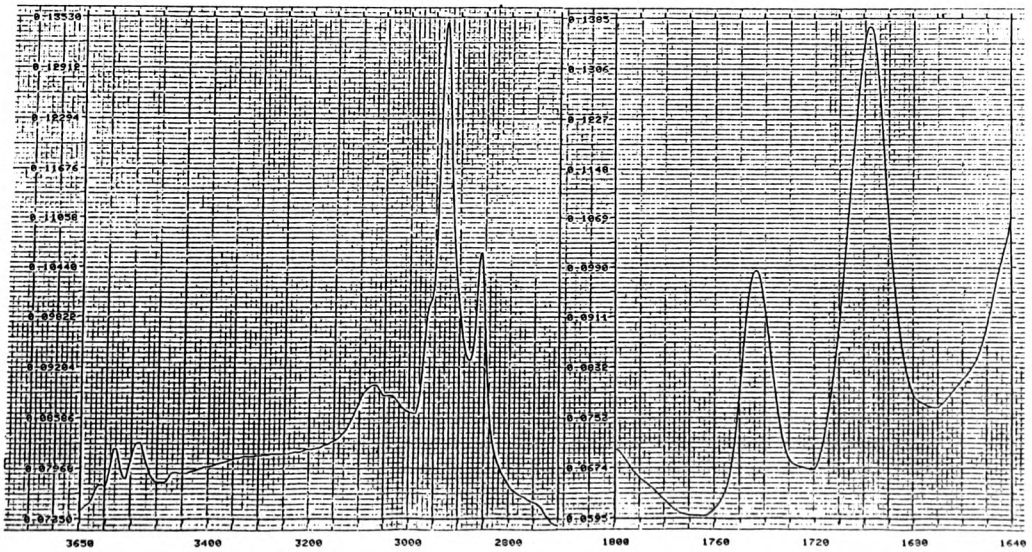

cm^{-1}

(c) 1.2 X 10 $^{-3}$ M

Fig.4.4. Infrared spectra of Benzoic acid in CCl_4 at 1.0 mm path length. PE 880, Slit Prog.1, Filter 16, Smooth level 2.

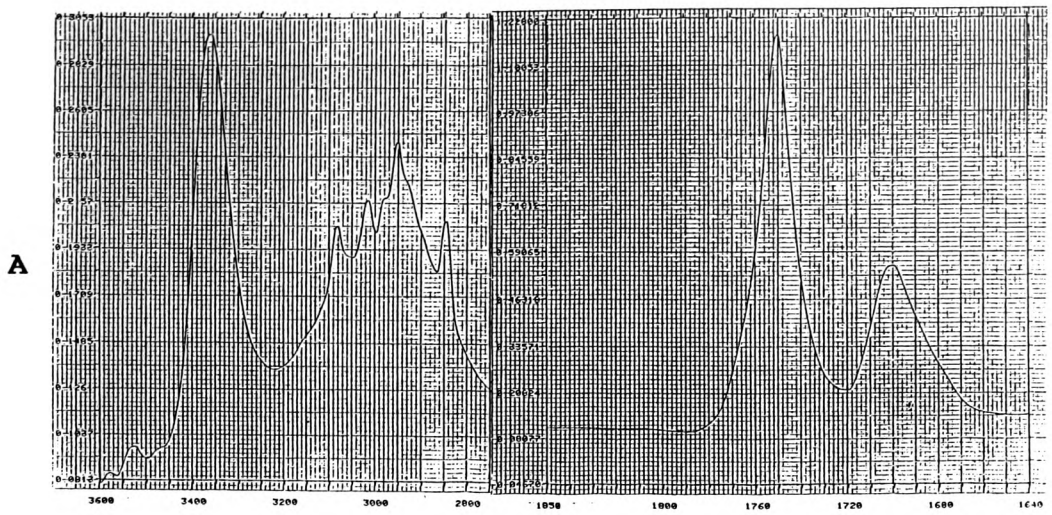

(a) 3 X 10 $^{-2}$ M

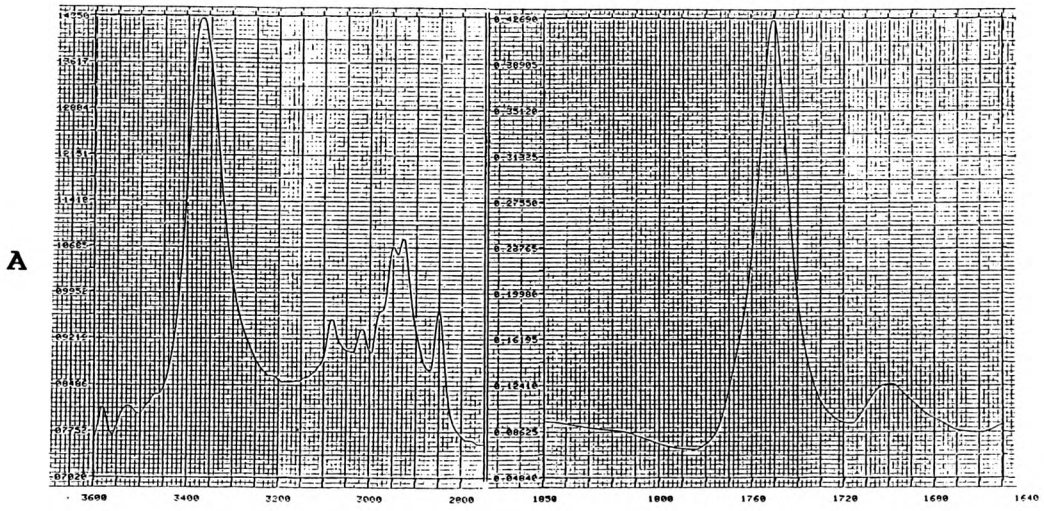

(b) 6 X 10 $^{-3}$ M

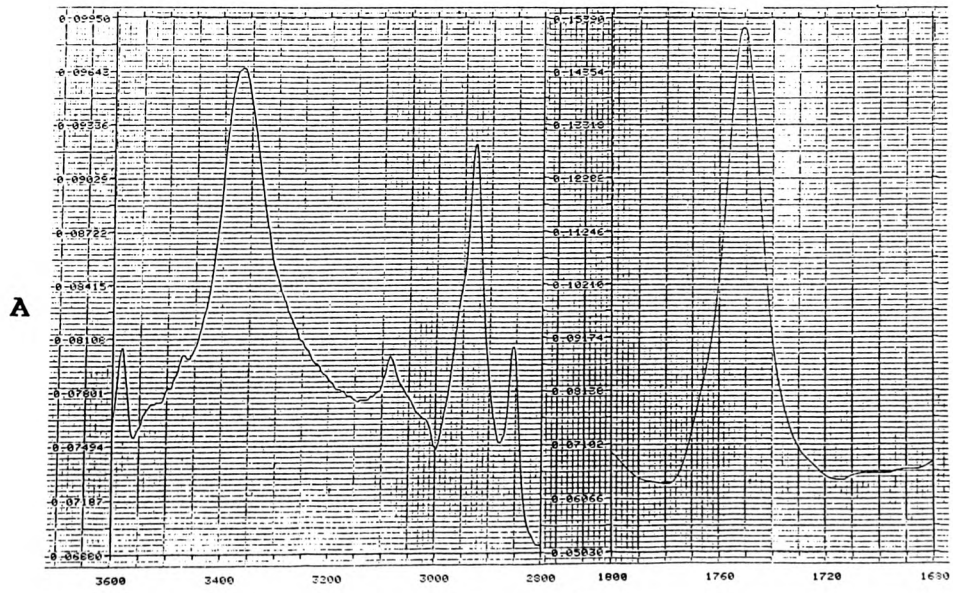

cm^{-1}

(c) 1.2 X 10 $^{-3}$ M

Fig.4.5. Infrared spectra of o-Methoxy Benzoic acid in CCl_4 at 1.0 mm path length. PE 880, Slit Prog.1 Filter 16, Smooth level 2.

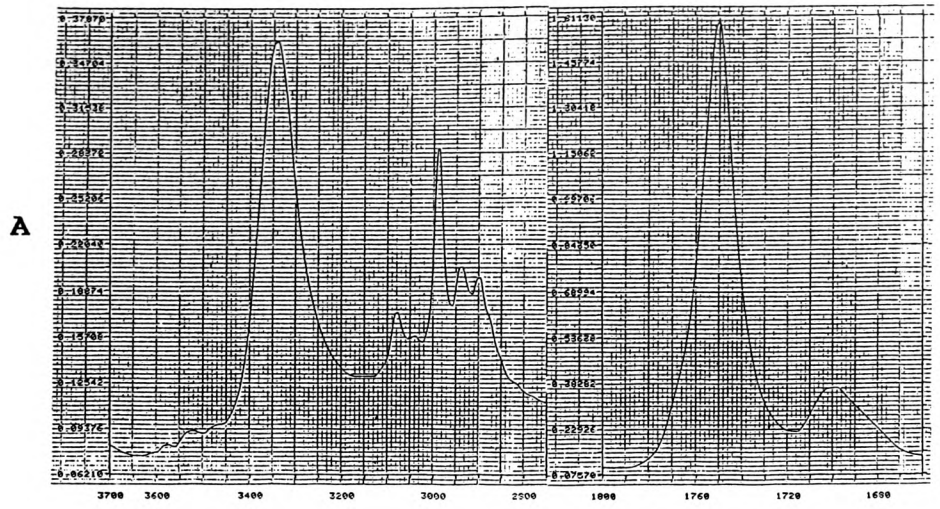

(a) 3 X 10 $^{-2}$ M

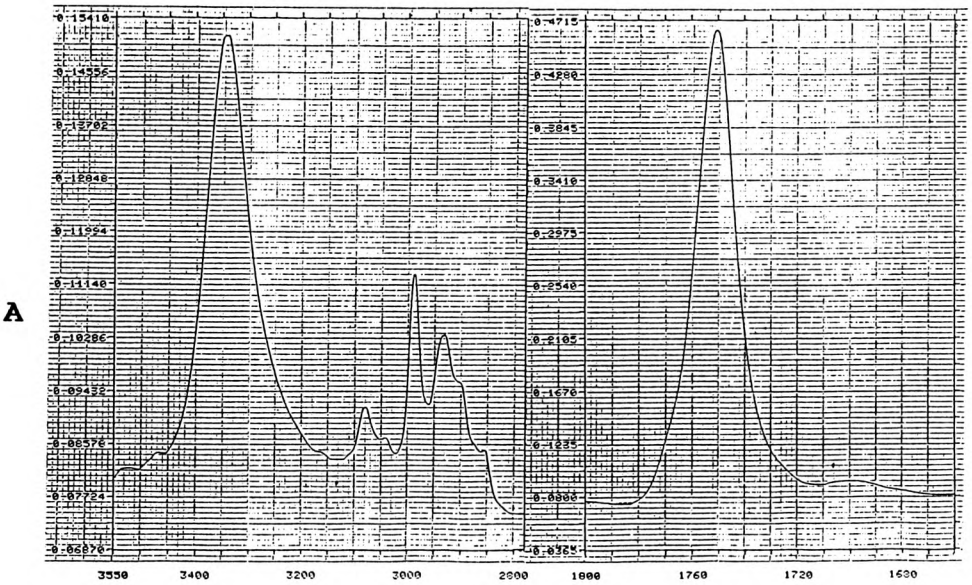

(b) 6 X 10 $^{-3}$ M

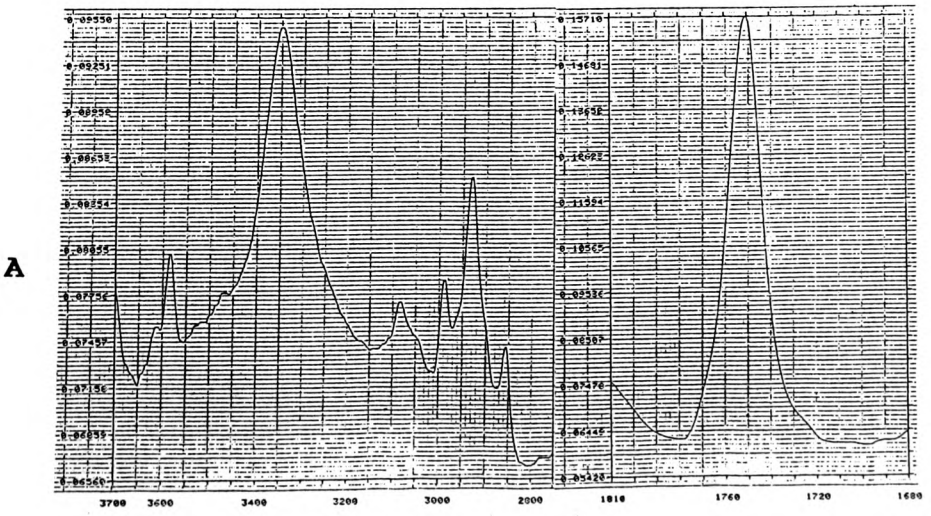

cm^{-1}

(c) 1.2 X 10 $^{-3}$ M

Fig.4.6. Infrared spectra of o-Ethoxy Benzoic acid in CCl_4 at 1.0 mm path length. PE 880, Slit Prog.1, Filter 16, Smooth level 2.

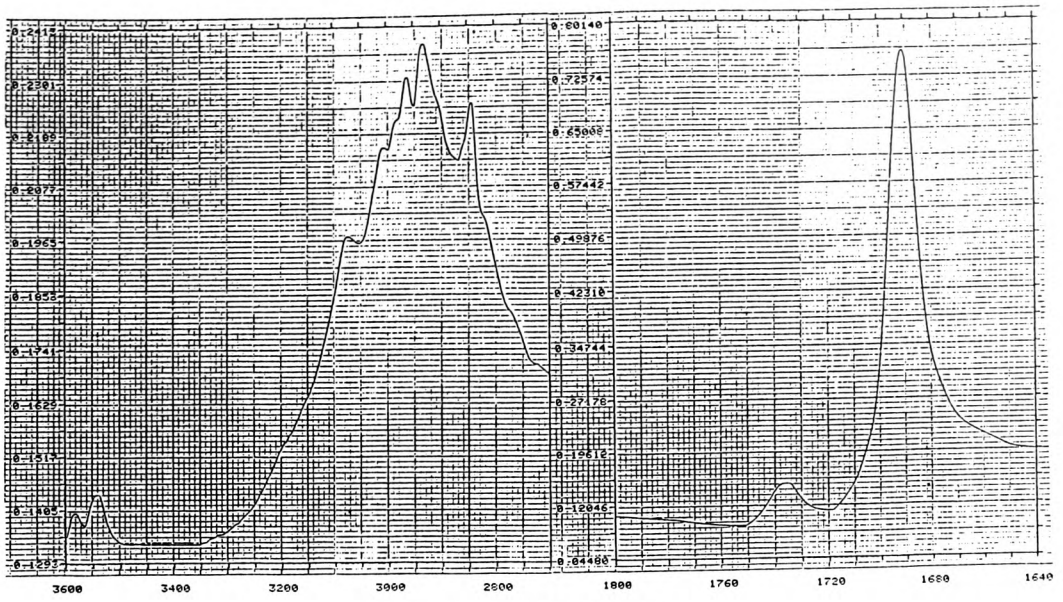

(a) 3 X 10 $^{-2}$ M

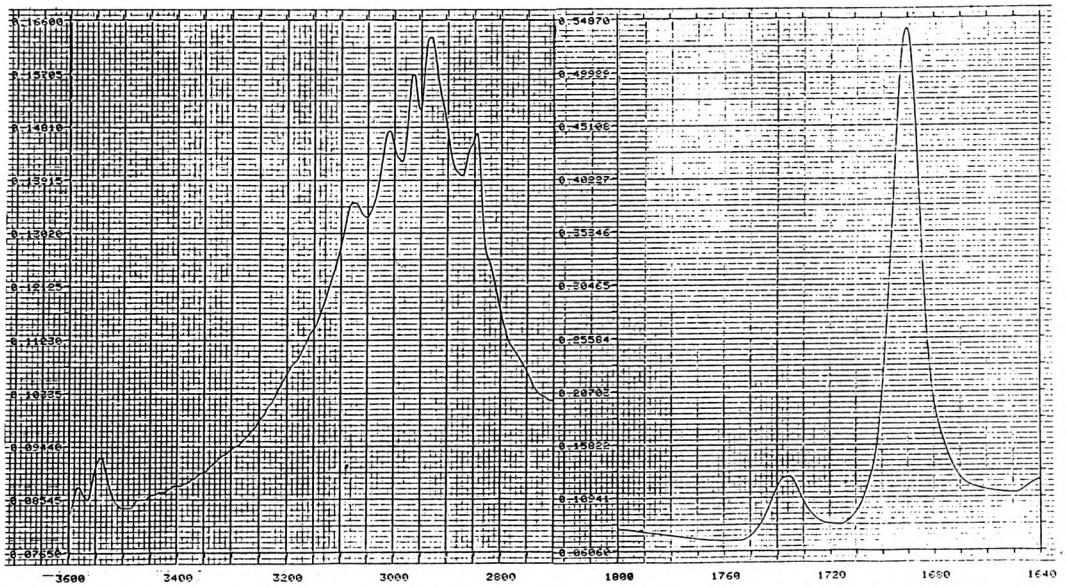

(b) 6 X 10 $^{-3}$ M

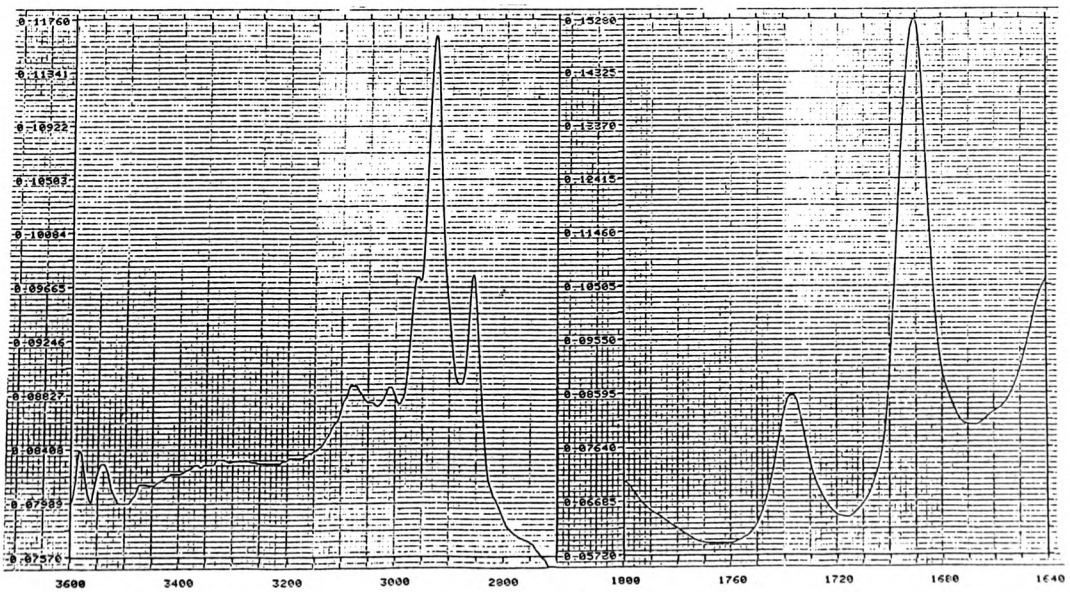

cm^{-1}

(c) 1.2 X 10 $^{-3}$ M

Fig.4.7. Infrared spectra of p-Methoxy Benzoic acid in CCl_4 at 1.0 mm path length. PE 880, Slit Prog.1, Filter 16, Smooth level 2.

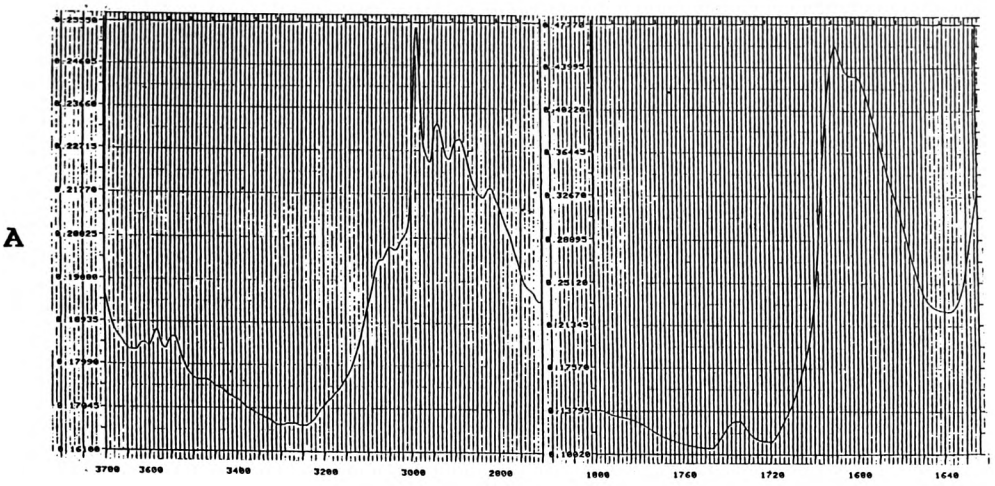

(a) 3 X 10 $^{-2}$ M

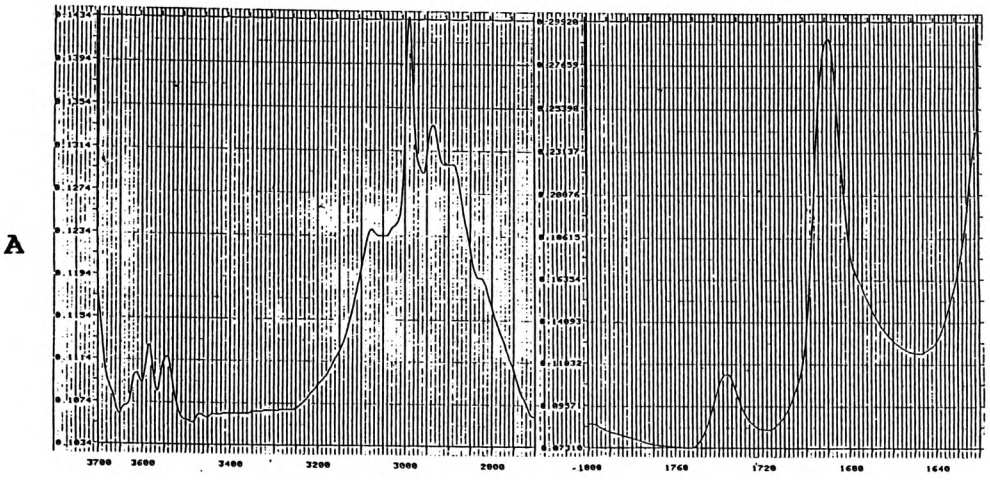

(b) 6 X 10 $^{-3}$ M

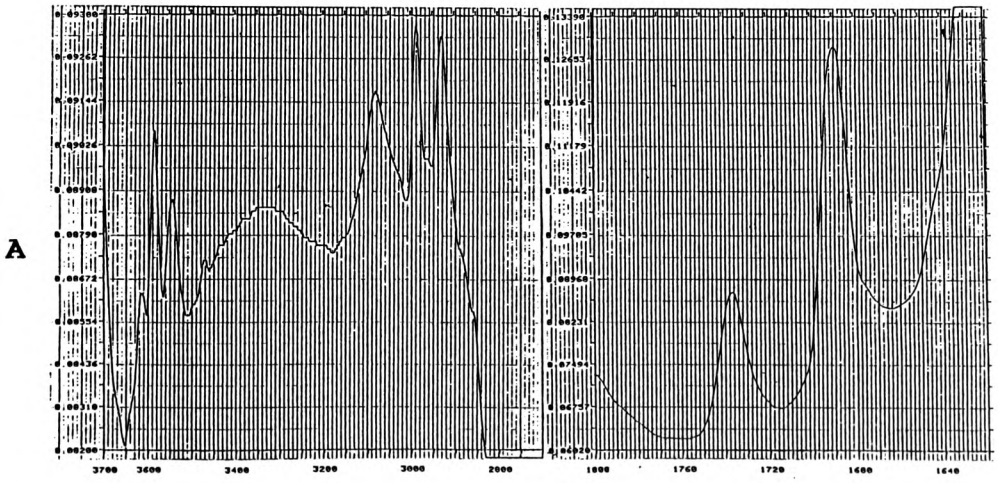

cm^{-1}

(C) 1.2 X 10 $^{-3}$ M

Fig.4.8. Infrared spectra of p-Ethoxy Benzoic acid in CCl_4 at 1.0 mm path length. PE 880, Slit Prog.1, Filter 16, Smooth level 2.

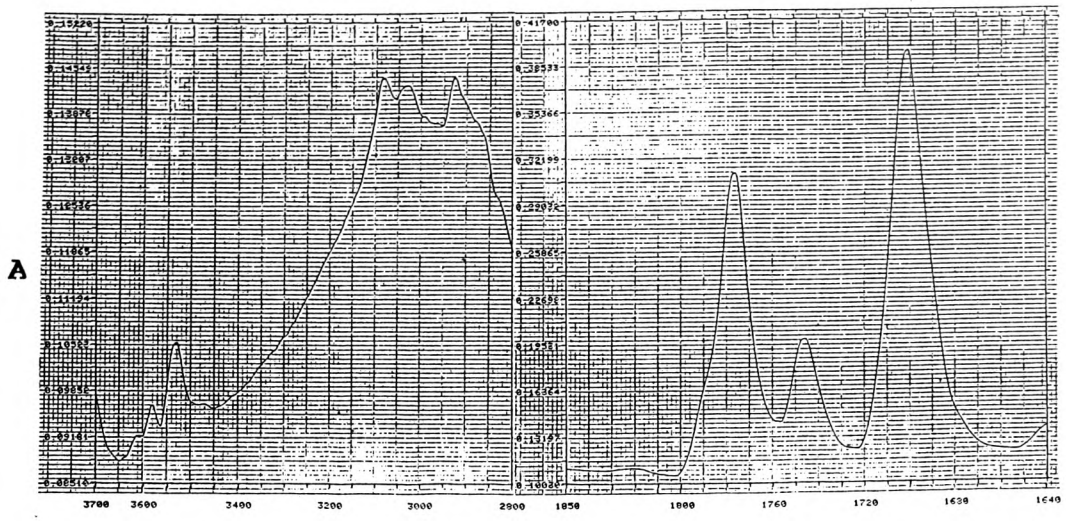

(a) 3 X 10 $^{-2}$ M

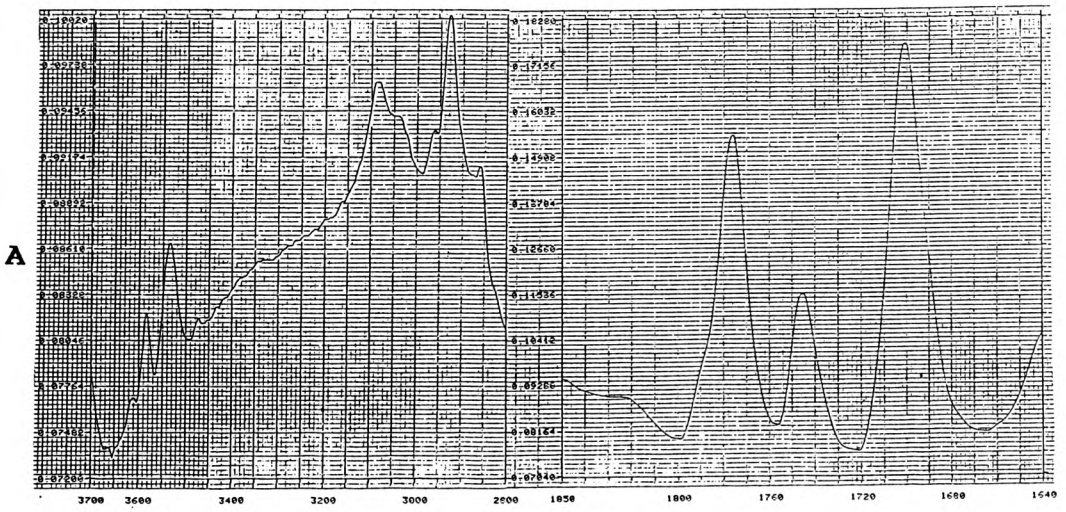

(b) 6 X 10 $^{-3}$ M

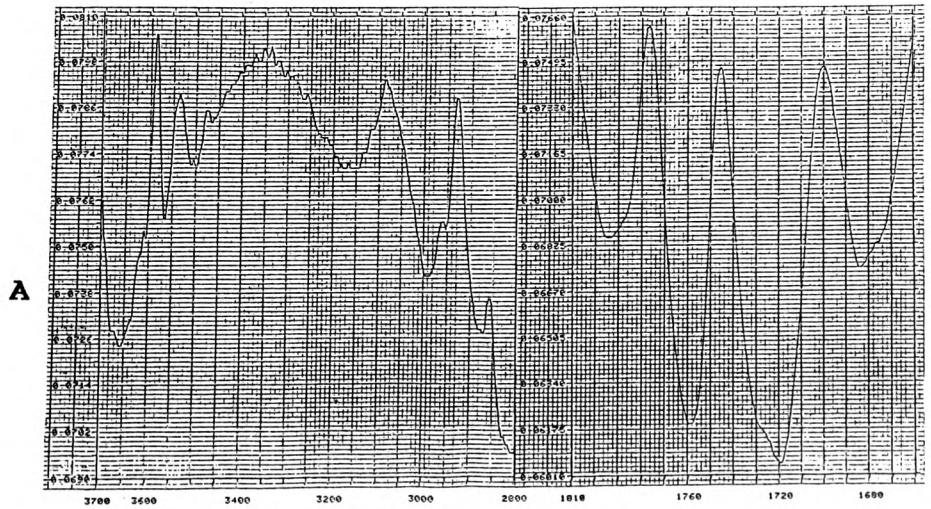

cm^{-1}

(c) 1.2 X 10 $^{-3}$ M

Fig.4.9. Infrared spectra of o-Acetyl Salicylic acid in CCl_4 at 1.0 mm path length. PE 880, Slit Prog.1, Filter 16, Smooth level 2.

CHAPTER FIVE

CALCULATION OF ENERGY AND ANALYSIS OF CONFORMERS USING THE CHEM-X MOLECULAR MODELLING PROGRAMME

5. CALCULATION OF ENERGY AND ANALYSIS OF CONFORMERS USING THE CHEM-X MOLECULAR MODELLING PROGRAMME

5.1. Introduction

Chem-X is a "default" software package marketed by Chemical Design Ltd. which has powerful visualisation, computation and database facilities for molecular modelling. It provides many ways in which a particular molecular system can be described.

In this study molecular models were constructed for a series of carboxylic acid monomer and dimer species whose infrared spectral characteristics were studied in the previous chapter. These were built and displayed using the facilities of Chem-X. The most favoured geometries were determined from the minimum interaction energy calculations. The Molecular Mechanics (MM) Chem-X option used in this study is a force field which employs a set of parameters for calculating the energy of a molecule[123].

The Chem-X package reports energies in kcals per mole. In chapter 3 energy is expressed in kJoule per mole in line with SI and IUPAC recommendations. The two sets of units are interconvertable by-

$$1 \text{ kcal mol}^{-1} = 4.184 \text{ kJ mol}^{-1}$$

5.2. Modelling structures in Chem-X

5.2.1. Drawing structures

The first stage of a Chem-X modelling study is to create a chemical structure of a molecule. A 2-dimensional drawing panel is generally used for sketching small molecular frameworks. Small chain molecules (1 - 3 compounds in table 5.1) were built using a chain option which continuously draws bonds as carbon chains. An element selector substitutes a predefined atom into the framework. The ring fragment is chosen from the supplied fragment library for building benzenoid molecules (4 - 9 compounds in table 5.1) and then appropriate substituents are added. The built structure is in turn converted into 3-dimensional coordinates with valid bond lengths and angles. To satisfy all valencies, hydrogen atoms are added automatically in this operation.

5.2.2. Displaying structures

Chem-X offers a variety of techniques to view and to manipulate 3-dimensional images of molecules. Certain colours, sizes and display style for atoms and bonds may be chosen which greatly enhance or emphasise different aspects of chemical structure. The default style which shows bonding framework and type of atoms is called 'atoms coloured stick'. For improved visibility, a combination of increased bond thickness and atomic radius can be made with a ball and stick display style. The structure of the molecule on the screen can be move by rotations,

translations, scaling, clipping and bond rotations. This ability provides opportunity to view the structure in plane or to view interacting molecules from many different orientations in order to appreciate where there are favourable interactions and where there are undesirable contacts or overlap.

5.2.3. Calculating Geometry

Information on the geometry of a structure is of fundamental importance where studying any model for determining the behaviour of a molecular model in different circumstances. Chem-X provides a facility to obtain structures with standard values for geometry and bond order. When more accurate information for bond length and bond angle is known this value can be incorporated in the model structure.

5.2.4. Minimising structures

The structures which are built using the 2-dimensional to 3-dimensional builder may be minimised in energy in order to refine the energy and geometry of molecules. In many structures especially in strained rings and sterically crowded molecules, bond lengths and angles can vary significantly from accepted values. Atoms from different parts of those structures may be in contact. This is reflected in high molecular energies and can be resolved by producing low energy structure through minimisation operations. Chem-X provides two ways to minimise the

structure. The van der Waals (VDW) minimisation adjust the bond torsions and interfragement orientations automatically. Molecular Mechanics Energy (MME) optimisation refines the structure by altering the full x y z coordinates to generate a more acceptable low energy model than the VDW minimiser.

5.2.5. Energy calculations

The structures of molecules are not static but change by constant vibration of bonds, and change of angles, and torsion angles of bonded atoms in their spatial relationships to one another. Chem-X uses molecular mechanics techniques to calculate the energy of the most favoured geometry and the minimised molecular mechanics energy determine the optimal molecular geometries.

There are two distinct methods in Chem-X for computing energy. These are

Van der Waals (VDW) Energy : The VDW energy is the measure of non bonded or through space effects on energy which omits any bond length and angle contributions. It is very quick and useful method to calculate energy differences when any significant changes such as conformational changes occur in a molecule.

***Molecular Mechanics (MM) energy*:** The MM energy is the change in energy when bond distortions changes molecular geometry[125]. In Molecular Mechanics (MM), a molecule is represented in terms of Newtonian ball and spring model and

takes account of complex electronic interactions between atoms. On this basis the internal energy of a molecule is calculated in terms of potential energy functions for each of the various structural aspects, such as bond lengths, non bonded interactions and electrostatic interactions. The combination of these potential energy functions is the molecular mechanics force field which give the molecular energy[124]. This calculation is necessary when optimisation process is carried out to find the minimum energy or in studying changes in strained or ring systems. In Chem-X a set of parameters provides for a full molecular mechanics force field for calculating the energy of a molecule.

The energy of the minimised model may be automatically calculated in both VDW and MM approximation. For the present work the energy calculated by MM methods was assumed to be most suitable for comparisons with related molecules.

5.2.6. Conformational analysis

The different arrangement of atoms in molecule caused by rotation about a single bond are called conformations, and a specific structure is called a conformational isomer.

Molecules are considered as dynamic entities which are freely interchanging between different number of conformational states. The lowest energy conformations are the most abundant.

The different three-dimensional arrangements in space of the atoms in a molecule are interconvertable by free rotation about single bonds and cannot usually be isolated because of the fact that the interconversion takes place very rapidly[126]. Free rotation is possible around all the single bond except when the single bonds are constrained as, for example, part of a ring.

Conformers differ only in the rotation of their atoms about single bonds and because of this there are an infinite number of conformations possible for a given molecule.

5.2.7. Creating Log files

A Chem-X log file is a text file created by the program where a sequence of operation containing commands, instructions and menu picks are normally recorded during a session. It can be replayed several times and it is often useful to see the information written to the log file. By adding comments using a normal text editor to manually created log files it is possible to make it easier to read and understand. These can be added at the end of session. Only one log file is open in one session and remains open until the end of the Chem-X session. To open a new log file the current file must be closed and will be deleted by opening a further log file when commencing a new session. Log files may be renamed and saved when a record of the relative operations is required.

5.2.8. The analysis of conformations by the Chem-X programme

Chem-X uses study plots for analysing conformations of molecules. This method involves generating conformations for all rotatable bonds and performing a systematic search about each bond using the default torsion increment of 30^{o}. These incremental steps may be changed to increase or decrease the number of points and the associated conformers measured. The results create a plot automatically using all of the torsion angle variables from the conformation generation. This is one dimensional (1D) plot of energy against change in angle during rotation through 360^{o} about the selected bond. Each conformation or datapoint is shown by a symbol for which point the energy can be determined and the structure can be displayed or printed. This allows the identification of the number of steps involved when a bond is rotated through 360^{o}. The value of energy of each number (typically 1 - 72) can be determined together with the structure of the conformer at that number.

Consider the molecule ethane. This was the subject of the earliest works on conformational analysis and calorimetric values were consistent with values derived from statistical thermodynamical calculations assuming a resonable value for the energy barrier. More refined calculation by Aston et al[127] account for a potential barrier to internal rotation and led to better agreement between theory and experiment.

The potential energy changes that accompany the rotation of the carbon-carbon single bond in ethane as calculated using the Chem-X package are shown in fig.5.1. The most and least stable conformations are staggered and eclipsed respectively. In the eclipsed conformation each C-H bond of one carbon is lined up with a C-H bond of the other carbon. On the other hand in the staggered conformation each C-H bond of one carbon lies in a plane that bisects an H-C-H angle of the other carbon. As the C-C bond rotates the energy gradually increases until the state of highest potential energy is reached which is the eclipsed conformation. The difference in energy between the two conformations for ethane is about 2.9 kcal mol^{-1}. This difference is called the energy barrier and for free rotation to occur about a single bond there must be sufficient rotational energy present to overcome this barrier every time two hydrogen atoms are opposite each other.

The greater stability of the staggered conformation is due to the maximum separation of the adjacent atoms. The eclipsed conformation of ethane is strained by interactions of bonds on adjacent atoms. This type of strain is called torsional strain.

Fig.5.2 shows the two conformations of ethane as determined using the Chem-X package. The angle of rotation, is 60^{o} for staggered conformation. As the methyl groups rotate

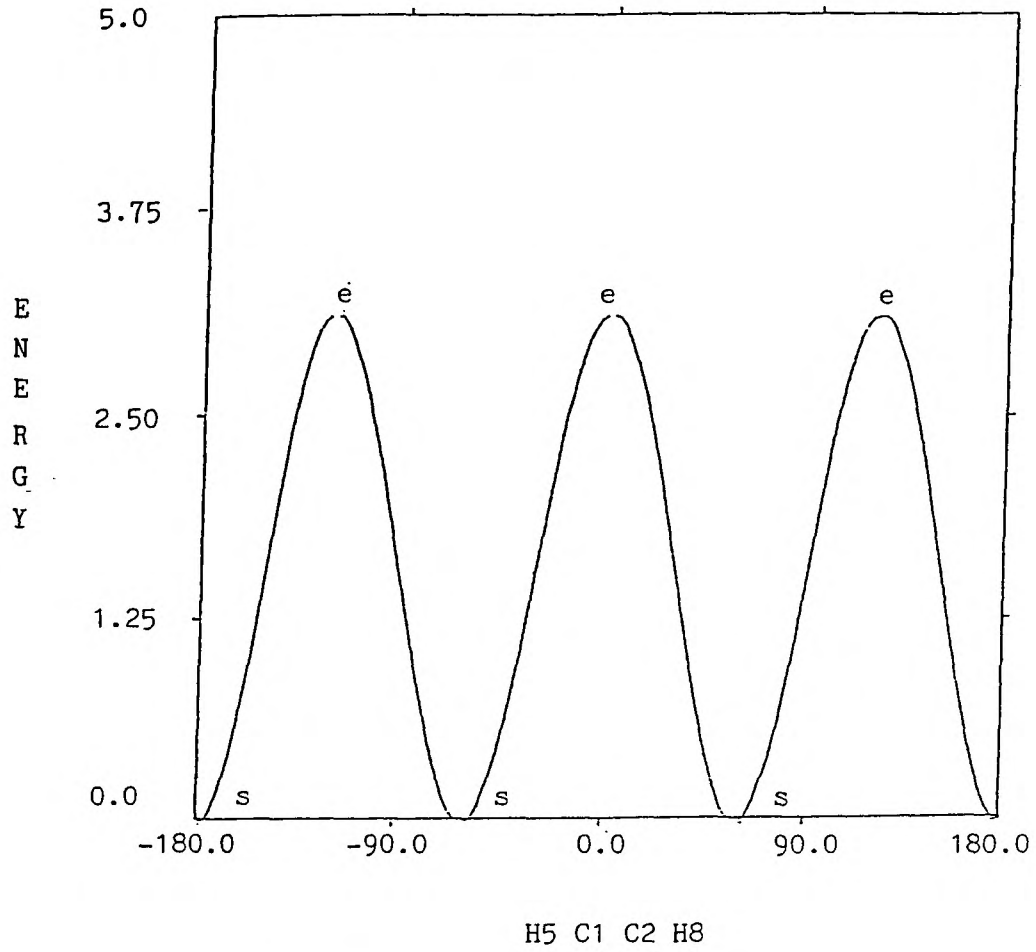

Fig.5.1. Variation of potential energy of ethane during the internal rotation of C-C bond (s = staggered, e = eclipsed).

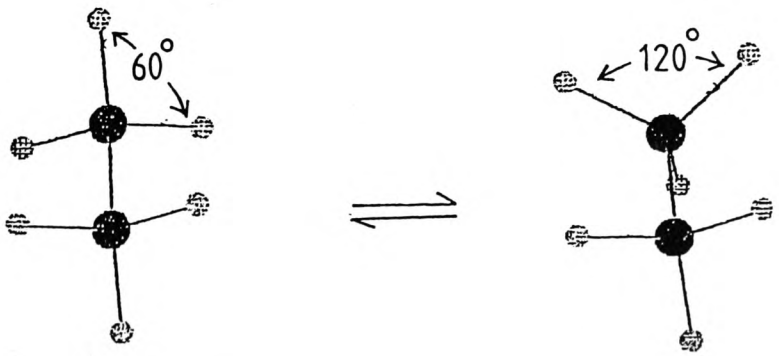

(a) Staggered form **(b) Eclipsed form**

Fig.5.2. Two conformational forms of ethane.

through 60° relative to each other, the angle of rotation between C-H bonds on adjacent carbon atoms become 0° (or 120°) leading to an eclipsed conformation.

5.3. Results and discussions

5.3.1. The calculation of Molecular Mechanics energy

The geometry of the carboxylic acid group in monomer and dimer form were taken from the acetic acid monomer and dimer values[59]. These values were found using electron diffraction in the gas phase but the values are takes to be the same for the solution phase.

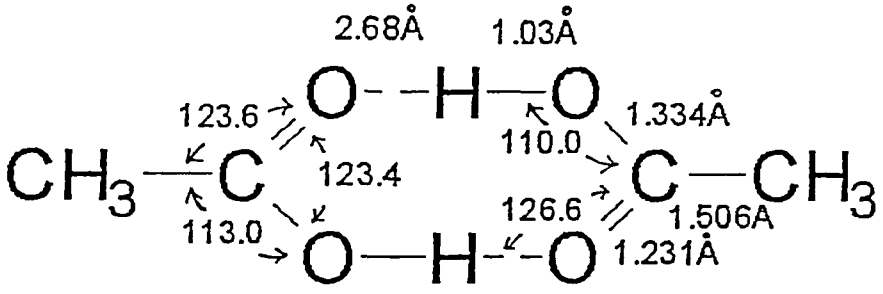

Using these parameters the molecules in table 5.1 were constructed. Structures were minimised as discussed in section 5.2.4. The calculation of energy for the o- methoxy benzoic acid is shown in the log file (appendix 1).

The "minimised" monomer of all carboxylic acids studied were designated as CM. In table 5.1 this reveals the lowest MM energy in all cases with lowest energy in acetic acid

(-12.0282 kcals) and highest energy (+4.2084 kcals) in o-methoxy benzoic acid.

The form favoured in the condensed state is dimeric (DM) and this reveals lower energy than the monomeric form in all cases except o-methoxy benzoic acid and o-ethoxy benzoic acid.

Here it is significant that o-methoxy and o-ethoxy benzoic acid permit internal hydrogen-bonding in which the alternative monomeric form (AM) permits close proximity between the carboxylic OH and the methoxy O for which spectroscopic evidence for hydrogen-bonding is present (chapter 4, p.94). The energy of these two bonded forms is calculated to be less than the monomer form in either conformation. This reduction in energy may be correlated with hydrogen bond formation from which greater stability is derived. The monomer form B is shown to have a calculated energy greater than the monomer form C in all cases.

Table 5.1

Calculation of Molecular Mechanics (MM) energy

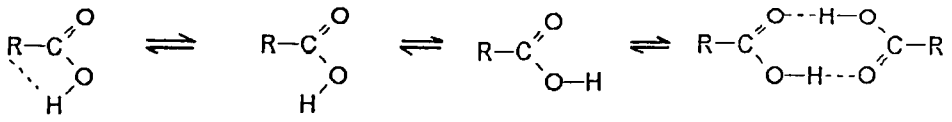

R	AM	BM	CM	DM
1 CH_3—		-8.5917	-12.0282	-25.2835
2 C_2H_5—		-4.831	-8.121	-17.522
3 C_3H_7—		-4.3343	-7.6639	-16.5908
4 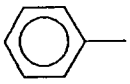		+4.6379	-0.0584	-1.4357
5 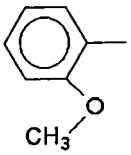	+2.8191	+6.2473	+4.2084	+6.5383
6 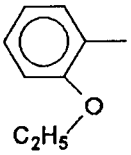	+0.1992	+3.6667	+1.7214	+2.2327
7 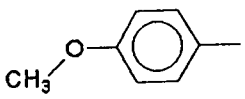		+6.6446	+1.9203	+1.4067
8 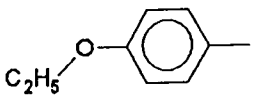		+4.2794	-0.435	-0.6371
9 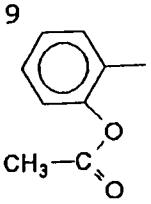		-1.321	-3.9389	-11.9511

5.3.2. The calculation of conformational energy for a number of rotating bonds

Since rotation about each bond in a molecule can lead to a number of conformers, the total possibilities of conformers for all bond rotations is considerable. It is also possible that the conformational energies associated with each rotation within a particular molecule interact with each other in a non-linear manner.

In case of o-methoxy benzoic acid there are four possible mode of rotation shown below

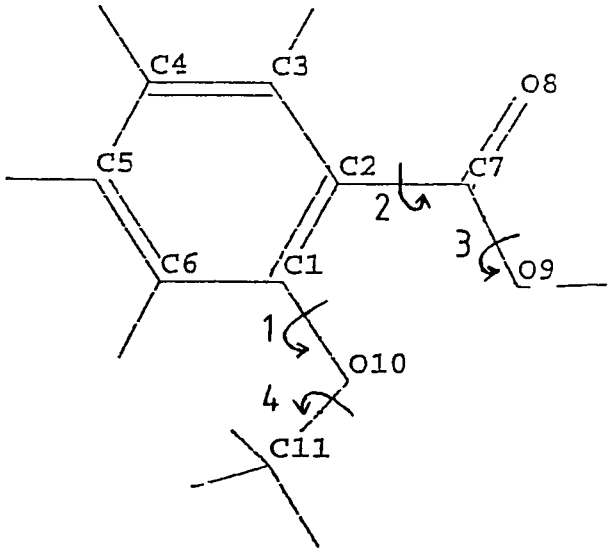

Using the Chem-X package it is possible to pick each bond in turn and determine

1. The potential energy changes associated with the bond rotation
2. The structure of conformers for each of the steps of angle rotation

3. The VDW energy for each of the steps

4. The MM energy for each of the steps.

Having established the molecular structure of the conformers for a particular rotation it is possible to select conformers and tabulated the potential energy (PE) of the rotatable bond, and determine the most stable conformer as indicated within the force field parameters within the Chem-X software.

These operations are described in the log file for the operation (appendix 2). The number of steps for rotating the O10 - C1 bond through 360 degrees was selected as 72 i.e. one every 5 degrees. The lowest energy conformer was determined as 5CM(17) for which the associated VDW energy was calculated as 8.1598 kcals. The total variation was determined graphically as shown in fig.5.3 (5CM). Each of the 72 conformers [5CM(1) to 5CM(72)] stored in the database (methocon.dbs) may be shown and the VDW and for MM energy calculated.

In order to analyse conformers derived from subsequent rotations it is necessary to rename the segment containing this conformer. This uses the "Selection" and "Create Structure" command within the "Edit" menu on the toolbar. The segment was renamed "m17" and a new database "Carbocon.dbs" opened to carry out a conformational analysis of the rotations of the carboxylic acid group about atoms C7 - C2. Here the Potential Energy (PE) diagram is determined as before [fig.5.4 (m17)]. Because the

carboxylic group is rotating against a non-planar framework the PE diagram is asymmetrical and the interactions of the carboxylic group on the same side as the methoxy group are different from those on the opposite side.

The conformer with the lowest calculated value is M17(7) leading to VDW energy of 7.7779 kcals. The conformer with highest energy is M17(37). These are shown in fig.5.5. It is worth noting that the experimental spectroscopic information on o-methoxy benzoic acid (chapter 4, section 4.3.5) indicated intramolecular hydrogen-bonding which is feasible in M17(37) but not in M17(7). This indicates the energy stabilisation associated with hydrogen-bonding overides the force field characteristics which determine the relative energies of these two models.

In order to measure the conformations associated with the rotation of the O-H group about the O9 - C7 bond the segment was renamed "m37" and a database "hydrocon.dbs" opened. The PE diagram (fig.5.6 M37) reveals a deep single minimum corresponding to the O-H group far removed from the methoxy group. The experimental evidence discussed earlier indicated the OH group is in closer proximity to the methoxy group and therefore corresponds to a maximum rather than a minimum energy [see figures 5.5 (a) and (b)]. The maximum energy was determined at m37(19) and the structure is shown in fig.5.7 M37(19) for which the VDW and MM energies were determined as 411.418 and 182.547 kcals respectively.

It is noted that these values for potential energy are considerably different from the energy values calculated in table 5.1. Here each set provides some internal comparison but further correlations between different methodologies are more difficult to analyse.

In accordance with the experimental information discussed earlier M37(19) was converted into the hydrogen-bonded form. In addition, the conformations associated with rotation of the methyl group were measured leading to a three-fold barrier (fig.5.8 M19). The minimum value corresponding to hydrogens staggered with respect to the O-H group is shown in fig.5.9 M19(36).

The stabilisation conferred by hydrogen-bonding is reflected in the calculated VDW and MM PE values of 53.4351 and 22.9913 kcals respectively. On removing the hydrogen bond in the model these values rise to 411.325 and 182.601 kcals. These values show small differences from those in m37(19) listed above because of the effect of minimising the conformers of the methyl group.

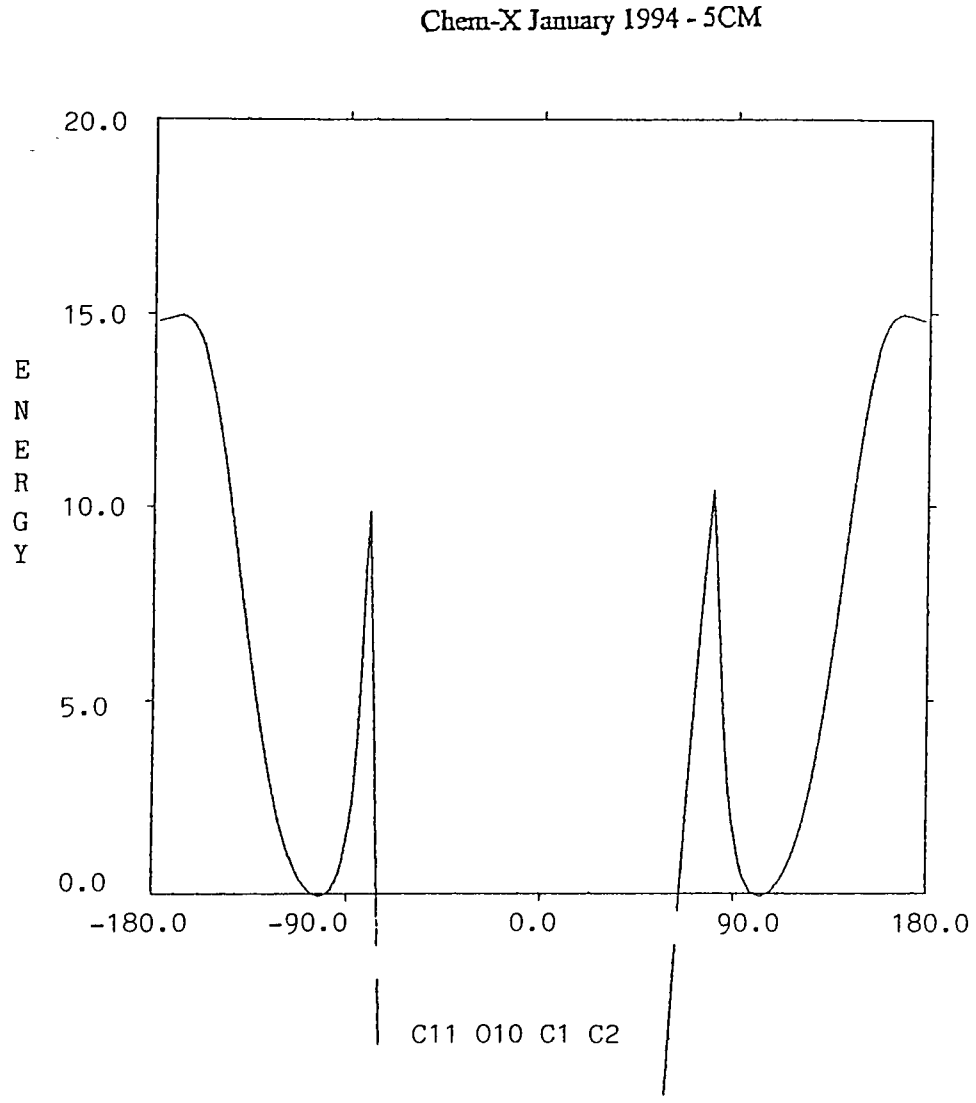

Fig.5.3 (5CM). Variation of potential energy of o-methoxy benzoic acid with rotation of O10 - C1 bond.

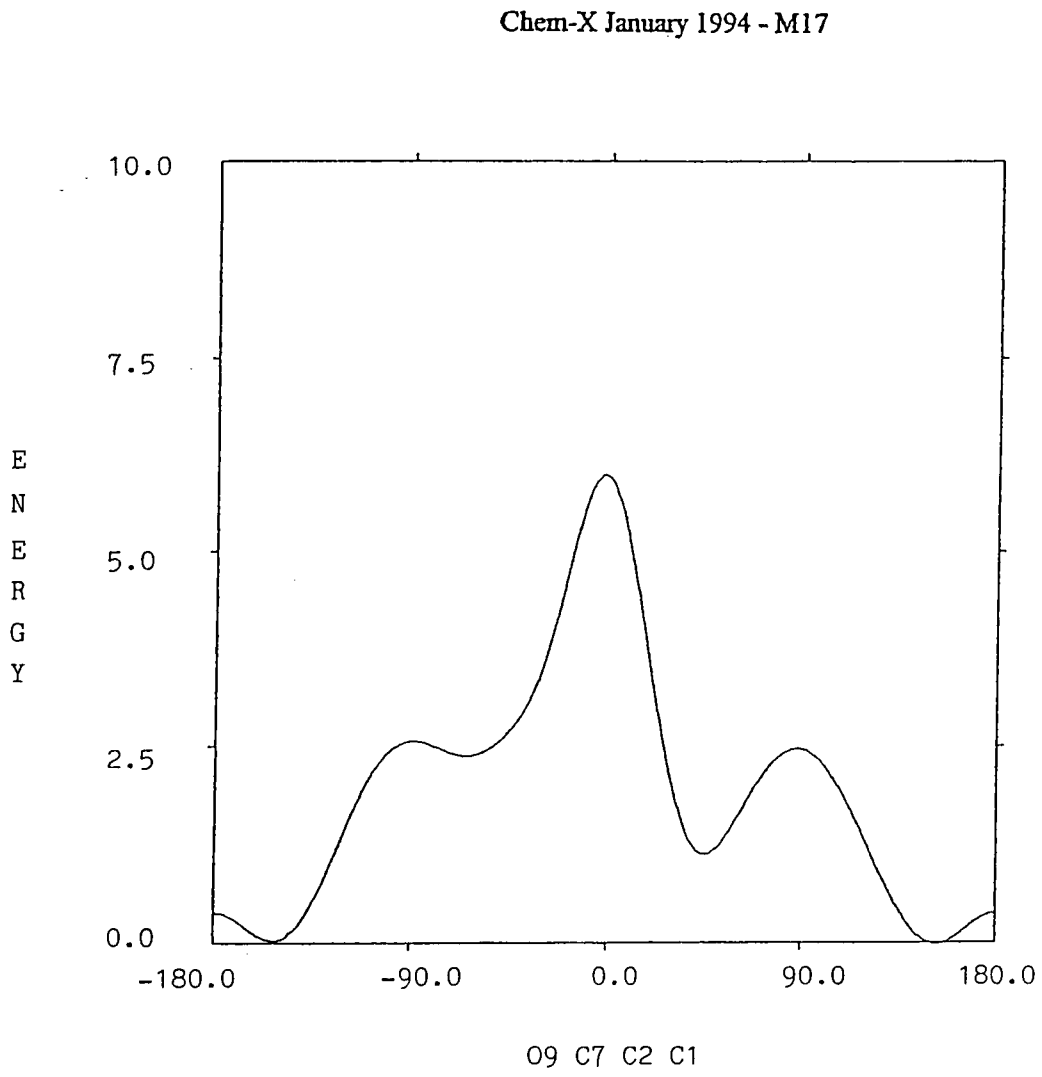

Fig.5.4 (m17). Variation of potential energy of o-methoxy benzoic acid with rotation of C7 - C2 bond.

Chem-X January 1994 - M17(7)

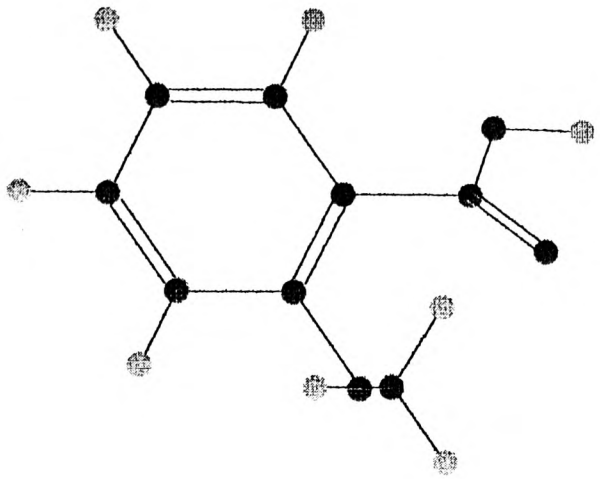

(a) Lowest energy conformer

Chem-X January 1994 - M17(37)

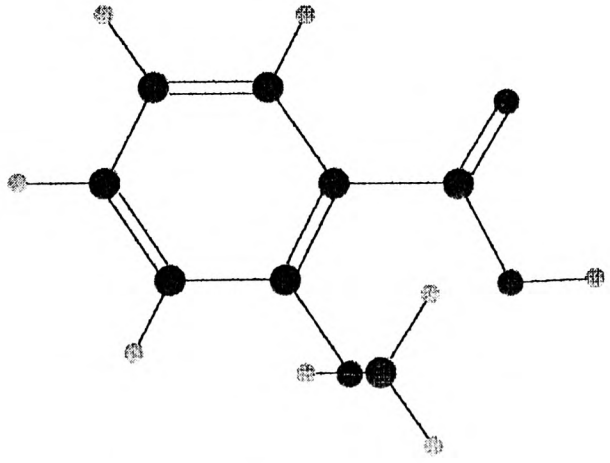

(b) Highest energy conformer

Fig.5.5. Conformations of o-methoxy benzoic acid during the rotation of C7 - C2 bond.

Chem-X January 1994 - M37

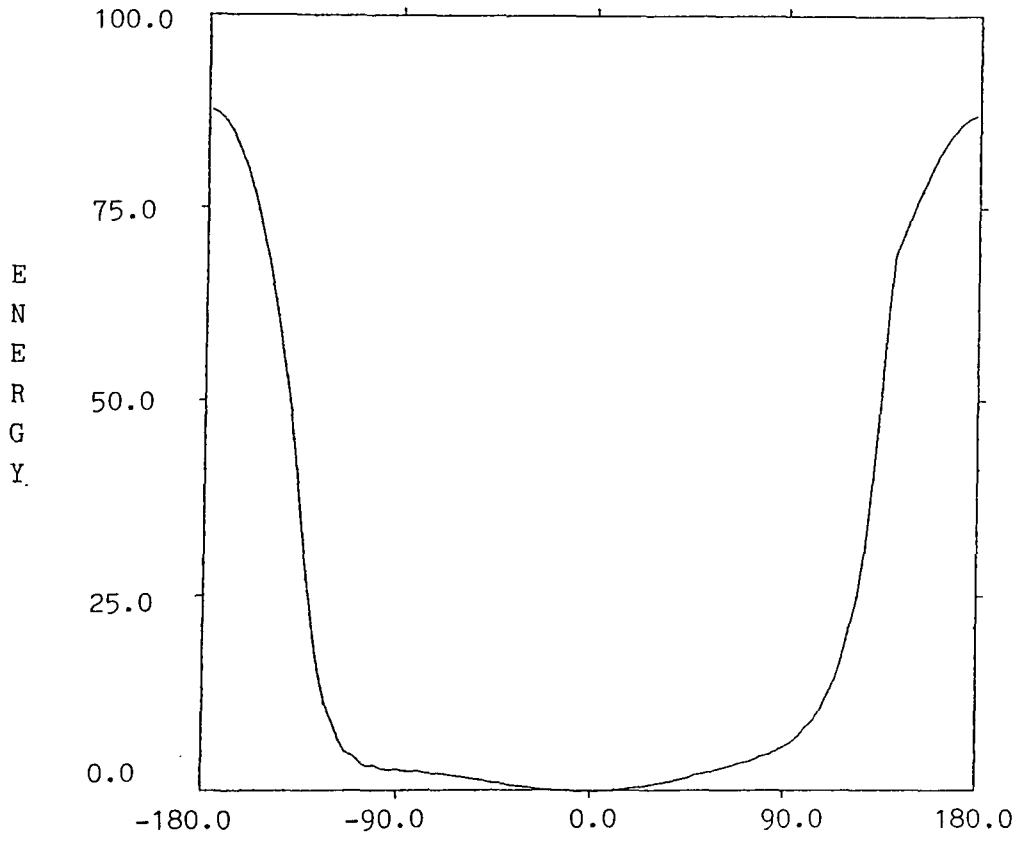

Fig.5.6 (M37). Variation of potential energy of o-methoxy benzoic acid with rotation of O9 - C7 bond.

Chem-X January 1994 - M37(19)

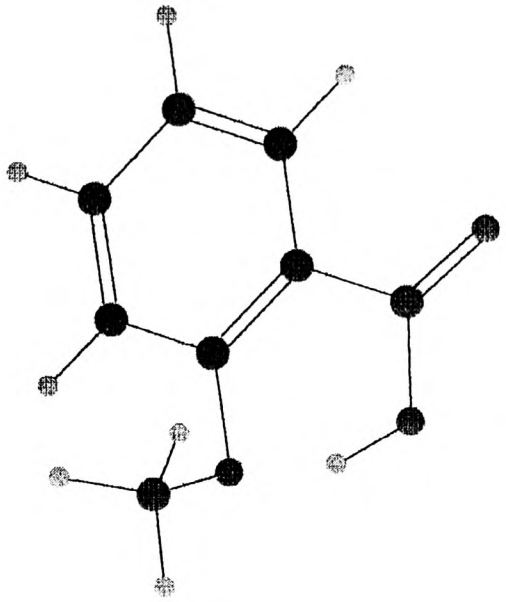

Fig.5.7 M37(19). The highest energy conformation of o-methoxy benzoic acid during the rotation of O9 - C7 bond.

Chem-X January 1994 - M19(36)

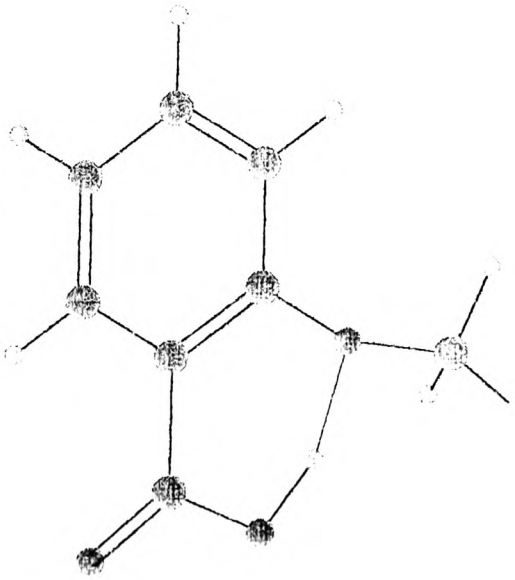

Fig.5.9 M19(36). The lowest energy conformation of o-methoxy benzoic acid during the rotation of O9 - C7 bond.

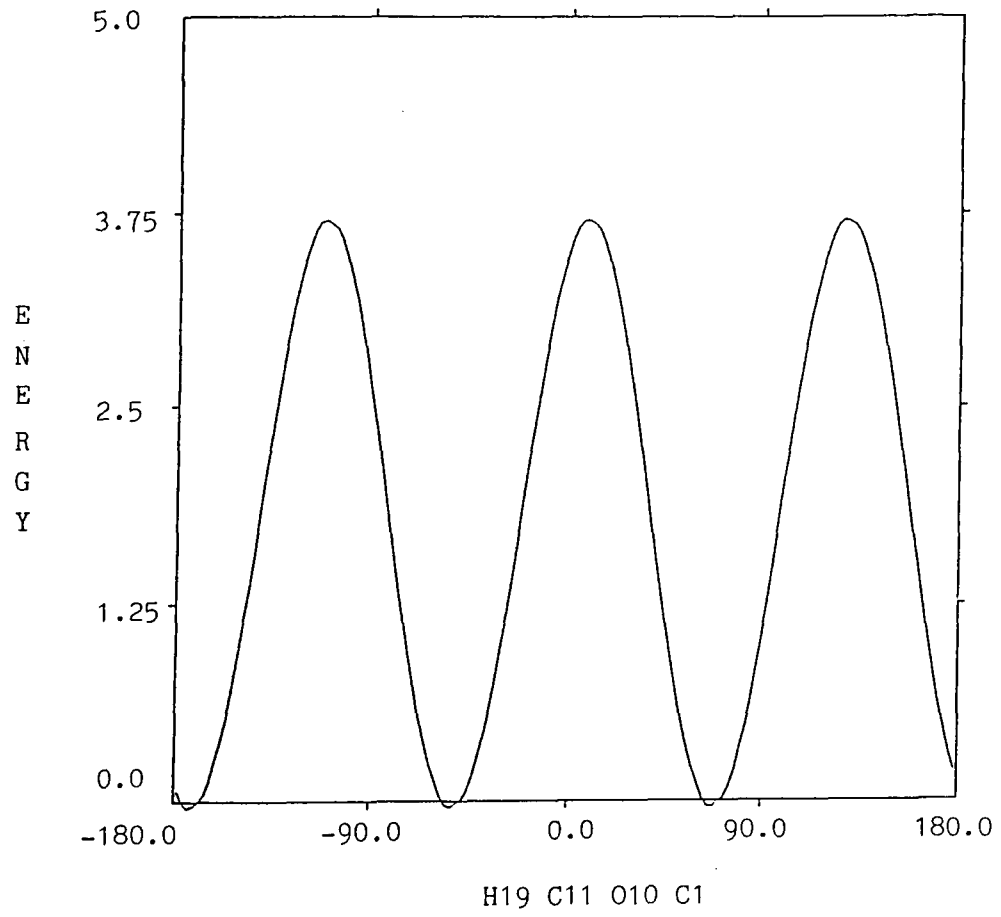

Fig.5.8 M19. Variation of potential energy of o- methoxy benzoic acid with rotation of C11 - O10 bond.

5.4. The incorporation of Spectra into the Chem-X package using the JCAMP.DX File Transfer Protocol

The JCAMP.DX format was determined as a spectral file transfer protocol for transfer of spectra between different spectrometers and other computer based systems[128]. Using a range of spectral files converted into the JCAMP.DX format software was developed for incorporation of spectra into the Chem-X package[129]. This software was loaded into the IPC Porta- PC-486/TFT computer which operates a number of packages including Chem-X via the Windows 3.1 operating system.

On switching from a screen containing a Chem-X constructed molecular model to the JCAMP command the following information appears

A - List DX files in spectra directory

B - Run JCAMP Conversion Program

C - Exit JCAMP Converter

Fig.5.10 was obtained by converting the spectra of o-methoxy benzoic acid recorded as solution in CCl_4 at 1.2 X 10^{-3} M on the PE model 1760 FT-IR into the JCAMP.DX format and transferred from the appropriate directory in the C drive of the spectrometer computer to the directory named "Spectra" within the C drive of the Chem-X computer using a diskette and the respective A drives.

The commands to import the spectra onto the screen displaying the Chem-X model are as follows:

A - the required spectra (5cm.dx) was loaded

B - 5cm.dx was entered

C - The SPK file name was entered (5cm.spk)

The screen was switched to Chem-X and a database opened (spectra.dbs) within the directory (Bill) in the C drive. Using the commands Computer/Diffraction, View/experimental, within the toolbar file names were read in the "spectral" directory of the C drive (enter 5cm.spk and O.K.). To exit View/none.

The spectrum is now displayed along side the model structure with which it is associated. This model can be manipulated using the normal toolbars on the right of the screen.

5.5. Further work

The information in fig.5.10 at a basic level comprises an infrared spectrum and an associated structure for a o-methoxy benzoic acid. In this case the structure and spectra indicate hydrogen-bonding as described in chapter 4. Both representations (structure and spectra) are amenable to considerable manipulation through their respective computer packages.

Thus the structure may be modified in terms of geometrical and chemical properties via Chem-X. The spectra can be manipulated and various bands studied and measured under optimum conditions using a suitable package based either

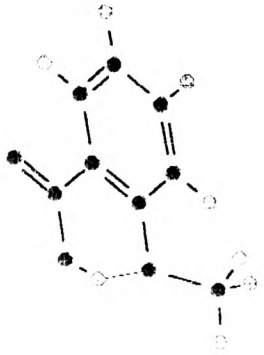

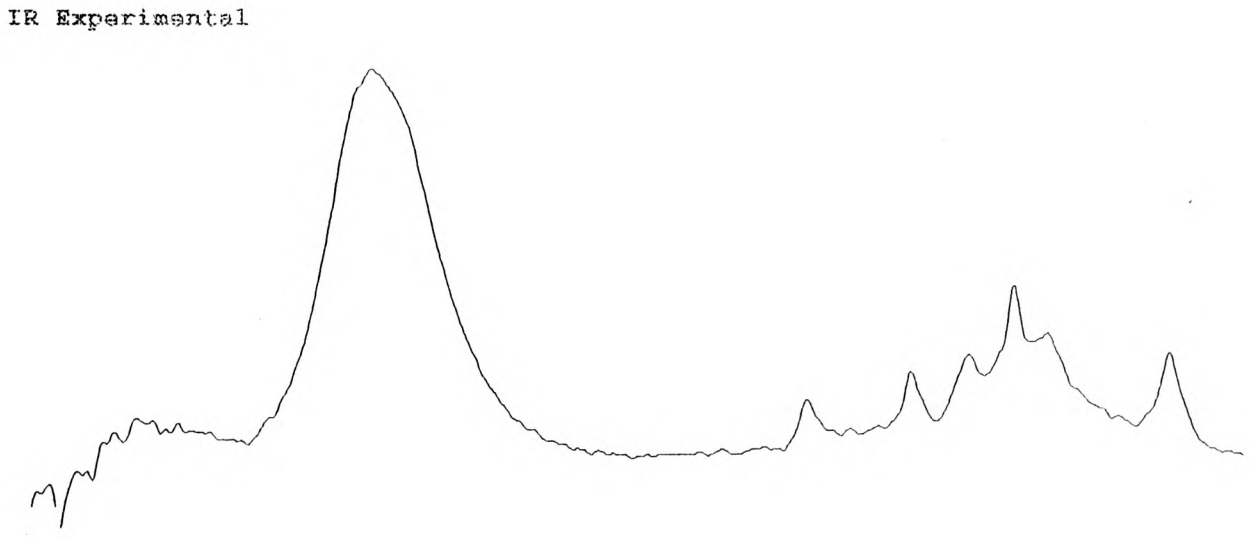

Fig.5.10. Incorporation of infrared spectra into Chem-X package for o-methoxy benzoic acid.

within the spectrometer controls or as a free standing package e.g. QSNEW from Sprouse Scientific or spectral packages from Galactic industries corporation[130]. Other structures and spectra can be brought to the screen for comparisons within like families of compounds.

Although feasible to manipulate the structure and spectra separately it would be highly desirable to be able to manipulate these simultaneously and to link them together. This would enable the basic experimental information which enables structures to be formulated to be more readily inputted into the model. This would provide a better link between theory and experiment which in turn provides greater incentives to refine and improve experimental and theoretical understanding of structure and hydrogen bonding phenomena[131].

CHAPTER SIX

CONCLUSIONS AND FURTHER WORK

6. CONCLUSIONS AND FURTHER WORK

Infrared spectroscopy has been used in this thesis as a sensitive probe of hydrogen-bonding interactions in alcohol and carboxylic acids systems. Measurements have been made firstly, to investigate thermodynamic properties associated with hydrogen-bonded alcohol-base system, secondly, to study the hydrogen-bonding effect on the spectra of carboxylic acids.

The hydrogen-bonding interactions between OH and C=O compounds may be considered in two categories. Firstly, alcohols as proton donors with carbonyl compounds as proton acceptors. Secondly, in terms of carboxylic acids where these functions are present in the same molecule.

The $\Delta H^{\ominus}$ value for the reaction of ethanol with acetone in CCl_4 agrees favourably with the determinations made by previous workers for similar systems. Since the hydrogen bond is relatively localised, it is expected that the most important factor controlling $\Delta H^{\ominus}$ will be the nature of the interacting centres involved in the interaction i.e. C=O...H-O. $\Delta S^{\ominus}$ values, as expected, are appreciably different for different ketones or alcohols, reflecting different degrees of steric repulsion for molecules with different alkyl groups or substituents.

The spectra of acetic acid in the vapour phase confirms that it is extensively dimerized, even at relatively low partial pressures ($\approx$0.05 torr) of acid whereas even at 20

torr the spectrum of pure alcohol show very little-complexation. Acid dimerization persists even in the presence of alcohol molecules. The existence of higher acid polymers ($[CH_3CO_2H]_n$) is more difficult to verify at the low resolution used in this work.

The measurements of thermodynamic parameters reported in chapter 3 also highlight some of the difficulties associated with such experiments. In principle, the determination of a equilibrium constant simply requires the simultaneous measurement of reactant and product concentrations. However, obtaining equilibrium concentrations by spectroscopic measurements of the acid, base and complex is generally difficult, due to the low concentration of the complexes at room temperature and complicated because we need to be sure that a complex spectral transition due to a complex is being unambiguously monitored.

Equilibrium constants generated by the solution phase work involving ethanol and acetone are considered to be more reliable and reproducible than experiments involving the corresponding gas-phase mixtures. Two explanations for this irreproducibility have been considered. Firstly, evidence suggests that adsorption is taking place within the gas cell. This reduces the ethanol and acetone concentrations by an unknown amount. Second, band enhancement of ketone and alcohol bands (an effect initiated by collisions of the absorber with molecules of the other component) could destroy the assumption that the monitored monomer band is

simply related to alcohol concentration. Work by George and Lewis et al[91,132] suggests that band enhancement is maximised by polar molecules (including ketones and alcohols). Solute/solute band enhancement is less important in solution where solute/solvent collisions dominate and where enhancement appears to be maximised.

Further work might usefully employ Teflon coated cells to minimise adsorption. One way of assessing the importance of band enhancement in affecting the determination of thermodynamic parameters for gaseous systems would be to determine the equilibrium constant K_C independently by two independent techniques e.g. IR and UV spectroscopy.

The second category of hydrogen-bonding considered in this work involves single component measurements on carboxylic acids. Here, the different species arising from hydrogen bonding interactions are well known. The present work seeks to add to this knowledge using the Chem-X software package.

The increase in the intensity of the absorption band of propionic acid in the monomeric hydroxyl region with decreasing concentration in carbon tetrachloride solution is consistent with the known effect of hydrogen-bonding on carboxylic acids. Examination of the infrared spectra of acetic acid vapour in the range of pressure $0.05 < 0.5 < 10$ torr indicates that acetic acid vapour is composed of a mixture of monomers and cyclic dimers. Spectra at different pressure are shown in chapter three. The band associated with the hydrogen stretching frequency centred at 3050 cm^{-1}

is found to be broad in each case. When pressure falls its intensity decrease but the intensity of free OH band increases.

The general character of the infrared spectra indicative of hydrogen-bonding is discussed in chapter one. The possible effect on a series of simple carboxylic acids as a result of hydrogen-bonding was obtained in chapter four. Spectra are shown for the OH and CO frequencies under various concentrations. All of these acids exist as an equilibrium mixture of monomer and dimer in dilute carbon tetrachloride solution. Inter and intramolecular hydrogen-bonding are observed in the spectra of o-methoxy and o-ethoxy benzoic acid which is consistent with the structure. The corresponding para compounds only show evidence for intermolecular association band of carboxylic acid.

The molecular modelling programme Chem-X offers innovative modelling solutions for all types of chemical structures including complex molecules such as polypeptides and proteins. A wide range of programmes may be used as Chem-X packages to perform modelling tasks. For creating molecular structure models, a 3-dimensional representation is available to provide the most probable geometry. In the present work values for potential energy of structures were determined. The structures were analysed in terms of conformers arising from the rotation, in turn, of each bond which could give rise to conformers of different energy. For each such bond a plot of energy against rotation may be

obtained from which structures and energies were determined as a function of angle of rotation from 0-360^{o}.

The significance of the values determined for particular structure depend on the assumptions of theory for force fields and interactions within the modelling package. There are also uncertainties in the choice of method of calculations. Both of these limitations require more detailed analysis before the energy values can be established with reasonable confidence.

One important feature of the calculations in this work is the opportunity to measure the change in energy on formation of a hydrogen bond. Here the changes of energies associated with different structures are likely to have relative significance. The opportunity to bring forward experimental information on hydrogen-bonding from infrared spectra into the Chem-X package shows promise in terms of improving the links between laboratory experiments on materials and computer based calculation arising from modelling theory.

These potential applications of interactive links between modelling package and spectroscopic measurements have been initiated for studies of hydrogen-bonding on carboxylic acids. This work also has potential for the study of other proton donor interactions described in this thesis and additionally to large molecules of biological significance.

REFERENCES

1. F.A. Cotton and G. Wilkinson, "Advanced Inorganic Chemistry", John Wiley & Sons, New York, Chichester, Brisbane, Toronto, 4th ed, (1972), Chap.6, p.215.

2. G.C. Pimentel and A.L. McClellan, "The Hydrogen Bond", W.H.Freeman and Co., San Francisco and London, (1960), Chap.1, p.6.

3. C.A. Coulson, Research, **10**, (1957), p.149.

4. J.C. Speakman, "The Hydrogen Bond and Other Intermolecular Forces", The Chemical Society, London, No.27, (1975), p.14.

5. C.G. Cannon, Spectrochim.Acta., **10**, (1958), p.341.

6. W.C. Hamilton and J.A. Ibers, "Hydrogen Bonding in Solids", W.A.Benjamin, Inc., New York, Amsterdam, (1968), Chap.1, p.13.

7. H. Ratajczak and W.J. Orville-Thomas, "Molecular Interactions ", John Wiley & Sons., Chichester, New York, Brisbane, Toronto, (1980), Vol.1, Chap.1, p.9.

8. M.M. Davies, Rep.Prog.Chem., **43**, (1946), p.5.

9. W.S. Fyfe, J.Chem.Phys., **21**, (1953), p.2.

10. G.L. Miessler and D.A. Tarr, "Inorganic Chemistry", Prentice-Hall International Editions, (1991), Chap.3, p.77.

11. S.N. Vinogradov and R.H. Linnel, "Hydrogen Bonding", Van Nostrand-Reinhold Co., New York, Cincinnati, Toronto, London, Melbourne, (1971) , Chap.1, p.11.

12. J.E. Huheey, "Inorganic Chemistry", Harper & Row Publishing Co., New York, 3rd ed., (1983), Chap.6, p.269.

13. M. Davies, ed., "Infrared Spectroscopy and Molecular Structure", Elsvier Publishing Co., Amsterdam, London, New York, (1963), Chap.12, p.405.

14. W.M. Latimer and W.H. Rodebush, J.Am.Chem.Soc., **42**, (1920), p.1419.

15. M.D. Joesten and L.J. Schaad, "Hydrogen Bonding", Marcel Dekker, Inc., New York, (1974), Chap.1, p.35.

16. P. Schuster, G. Zundel and C. Sandorfy, "The Hydrogen Bond", North-Holland Publishing Co., Amsterdam, New York, Oxford, (1976), Vol.II, Chap.8, p.395.

17. D.J. Millen, J.Mol.Struct., **45**, (1978), p.1.

18. M.D. Joesten, J.Chem.Educ., **59**, No.5, (1982), p.362.

19. J.T. Arnold and M.E. Packard, J.Chem.Phys., **19**, (1951), p.1608.

20. J.T. Arnold and M.E. Packard, Phys.Rev., **83**, (1951), p.210.

21. E.D. Becker, U. Liddel and J.N. Shoolery, J.Mol. Spectrosco., **2**, (1958), p.1-8.

22. J.L. Wood, "Spectroscopy and Structure of Molecular Complexes", J.Yarwood ed., Plenum Publishing Co., London, New York, (1973), Chap.4, p.308.

23. B.A. Wofford, J.W. Bevan, W.B. Olson and W.J. Lafferty, Chem.Phys.Lett., **124**, No.6, (1986), p.579.

24. L. Hunter, Rep.Prog.Chem., **43**, (1946), p.141.

25. J.S. Craw, M.A.C. Nascimento and M.N. Ramos, Spectrochim.Acta., **47A**, No.1, (1991), p.69.

26. A.C. Legon and D.J. Millen, Chem.Rev., **86**, No.3, (1986), p.636.

27. W.C. Hamilton and J.A. Ibers, "Hydrogen Bonding in Solids", W.A.Benjamin, Inc., New York, Amsterdam, (1968), Chap.3, p.85.

28. C.M. Huggins and G.C. Pimentel, J.Chem.Phys., **60**, (1956), p.1615.

29. G.M. Barrow, J.Chem.Phys., 59, (1955), p.1129.

30. W.O. George and Rh. Lewis, Educ.in Chem., **30**, No.3, (1993), p.78.

31. A. Allerhand and P.V.R. Schleyer, J.Am.Chem.Soc., **85**, (1963), p.371.

32. D.J. Millen, J.Mol.Struct., **100**, (1983), p.351.

33. J.E. Bertie and D.J. Millen, J.Chem.Soc., (1965), p.497.

34. J.T. Arnold and D.J.Millen, J.Chem.Soc., (1965), p.503.

35. J.E. Bertie and M.V. Falk, Can.J.Chem., 51, (1973), p.1713.

36. N. Sheppard, "Hydrogen Bonding", D.Hadzi ed., Pergamon Press, London, New York, Paris, Los Angels, (1959), p.101.

37. D.J. Millen and J. Zabicky, J.Chem.Soc., (1965), p.3080.

38. L.Al-Adhami and D.J. Millen, Nature, 211, (1966), p.1291.

39. R.G.J. Miller and B.C. Stace, eds., "Laboratory Methods in Infrared Spectroscopy", Heyden & Son Ltd., London, New York, Rheine, 2nd ed., (1972).

40. J.R. Ferraro and L.J. Basile, "Fourier Transform Infrared Spectroscopy", Academic Press, (1978), Chap.3, p.18.

41. J.M. Hollas, "Modern Spectroscopy", John Wiley & Sons., Chichester, New York, Brisbane, Toronto, Singapore, (1987), Chap.3, p.55.

42. A.A. Michelson, Phil.Mag., Ser.5., 31, (1891), p.256.

43. A.A. Michelson, Phil.Mag., Ser.5., 34, (1892), p.280.

44. R.J. Bell, "Introductory Fourier Transform Spectroscopy", Academic Press, Orlando, San Diego, New York,

London, Toronto, Montreal, Sydney, Tokyo, (1972), Chap.2, p.18.

45. R.C. Denney, "A Dictionary of Spectroscopy", Macmillan Press Ltd., London & Basingstoke, (1973), p.71.

46. P. Fellgett, J.Phys.Radium, 19, (1958). p.187.

47. P. Jacquinot and J.C. Dufour, J.Rech.C.N.R.S., 6, (1948), p.91.

48. J. Connes and P. Connes, J.Opt.Soc.Am., 56, (1966), p.896.

49. A.J. Barnes and W.J. Orville-Thomas, eds., "Vibrational Spectroscopy Modern Trends", Elsevier Scientific Publishing Co., Amsterdam, Oxford, New York, (1977), Chap.6, p.56.

50. W. Kemp., "Organic Spectroscopy", Macmillian Education Ltd., (1991), Chap.2, p.41.

51. P.R. Griffiths, "Chemical Infrared Fourier Transform Spectroscopy", John Wiley & Sons., New York, London, Sydney, Toronto, (1975), Chap.13, p.332.

52. D.R. Mattson, International Laboratory, Nov., (1989), p.46.

53. R.P. Bauman, "Absorption Spectroscopy", John Wiley & Sons., New York, London, (1962), Chap.4, p.177.

54. R.A. Nyquist and S.L. Fielder, Appl.Spectrosco., 47, No.10, (1993), p.1670.

55. N.L. Alpert, W.E. Keiser and H.A. Szymanski, "Theory and Practice of Infrared Spectroscopy", Plenum Press, New York, 2nd ed., (1970), Chap.3.

56. C.N.R. Rao, "Chemical Applications of Infrared Spectroscopy", Academic Press, New York, London, (1963), Chap.1, p.62.

57. W.O. George and P.S. McIntyre, "Infrared Spectroscopy", John Wiley & Sons., Chichester, New York, Brisbane, Toronto, Singapore, (1990), Chap.3.

58. E.F.H. Brittain, W.O. George, and C.H.J. Wells, "Introduction to Molecular Spectroscopy, Theory and Experiment", Academic Press, London, New York, (1970), Chap.3, p.175.

59. J.L Derissen, J.Mol.Struct., 7, (1971), p.67.

60. G.S. Hammond and W.M. Moore, J.Am.Chem.Soc., 81, (1959), p.6334.

61. W.M. Moore, G.S. Hammond and R.P. Foss, J.Chem.Phys., 32, (1960), p.1594.

62. W.M. Moore, G.S. Hammond and R.P. Foss, J.Am.Chem.Soc., 83, (1961), p.2789.

63. G.S. Hammond, W.P. Baker and W.M. Moore, J.Am.Chem. Soc., 83, (1961), p.2795.

64. U. Liddel and E.D. Becker, Spectrochim.Acta., **4**, (1952), p.229.

65. G. Geisler and E. Stockel, Spectrochim.Acta., **17**, (1961), p.1185.

66. S.N. Vinogradov, Can.J.Chem., **41**, (1963), p.2719.

67. A.C. Legon, D.J. Millen and S.C. Rogers, Proc.Roy. Soc.Lond., **A370**, (1980), P.213.

68. A.S. Pine and B.J. Howard, J.Chem.Phys., **84**, (1986), p.590.

69. F.A. Smith and E.C. Creitz, J.Res.Nat.Bur.Stand., **46**, (1951), p.145.

70. N.D. Coggeshall and E.L. Saier, J.Am.Chem.Soc., **73**, (1951), p.5414.

71. E.D. Becker, Spectrochim.Acta., **17**, (1961), p.436 .

72. P.J. Krueger and H.D. Mettee, Can.J.Chem., **42**, (1964), p.288.

73. H. Dunken and H. Fritzsche, Z.Chem., **1**, (1961), p.127.

74. H. Dunken and H. Fritzsche, Z.Chem., **1**, (1961), p.249.

75. H. Dunken and H. Fritzsche, Z.Chem., **2**, (1962), p.345.

76. S. Singh, A.S.N. Murthy and C.N.R. Rao, Trans.Faraday Soc., **62**, (1966), p.1056.

77. S. Singh and C.N.R. Rao, J.Am.Chem.Soc., 88, (1966), p.2142.

78. I.M. Arefev and V.I. Malyshev, Opt.i Spektroskopiya, 13, (1962), p.206, [English transl., Opt.Spectrosco., 13, (1962), p.112].

79. P. Pineau and M.L. Josien, Proc.Intern.Meeting.Mol. Spectrosco., 4th Bologna, 2, (1962), p.924.

80. Y. Sato, Nippon Kagaka Zasshi, 79, (1958), p.538.

81. A.C. Legon, D.J. Millen and O. Schrems, J.Chem.Soc., Faraday II, 75, (1979), p.592.

82. I.S. Perelygin and M.A. Klimchuk, Opt.i Spektroskopiya, 29, (1970), p.37, [English transl., Opt.Spectrosco., 29, (1970), p.20].

83. W.A.P. Luck and O. Schrems, Chem.Phys.Lett., 76, No.1, (1980), p.75.

84. J. Errera and P. Mollet, Nature, London, 138, (1936), p.882.

85. J. Errera, R. Gaspart and H. Sack., J.Chem.Phys., 8, (1940), p.63.

86. U. Liddel and E.D. Becker, Spectrochim.Acta., 10, (1957), p.70.

87. J.J. Fox and A.E. Martin, Proc.Roy.Soc., A162, (1937), p.419.

88. Ying-Sing Li and Mei-Lee H. Jeng, J.Chem.Educ., 65, No.10, (1988), p.920.

89. M.M. Hoeke, A.L. Koevoet, Recueil, **17**, (1963), p.82.

90. L.A. Curtiss and M. Blander, Chem.Rev., **88**, (1988), p.827.

91. W.O. George, Rh. Lewis, G. Hossain and G.J. Rees, J.Mol.Struct., **189**, (1988), p.211.

92. D. Hadzi and N. Sheppard, Proc.Roy.Soc., **A216**, (1953), P.274.

93. S. Bratoz, D. Hadzi and N. Sheppard, Spectrochim.Acta., **8**, (1956), p.249.

94. R.M. Badger and S.H. Bauer, J.Chem.Phys., **5**, (1937), p.605.

95. J.D.S. Goulden, Spectrochim.Acta., **6**, (1954), p.129.

96. A.M. Buswell, W.H. Rodebush and M.F. Roy, J.Am.Chem. Soc., **60**, (1938), p.2239.

97. M.M. Davies and G.B.B.M. Sutherland, J.Chem.Phys., **6**, (1938), p.755.

98. G. Allen and E.F. Caldin, Quartz.Rev.London., 7, (1953), p.255.

99. A.D.H. Clague and H.J. Bernstein, Spectrochim.Acta., **25A**, (1969), P.593.

100. R.C. Herman and R. Hofstadter, J.Chem.Phys., 6, (1938), p.534.

101. J.K. Wilmshurst, J.Chem.Phys., 25, (1956), p.1171.

102. M. Haurie and A. Novak, J.Chim.Phys., 62, (1965), p.137.

103. W. Weltner, J.Am.Chem.Soc., 77, (1955), p.3941.

104. Y. Marechal, Can.J.Chem., 63, (1985), p.1684.

105. K. Hirota and Y. Nakai; Bull.Chem.Soc.Japan., 32, (1959), p.769.

106. Y. Marechal, J.Chem.Phys., **87(II)**, (1987), p.6344.

107. J.L. Leviel and Y. Marechal, J.Chem.Phys., 54, (1971), p.1104.

108. D. Jaffe, Spectrochim.Acta., **43A**, No.11, (1987), p.1393.

109. D. Lin-Vien, N.B. Colthup, W.C. Fateley and J.G. Grasselli, "The Handbook of Infrared and Raman Characteristic Frequencies of Organic Molecules", Academic Press, Inc., New York, London, Tokyo, (1991), Chap.9, p.137.

110. J. Wenograd and R.A. Spurr, J.Am.Chem.Soc., 79, (1957), p.5844.

111. L.J. Bellamy, "The Infrared Spectra of Complex Molecules", Methuen and Co., London, (1954).

112. M. Davies and O. Thomas, Discuss.Faraday Soc., 9, (1950), p.335.

113. P.W. Allen and L.E. Sutton, Acta.Cryst., 3, (1950), p.46.

114. C.P. Smyth, "Dielectric Behavior and Structure", McGraw-Hill Co., New York, (1955), p.305-307.

115. M. Oki and M. Hirota, Spectrochim.Acta., 17, (1961), p.583.

116. N.M. Cullinane, R.A. Woothouse and V.V. Balley-Wood, Recueil, **80**, (1961), p.116.

117. M.C. Etter, Z.U. Lipkowska, P.A. Fish, T.W. Panunto and P.W. Baures, J.Crystallogra.Spectrosco.Res., **18**, No.4, (1988), p.311.

118. D. Peltier and A. Pichevin, Bull.Soc.Chim.France., (1960), p.1141.

119. J.J. Fox and A.E. Mertin, Nature, **143**, (1939), p.199.

120. Y. Nakai, S. Nakajima, K. Yamamoto, K. Terada and T. Konno, Chem.Pharm.Bull., **28(2)**, (1980), p.652.

121. T.I. Nagibina and A.L. Smolyanskii, Zh.Obshch.Khim., (Russ), **52**, (1982), p.754.

122. M.J. Wojcik, Chem.Phys.Lett., **83**, No.3, (1981), p.503.

123. Chem-X User Guide, January, (1994), Chemical Design Ltd., Roundway House, Cromwell Park, Chipping Norton,

Oxfordshire OX7 5SR, U.K.

124. Chem.Lib Programming Guide, Vol.II, July, (1993), Chemical Design Ltd., Roundway House, Cromwell Park, Chipping Norton, Oxfordshire OX7 5SR, U.K.

125. U. Burket and N.L. Allinger, "Molecular Mechanics", American Chemical Society, Washington, D.C., (1982), Chap.3, p.59.

126. R.C. Atkins and C.A. Carey, "Organic Chemistry", McGraw-Hill Publishing Co., New York, London, Mexico, Montreal, Sydney, Tokyo, Toronto, (1990), Chap.2, p.27.

127. M.L. Eidinoff and J.G. Aston, J.Chem.Phys., 3, (1935), p.379.

128. W.O. George and H.A. Willis, eds., "Computer Methods in UV, Visible and IR Spectroscopy", The Royal Society of Chemistry, (1990), Chap.11, p.167.

129. R. Upton and J. Gilbert, Chemical Design Ltd., Roundway House, Cromwell Park, Chipping Norton, Oxfordshire OX7 5SR, U.K.

130. Galactic Industries Corporation, 395 main St., Salem, NH 03079, USA.

131. R. Dilshad, J.R. Dixon, W.O. George, Rh. Lewis, B. Minty and R. Upton, Spie, **2089**, (1993), p.155.

132. W.O. George, I.W. Griffiths, B. Minty and Rh. Lewis, J.Chem.Educ., 71, No.7, (1994), p.621.

APPENDICES

APPENDIX 1

THE CALCULATION OF MOLECULAR MECHANICS (MM) ENERGY FOR THE o-METHOXY BENZOIC ACID

{ Menu | Open }
{ Open | Replace Structure }
{ Open | Open Database }
{ File Selection | A:\DILSHAD.DBS }
{ SCROLL-DOWN | 2DM }
{ SCROLL-DOWN | 7CM }
{ Open | 5CMR }
! Segment : 5CMR read from database 19 atoms in 1 entry
{ Open | OK }
{ Menu | Energy }
{ Energy | (1) : VDW_ENERGY }
{ * | VdW Minimise Torsions etc }
{ Energy | Add : AUTO BONDS }
{ * | Auto Bonds }
{ Energy | Add Variable(s) }
{ Energy | Calculate }
100
! VDW energy : 28.5105 kcals Cycle : 1
! % Convergence criterion reached
{ Energy | (1) : VDW_MINIMISE }
{ * | MM Optimise XYZ }
{ Energy | Calculate }
100
! MM energy : 16.7471 kcals Cycle : 1
! MM energy : 4.2084 kcals Cycle : 33
! % Energy convergence criterion reached - optimisation terminated
{ Energy | OK }
{ Menu | Geometry(1) }
{ Edit Geometry | Set Torsion (Twist) }
{ PICK ATOM | H16^5CMR }
{ PICK ATOM | O9^5CMR }
{ PICK ATOM | C7^5CMR }
{ PICK ATOM | C2^5CMR }
0
{ Edit Geometry | OK }
{ Menu | Energy }
{ Energy | (1) : MM_OPTIMISE }
{ * | VdW Minimise Torsions etc }
{ Energy | Add : AUTO BONDS }
{ * | Auto Bonds }
{ Energy | Add Variable(s) }
{ Energy | Calculate }
100
! % Convergence criterion reached
! VDW energy : 79.085 kcals Cycle : 1
{ Energy | (1) : VDW_MINIMISE }
{ * | MM Optimise XYZ }
{ Energy | Calculate }
100

```
! MM energy   : 12.7556 kcals       Cycle      : 1
! MM energy   : 6.2473kcals        Cycle      : 34
! % Energy convergence criterion reached - optimisation terminated
{ Energy | OK }
{ Menu | Hydrogen Bonds }
{ Hydrogen Bonds | Add H-Bond }
{ PICK ATOM | H16^5CMR }
{ PICK ATOM | O10^5CMR }
{ Hydrogen Bonds | OK }
{ Menu | Energy }
{ Energy | (1) : MM_OPTIMISE }
{ * | VdW Minimise Torsions etc }
{ Energy | Add : AUTO BONDS }
{ * | Auto Bonds }
{ Energy | Add Variable(s) }
{ Energy | Calculate }
100
! VDW energy  : 2.1116 kcals       Cycle      : 1
! % Convergence criterion reached
{ Energy | (1) : VDW_MINIMISE }
{ * | MM Optimise XYZ }
{ Energy | Calculate }
100
! MM energy   : 4.3974 kcals       Cycle      : 1
! MM energy   : 2.8191 kcals       Cycle      : 42
! % Energy convergence criterion reached - optimisation terminated
{ Energy | OK }
{ Menu | Open }
{ SCROLL-DOWN | 2DM }
{ SCROLL-DOWN | 1CM }
{ Open | 5DM }
! Segment : 5DM read from database  38 atoms in  1 entry
{ Open | OK }
{ Menu | Energy }
{ Energy | (1) : MM_OPTIMISE }
{ * | VdW Minimise Torsions etc }
{ Energy | Add : AUTO BONDS }
{ * | Auto Bonds }
{ Energy | Add Variable(s) }
{ Energy | Calculate }
100
! VDW energy  : 41.8402 kcals      Cycle      : 1
! % Convergence criterion reached
{ Energy | (1) : VDW_MINIMISE }
{ * | MM Optimise XYZ }
{ Energy | Calculate }
100
! MM energy   : 29.2705 kcals      Cycle      : 1
! MM energy   : 6.5383 kcals       Cycle      : 52
! % Energy convergence criterion reached - optimisation terminated
{ Energy | OK }
{ Menu | 2D Draw }
{ Tool Bar | DUSTBIN }
{ Menu | Exit }
```

APPENDIX 2

THE CALCULATION OF CONFORMATIONAL ENERGY FOR A NUMBER OF ROTATING BONDS OF o-METHOXY BENZOIC ACID

{ Menu | Open }
{ Open | Open Database }
{ File Selection | A:\DILSHAD.DBS }
{ SCROLL-DOWN | 2DM }
{ SCROLL-DOWN | 1CM }
{ Open | 5CM }
! Segment : 5CM read from database 19 atoms in 1 entry
{ Open | OK }
{ Menu | Conformers }
{ Conformers | Add : AUTO BONDS }
{ * | One Bond }
{ Conformers | Database : DILSHAD }
{ * | [Open] }
{ File Selection | C:\BILL\METHOCON.DBS }
{ Conformers | Add Variable(s) }
{ PICK ATOM | O10^5CM }
{ PICK ATOM | C1^5CM }
{Conformers | O10 C1 }
{ SCROLL-DOWN | Single }
{ SCROLL-DOWN | O10 C1 }
{ Conformers | Steps = 72 }
{ Conformers | Generate Conformers }
! Lowest VDW energy = 8.1598 Reference no. = 17
{ Conformers | OK }
{ Menu | Plot }
{ Plot | Plot Style : 2-D }
{ * | 1 Dimensional }
{ Plot | Generate Plot }
{ Plot | Relative = 20 }
{ Plot | OK }
{ Menu | Plot }
{ Plot | Plot Style : 1-D }
{ * | 2 Dimensional }
{ Plot | OK }
{ Menu | Open }
{ Open | Show Conformers }
{ Open | Replace Structure }
{ SCROLL-DOWN | 5CM(0) }
{ SCROLL-DOWN | 5CM(7) }
{ Open | 5CM(17) }
! Segment : 5CM(17) read from database 19 atoms in 1 entry
{ Open | OK }
{ Menu | Selection }
{ Selection | (1) : Create Structure }
{ * | Create Structure }
{ Selection | Name = m17 }
{ Selection | OK }
{ Menu | Conformers }

{ Conformers | Database : METHOCON }
{ * | [Open] }
{ File Selection | C:\BILL\CARBOCON.DBS }
{ Conformers | Add Variable(s) }
{ PICK ATOM | C7^M17 }
{ PICK ATOM | C2^M17 }
{ Conformers | C7 C2 }
{ SCROLL-DOWN | Single }
{ SCROLL-DOWN | C7 C2 }
{ Conformers | C7 C2 }
{ Conformers | Steps = 72 }
{ Conformers | Generate Conformers }
! Lowest VDW energy = 7.7778 Reference no. = 7
{ Conformers | OK }
{ Menu | Plot }
{ Plot | Plot Style : 2-D }
{ * | 1 Dimensional }
{ Plot | Generate Plot }
{ Plot | Relative = 10 }
{ Plot | OK }
{ Menu | Plot }
{ Plot | Plot Style : 1-D }
{ * | 2 Dimensional }
{ Plot | OK }
{ Menu | Open }
{ Open | M17(7) }
! Segment : M17(7) read from database 19 atoms in 1 entry
{ Open | OK }
{ Menu | Structure }
{ Structure | (1) : Atom Coloured Stick }
{ * | Ball and Stick }
{ Structure | Style : LABELS }
{ * | Atoms }
{ Structure | Set Radius = .75 }
{ Structure | OK }
{ Tool Bar | XY-Rotate }
{ Tool Bar | Close }
{ Menu | Energy }
{ Energy | Calculate }
! VDW energy : 7.7779 kcals
{ Energy | (1) : VDW_ENERGY }
{ * | MM Energy }
{ Energy | Calculate }
! MM energy : 9.9993 kcals
{ Energy | OK }
{ Menu | Open }
{ SCROLL-DOWN | M17(0) }
{ SCROLL-DOWN | M17(27) }
{ Open | M17(37) }
! Segment : M17(37) read from database 19 atoms in 1 entry
{ Open | OK }
{ Tool Bar | XY-Rotate }
{ Tool Bar | Close }
{ Menu | Selection }

{ Selection | (1) : Create Structure }
{ * | Create Structure }
{ Selection | Name = m37 }
{ Selection | OK }
{ Menu | Conformers }
{ Conformers | Database : CARBOCON }
{ * | [Open] }
{ File Selection | C:\BILL\HYDROCON.DBS }
{ Conformers | Add Variable(s) }
{ PICK ATOM | O9^M37 }
{ PICK ATOM | C7^M37 }
{ Conformers | O9 C7 }
{ SCROLL-DOWN | Single }
{ SCROLL-DOWN | O9 C7 }
{ Conformers | Steps = 36 }
{ Conformers | Generate Conformers }
! Lowest VDW energy = 13.731 Reference no. = 1
{ Conformers | OK }
{ Menu | Plot }
{ Plot | Plot Style : 2-D }
{ * | 1 Dimensional }
{ Plot | Generate Plot }
{ Plot | Relative = 100 }
{ Plot | OK }
{ Menu | Plot }
{ Plot | Plot Style : 1-D }
{ * | 2 Dimensional }
{ Plot | OK }
{ Menu | Open }
{ SCROLL-DOWN | M37(0) }
{ SCROLL-DOWN | M37(14) }
{ Open | M37(24) }
! Segment : M37(24) read from database 19 atoms in 1 entry
{ Open | OK }
{ Menu | Energy }
{ Energy | Calculate }
! MM energy : 30.0756 kcals
{ Energy | OK }
{ Menu | Open }
{ SCROLL-DOWN | M37(0) }
{ SCROLL-DOWN | M37(13) }
{ Open | M37(23) }
! Segment : M37(23) read from database 19 atoms in 1 entry
{ Open | OK }
{ Menu | Energy }
{ Energy | Calculate }
! MM energy : 40.8191 kcals
{ Energy | OK }
{ Menu | Open }
{ SCROLL-DOWN | M37(0) }
{ SCROLL-DOWN | M37(13) }
{ Open | M37(22) }
! Segment : M37(22) read from database 19 atoms in 1 entry
{ Open | OK }

{ Menu | Energy }
{ Energy | Calculate }
! MM energy : 60.8237 kcals
{ Energy | OK }
{ Menu | Open }
{ SCROLL-DOWN | M37(0) }
{ SCROLL-DOWN | M37(11) }
{ Open | M37(21) }
! Segment : M37(21) read from database 19 atoms in 1 entry
{ Open | OK }
{ Menu | Energy }
{ Energy | Calculate }
! MM energy : 100.085 kcals
{ Energy | OK }
{ Menu | Open }
{ SCROLL-DOWN | M37(0) }
{ SCROLL-DOWN | M37(10) }
{ Open | M37(19) }
! Segment : M37(19) read from database 19 atoms in 1 entry
{ Open | OK }
{ Menu | Energy }
{ Energy | Calculate }
! MM energy : 182.547 kcals
{ Energy | OK }
{ Menu | Open }
{ SCROLL-DOWN | M37(0) }
{ SCROLL-DOWN | M37(8) }
{ Open | M37(18) }
! Segment : M37(18) read from database 19 atoms in 1 entry
{ Open | OK }
{ Menu | Energy }
{ Energy | Calculate }
! MM energy : 145.964 kcals
{ Energy | OK }
{ Menu | Open }
{ SCROLL-DOWN | M37(0) }
{ SCROLL-DOWN | M37(9) }
{ Open | M37(19) }
! Segment : M37(19) read from database 19 atoms in 1 entry
{ Open | OK }
{ Tool Bar | XY-Rotate }
{ Menu | Energy }
{ Energy | Calculate }
! MM energy : 182.547 kcals
{ Energy | (1) : MM_ENERGY }
{ * | VdW Energy }
{ Energy | Calculate }
! VDW energy : 411.418 kcals
{ Energy | OK }
{ Menu | Hydrogen Bonds }
{ Hydrogen Bonds | Auto Calculate }
{ Hydrogen Bonds | Add H-Bond }
{ Hydrogen Bonds | OK }
{ Tool Bar | XY-Rotate }

{ Tool Bar | Close }
{ Menu | Selection }
{ Selection | Name = m19 }
{ Selection | OK }
{ Menu | Conformers }
{ Conformers | Database : HYDROCON }
{ * | [Open] }
{ File Selection | C:\BILL\METCON.DBS }
{ Conformers | Add Variable(s) }
{ PICK ATOM | C11^M19 }
{ PICK ATOM | O10^M19 }
{ Conformers | C11 O10 }
{ SCROLL-DOWN | Single }
{ SCROLL-DOWN | C11 O10 }
{ Conformers | Steps = 36 }
{ Conformers | Generate Conformers }
! Lowest VDW energy = 53.4351 Reference no. = 36
{ Conformers | OK }
{ Menu | Plot }
{ Plot | Plot Style : 2-D }
{ * | 1 Dimensional }
{ Plot | Generate Plot }
{ Plot | Relative = 5 }
{ Plot | OK }
{ Menu | Plot }
{ Plot | Plot Style : 1-D }
{ * | 2 Dimensional }
{ Plot | OK }
{ Menu | Open }
{ SCROLL-DOWN | M19(0) }
{ SCROLL-DOWN | M19(26) }
{ Open | M19(36) }
! Segment : M19(36) read from database 19 atoms in 1 entry
{ Open | OK }
{ Menu | Energy }
{ Energy | Calculate }
! MM energy : 22.9913 kcals
{ Energy | (1) : MM_ENERGY }
{ * | VdW Energy }
{ Energy | Calculate }
! VDW energy : 53.4351 kcals
{ Energy | OK }
{ Menu | Hydrogen Bonds }
{ Hydrogen Bonds | Remove H-Bond }
{ Hydrogen Bonds | OK }
{ Menu | Energy }
{ Energy | Calculate }
! MM energy : 182.601 kcals
{ Energy | (1) : MM_ENERGY }
{ * | VdW Energy }
{ Energy | Calculate }
! VDW energy : 411.325 kcals
{ Energy | OK }
{ Menu | Exit }